COMBINED THEORETICAL AND EXPERIMENTAL STUDY OF THE LINEAR RHEOLOGY OF MODEL AND COMMERCIAL POLYMERS

by

Xue Chen

A dissertation submitted in partial fulfillment
of the requirements for the degree of
Doctor of Philosophy
(Chemical Engineering)
in The University of Michigan
2011

Doctoral Committee:

Professor Ronald G. Larson, Chair
Professor Alan S. Wineman
Professor Michael J. Solomon
Professor Robert M. Ziff

Dedication

This dissertation is dedicated to my husband Kai Zhang (张楷), my parents Lingqin Xie(谢令琴) and Yumin Chen (陈玉民) in appreciation of their enduring support and encouragement.

Acknowledgements

Five years ago, I decided to pursue my PhD degree in Chemical Engineering and started to work on polymer rheology projects. Doubtlessly, the most important person for the completion of my dissertation was my advisor Prof. Ronald G. Larson. I am indebted to Prof. Larson, for being such an excellent advisor and mentor to me over the past five years, and for providing insightful academic and professional guidance throughout my doctoral studies. I greatly appreciate his critical thinking and his wealth of knowledge along with my research, which make my thinking more deep and comprehensive. I am also very impressed by and learned a lot from his efficient working style. No matter how busy he was, he would always finish revising my manuscript within one week, sometimes even within three days. I still remember the exciting moments working together with him during my second and third year--dozens of emails a day and daily meetings--very highly interactive and productive. Besides the academic aspect, I also wish to thank Prof. Larson for his support for my personal life. I have experienced several significant stages of my life during the past five years in Larson's group, i.e., transitioning my life to a new culture, starting a new research area, getting married, giving birth to a baby, and pursuing my degrees. As a foreigner to the U.S. who has left home for long time, I have never felt lonely or helpless. Instead, I have been always feeling in a big family in Larson's group. It is Prof. Larson who makes me have such a feeling, because he always treats us with respects, invites us to lunches and dinners with his family, and encourages his students to become well-rounded. Furthermore, I would also like to thank Prof. Larson's patience and understanding in my various extra curricular organizations, studies, and involvements, and thank him for giving me a lot of flexibilities to balance my course studies, research and personal life.

I would like to sincerely thank to Professor Robert M. Ziff, Professor Michael J. Solomon, and Professor Alan S. Wineman for serving on my committee and for their constructive questions and suggestions. Furthermore, I also thank Prof. Ziff, who went to

Tianjin University to recruit graduate students and admitted me to this wonderful program, so that I have a chance to enhance my understanding of chemical engineering as well as explore a different but interesting culture. Prof. Ziff also taught us Advanced Mathematics and Fluid Dynamics during my first year. In the class, he always had a word "beautiful" on the tip of his tongue to describe an equation, a figure or a phenomenon, which motivated and inspired our passion for science. I also want to thank Prof. Solomon for allowing me to use his lab instruments (ARG2 rheometer, pH meters, centrifugal machine, et al.). His dedication to research also motivated and moved me a lot. I would also like to express my thanks to Prof. Wineman who taught me the linear viscoelasticity of polymers during my first year in his class. It can be said that my first systematic understanding about G' and G' started from Prof. Wineman's class.

Most importantly, I thank my family for making me what I am today. I thank my mom and dad for building a home that encourages education, for their strict training and strict demands on me since I was a little girl, for providing opportunities to send me to many clubs, such as traditional Chinese painting club, for being there for me whenever I needed them, and for always believing that I am the best in their eyes. I hope that I will continue to make them proud. Especially, I thank my husband Kai Zhang for his unfailing support, for helping me through the toughest times, and caring of our lovely daughter Hannah H. Zhang during my final busy PhD stage.

None of the work presented in this thesis would have been possible without the help of my collaborators. I wish to start with Prof. Zuowei Wang for our discussions about the hierarchical model and exchanging our ideas about how to compare the two advanced tube models. And then I wish to thank Prof. John Dealy for providing me a wonderful opportunity to visit his lab and thank Prof. Dealy's student Dr. Siwan Li for her hospitality during my stay in Montreal, Canada. Then, I wish to thank Dr. M. Shahinur Rahman and Prof. Jimmy Mays who have provided me with carefully prepared H-shaped polybutadiene samples. Next, I wish to acknowledge the assistance of Hyojoon Lee and Prof. Taihyun Chang for their temperature gradient interaction chromatography characterizations on the H-shaped polybutadiene samples. Next, I would like to thank Dr. Chunxia Costeux for blending the linear commercial polyethylenes with the branched commercial polyethylens. Last but not least of the collaborators, I wish to thank Prof.

Florian J. Stadler for providing his rheological data to me for my validation work described in Chapter 5. I especially cherish his friendship and our conversations in Madison, WI.

I am grateful for Prof. Ralph Yang and Prof. Henry Wang to give me the opportunities to be their Graduate Student Instructor for the courses ChE360, ChE460 and ChE696 to enrich my teaching experience. Their personal experience and insightful suggestions inspired and encouraged me a lot.

Many of my group members who were present in the beginning of my Ph.D. are now gone and others have arrived since then. To all of them, Weixian Shi, Zhicheng Long, Chulwoo Jung, Youngsuck Heo, Zuowei Wang, Qiang Zhou, Lin Fang, Indranil Saha Dalal, Susan Duncan, Xueming Tang, Shi Yu, Shihu Wang, et al. I wish to express my appreciation. I would especially like to thank former Larson group members Dr. Seung Joon Park and Chulwoo Jung, each provided me with some of their own previous work that I used to build my research upon.

I also wish to thank my personal friends in Chemical Engineering Department who gave me support and inspiration: Phapanin Charoenphol, Tanawan Pinnarat, Seyedeh Marjan Varedi Kolaei, Phillip Christopher, Hongliang Xin, Zhenyu Huang, Yu Chen, Hao Chen, Thomas Westrich, Chien Ching Lilian Hsiao, and Dr. Xiaoyin Chen.

Table of Contents

List of Figures

List of Tables

Abstract

Polymer rheology is a very sensitive indicator of polymer long chain branching, and therefore can be used as a tool to determine polymer structures. This dissertation is thus focused on the study of the relationship between polymer linear viscoelastic properties and their structures using both rheological experiments as well as theoretical modeling methods applied to both model polymer melts and commercial polymer melts. In this work, the two advanced tube models, namely the "hierarchical model" and the "BOB" (or "branch-on-branch") model, were firstly introduced and compared before being applied to predict the rheological properties of model polymer melts and commercial polymer melts. For the model polymer melts, symmetric and asymmetric "H" model polybutadienes of high quality were synthesized by a collaborator using a novel synthesis strategy, and characterized by another collaborator using temperature gradient interaction chromatography (TGIC) as well as by the rheological measurements carried out in our lab. The "hierarchical model" was employed to predict their rheological behaviors as well as to identify the impurities in the materials using the "analytical rheology" concept. After validating the tube model theory successfully on the model polymer melts, we developed and validated a method to obtain tube model parameters for commercial polyethylene copolymers and tried to access the validity of the modeling predictions for commercial polyolefins. We are the first team to work on the asymmetric "H" shaped polymers. The most interesting findings in this work include: (1) The methods of TGIC, rheology measurement and theory modeling need to be combined to determine reliable long-chain branching information for branched polymers, and to identity the impurities in the materials. (2) The polydispersity of a branched polymer is not only due to molecular weight variations but also due to different molecular structures. (3) Even long-chain branching levels as low as 0.335 long chain branches per million carbon atoms can be detected by polymer rheology, which is not detectable by any other experimental method. (4) The "hierarchical model" can predict the rheology for both

model polymers, such as star-, linear- and H-shaped polymers, and commercial polyolefins, and thus it is a useful tool to predict polymer linear rheology.

Chapter 1
Introduction

1.1 Motivation

Since the story of man-made plastic began in the nineteenth century, research on plastics has greatly progressed to the point that plastics have become a staple of human life. Nowadays, billions of pounds of polymers are produced worldwide every year and shaped into different products. The shaping process depends on their rheological properties, which depends on their molecular weight distribution and long chain branching. It is found that polymer melt rheology has two practical uses in the plastics industry: (1) to determine molecular characteristics, such as molecular weight distribution and long-chain branching (LCB) distribution; and (2) to characterize the processing behavior of the polymer melts [Dealy (1990)]. Thereby, as shown in Figure 1-1, polymer melt rheology forms an important link in the so-called "chain of knowledge" between polymer molecular structure and the final properties of plastics products [Cahleitner (2001)].

A better understanding of the relationship between polymer structures and their rheological properties can be significantly helpful to design polymer structures of interests [Dealy and Larson (2006)]. Also, by taking advantage of the desirable ability of polymer rheology, it is possible to tailor both processing and end-use properties [Vega, et al. (1996)].

Although rheological measurements provide the most sensitive indicator of the presence of long-chain branching in polymer melts, and that these long branches are of great importance in the processing behavior of polymers [Dealy (1999)], the rheological experimental itself cannot reveal the information of long-chain branching quantitatively. For example, in commercial polymer melts, assessing the role of long chain branching (LCB) is complicated by the effects of density of branch points, branch length, and the

location of the branches along the polymer backbone or along the other branches, making it difficult to study their effect on rheological properties of polymers from the experiment itself. However, the rheological modeling method makes it possible to determine the molecular characteristics accurately. My dissertation is thus to investigate the linear rheological properties of polymer melts using both modeling and experimental methods.

1.2 Tube model theory

Rapid advances in theoretical understanding of the linear and nonlinear viscoelasticity of entangled polymers have led to new models that can account for the effects of both polydispersity and long-chain branching (LCB) on rheology [McLeish (2002); Larson (2001); and Watanabe (1999)], and therefore it is of special interest to use molecular rheological theory to infer branching information from rheological experimental data. Recent molecular theories for long-chain-branched polymers are based on the well-known tube model for entangled polymers, in which relaxation occurs by a combination of reptation of linear chains along the tube, fluctuations of chain ends inside the tubes, and constraint release, whereby motions of surrounding chains release entanglements on the tube [Milner and McLeish (1998); Milner and McLeish (1997); Milner et al. (1998); McLeish (1999); McLeish (2002); Larson (2001)].

The "tube" idea arises from the notion that entanglements of one polymer with its neighbors creates a "tube-like" region that confines the polymer to quasi-one-dimensional motion [Doi (1983); Doi and Edwards (1978a), (1978b), and (1978b)]. Generally, there are three mechanisms of polymer motions [Doi and Edwards (2002)]:

1) Reptation of a linear polymer. "The molecule escapes from its tube by sliding back and forth in it, gradually protruding more and more of its mass outside of the tube. Every time a portion of the tube is vacated by the chain, that portion of the tube is "forgotten"—the portions of the chain no longer in the tube have freed themselves from their original entanglement." [de Gennes (1971); Dealy and Larson (2006)]

2) Arm retraction. When the arm fluctuates from its tip to the branch point, it has to diffuse up an entropic potential barrier. The entropic barrier represents the unlikelihood of compressed configurations required the chain to contract within the tube [Milner and McLeish (1998)].

3) Constraint release, which is especially important in polydisperse polymers. There are two kinds of constraint release mechanism: one is Rouse motion of the tube, which accounts for the fact that, "after reptation of the short chains, the long chain can only move a short distance before re-entangling with other short chains"[Dealy and Larson (2006)]; another one is dynamic dilution which means the short chain plays as a solvent "diluent" in the mixture with long chains. When the short chains relax, the tube diameter grows fatter [McLeish (1989)].

These physics were included in a linear viscoelastic model developed by Milner and McLeish and applied by them to simple monodisperse linear polymers [Milner and McLeish (1998)], star polymers [Milner and McLeish (1997)], mixtures of star with linear polymers [Milner et al. (1998)], nearly monodisperse "H" polymers [McLeish (1999); Daniels et al. (2001)], and nearly monodisperse comb polymers [Daniels et al. (2001); Inkson et al. (2006)]. Larson [Larson (2001)] developed a "hierarchical model" that incorporated the physics of the Milner-McLeish model, as well as some additional physics described below, in an algorithm applicable to general mixtures of polydisperse branched and linear polymers. Park and Larson et al. [2005] modified this "hierarchical model" to include the "early-time fluctuations." The latest version of the "hierarchical model" (v3.0) [Wang et al. (2010)] incorporates the "thin tube," "fat tube," as well as "arm-frozen" methods as separate options for constraint-release Rouse motion (the concept of "thin tube", "fat tube" and "arm frozen" will be discussed in Chapter 2). A related model was also developed by Das et al. [2006] which included the effect of branches on branches (BOB), i.e., hyper-branching. The differences between "hierarchical model" and "BOB" model will be discussed in detail in Chapter 2.

1.3 Significance and scope of my research work

This dissertation contains the work for two U.S. National Science Foundation projects. The significance and scope of my dissertation are listed below:

(1) The first project focuses on the study of linear viscoelastic properties of well-designed "H" model polybutadienes. This project is at the forefront of polymer science. Collaborating with an international team including synthesis chemists and polymer characterization experts, we are, for the first time, working on asymmetric "H" polymers, and this exciting work will bring in something new not only for comparison of our

measurements with the best available theories, but also for practical design of commercial polymers, since most “H” polymers of commercial interest are of asymmetric shape.

(2) The second project is related to commercial polyolefin copolymers, requiring me to collaborate with a leading world chemical company---Dow Chemical Co. in Midland, MI, with the goal to develop a predictive model of the effects of polymer melt structures on rheology to reduce the financial cost of plastics processing, and to improve the quality of plastics products. This project has enormous practical significance because over 100 billion pounds of polyethylene, with a market value of nearly $100 billion, is produced each year and its manufacturing and processing would be greatly aided by development of a predictive model of its rheology.

In what follows, Chapter 2 describes the comparisons of two advanced tube models. In particular, one example about the effect of branch point position on the linear rheology of asymmetric star polymers is discussed. The function of Chapter 2 in this dissertation is to introduce the “hierarchical model”, which is a “tool” used and validated in these two NSF projects. Chapter 3 and Chapter 4 are about the H-shaped polymer project, in which the work of synthesis, TGIC (Temperature Gradient Interaction Chromatography) characterization, rheological measurements and modeling on a series of symmetric H and asymmetric H are presented. Chapter 5 and Chapter 6 are about the commercial polyolefin project. The method to determine the tube model parameters for commercial copolymers is discussed in Chapter 5. The rheological measurements and modeling predictions on a series of commercial polyolefin are presented in Chapter 6. Conclusions and future work are presented in Chapter 7.

.

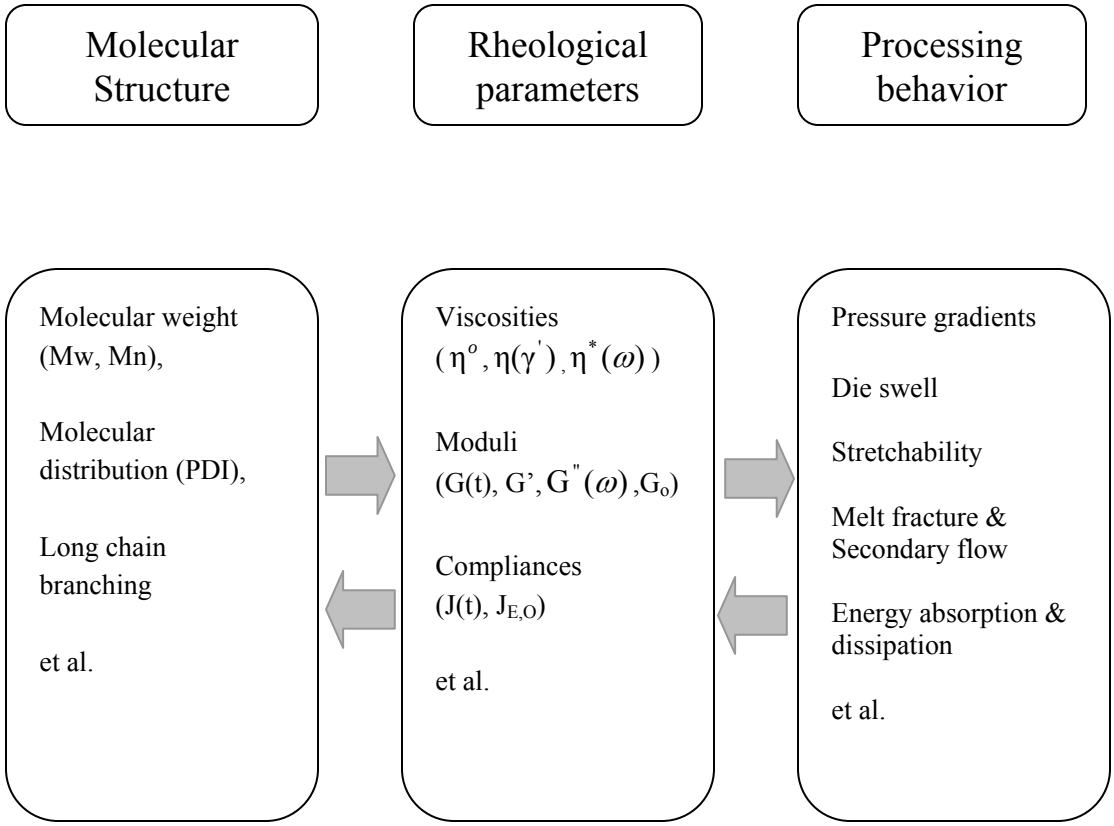

Figure 1-1. Rheological parameters acting as a "link" between molecular structure and final properties of a polymer [Adapted from Figure 1 in Ref. Cahleitner (2001)]

1.4 References

Ball, R. C., and T. C. B. McLeish, "Dynamic dilution and the viscosity of star polymer melts," Macromolecules 22, 1911-1913 (1989).

Cahleitner, M., "Melt rheology of polyolefins," Prog. Polym. Sci. 26, 895-944, (2001).

Daniels, D. R., T. C. B. McLeish, R. Kant, B. J. Crosby, R. N. Young, A. Pryke, J. Allgaier, D. J. Groves, and R. J. Hawkins, "Linear rheology of diluted linear, star and model long chain branched polymer melts," Rheol.Acta. 40, 403-415 (2001).

Daniels, D. R., T. C. B. McLeish, B. J. Crosby, R. N. Young, and C. M. Fernyhough, "Molecular rheology of comb polymer melts. 1. Linear viscoelastic response," Macromolecules, 34, 7025-7033 (2001).

Das, C., N. J. Inkson, D. J. Read, M. A. Kelmanson, and T. C. B. McLeish, "Computational linear rheology of general branch-on-branch polymers," J. Rheol. 50, 207-235 (2006).

de Gennes, P. G., "Reptation of a polymer chain in the presence of fixed obstacles," J.Chem. Phys. 55, 572-579 (1971).

Dealy J. M., and Larson R. G. Structure and rheology of Molten Polymers, Hanser Gardner Publications, Inc., Ohio (2006).

Dealy, J. M., Melt Rheology and its Role in Plastics Processing, New York: Van Nostrand Reinhold (1990).

Doi, M., and S. F. Edwards, "Dynamics of concentrated polymer systems. Part 1 - Brownian motion in the equilibrium state," J of the Chemical Society. Faraday Transactions II. 74, 1789-1801, (1978a).

Doi, M., and S. F. Edwards, "Dynamics of concentrated polymer systems. Part 2 - Molecular motion under flow," J of the Chemical Society. Faraday Transactions II. 74, 1802-1817, (1978b).

Doi, M., and S. F. Edwards, "Dynamics of concentrated polymer systems. Part 3 - The constitutive equation," J of the Chemical Society. Faraday Transactions II.; 74, 1818-1832, (1978c).

Doi, M., "Explanation for the 3.4 Power law of viscosity of polymeric liquids on the basis of the tube model," J. Polym. Sci.-Phys. 21, 667-684 (1983).

Doi, M., and S. F. Edwards, The Theory of Polymer Dynamics. Clarendon Press, Oxford (1986).

Inkson, N. J., R. S. Graham, T. C. B. McLeish, D. J. Groves, and C. M. Fernyhough, "Viscoelasticity of monodisperse comb polymer melts," Macromolecules 39, 4217-4227 (2006).

Janzen, J., and R.H. Colby, "Diagnosing long-chain branching in polyethylenes," J. Mol. Struct. 485, 569-584 (1999).

Larson, R. G., "Combinational rheology of branched polymer melts," Macromolecules 34, 4556-4571 (2001).

McLeish, T. C. B., "Tube theory of entangled polymer dynamics" Adv. Phys. 51, 1379-1527 (2002).

McLeish, T. C. B., J. Allgaier, D. K. Bick, G. Bishko , P. Biswas , R. Blackwell , B. Blottiere , N. Clarke , B. Gibbs , D. J. Groves , A . Hakiki , R. K. Heenan , J. M. Johnson , R. Kant , D. J. Read, and R. N. Young, "Dynamics of entangled H-polymers: Theory, rheology, and neutron-scattering," Macromolecules 32, 6734-6758 (1999).

Milner, S. T., and T. C. B. McLeish, "Parameter-free theory for stress relaxation in star polymer melts," Macromolecules 30, 2159-2166 (1997).

Milner, S. T., and T. C. B. McLeish, "Reptation and contour-length fluctuations in melts of linear polymers," Phys. Rev. Lett 81, 725-728 (1998).

Milner, S. T., T. C. B. McLeish, R. N. Young, A. Hakiki, and J. M. Johnson, "Dynamic dilution, constraint-release, and star-linear blends," Macromolecules 31, 9345-9353 (1998).

Park, S. J., S. Shanbhag, and R. G. Larson, "A hierarchical algorithm for predicting the linear viscoelastic properties of polymer melts with long-chain branching," Rheol. Acta 44, 319-330 (2005).

Vega, J. F., A. Muñoz-Escalona, A. Santamaría, M. E. Muñoz, and P. Lafuente. "Comparison of the Rheological Properties of Metallocene-Catalyzed and Conventional High-Density Polyethylenes," Macromolecules 29, 960 -965, (1996).

Wang, Z. W., X. Chen, and R. G. Larson, "Computational models for predicting the linear rheology of branched polymer melts," J. Rheol. 54, 223-260 (2010).

Watanabe, H. “Viscoelasticity and dynamics of entangled polymers,” Prog. Polym. Sci., 24, 1253-1403 (1999).

Chapter 2
Advanced tube models and polymer melt relaxation mechanism

2.1 Abstract

The "hierarchical model" and "BOB" (or branch-on-branch) model are advanced tube models recently developed for predicting the linear rheology of model polymers and general mixtures of polydisperse branched polymers. These two models are based on the well known tube model, but differ in some of the polymer relaxation mechanisms, tube model parameters as well as the numerical calculation implementation. An updated version of the "hierarchical model" (v3.0), which shows improved computational efficiency and refined relaxation mechanisms in previous publication [Wang, Chen and Larson (2010)], is introduced and compared with previous versions of "hierarchical model"(v1.0, v2.0) and the "BOB" model (v2.3). In Chapters 3, 4, 5 and 6, the latest version of hierarchical model (v3.0) is applied to predict the linear viscoelastic properties of all the polymer melts studied in this dissertation. The "BOB" model is used only in Chapter 5 to validate a method to obtain key tube model parameters of the commercial copolymers. Although in the next few chapters, the theory and modeling method will be described briefly, before applying these two advanced tube models into the next few chapters, a detailed overview of the similarities and differences of these models is presented in this chapter.

To test the ability of the "hierarchical model" and to study the polymer relaxation mechanism, the recent linear viscoelastic data of Archer and coworkers [Lee et al. (2005)] for asymmetric star-branched polymers having "T" and "Y" shapes are used to predict the effect of branch-point location on polymer relaxation. It is shown that the "hierarchical model" predicts correctly the effect of branch point placement on linear rheology.

2. 2 Comparisons of "hierarchical model" and "BOB" model

To describe commercial branched polymer melts, which are mixtures of polydisperse linear polymers with branched polymers of various architectures, the tube model must be generalized. Furthermore, for the model to be useful, the parameters used for prediction of simple polymers should not be readjusted when more complex branched structures are modeled. As a first step towards a generalized model for polydisperse branched melts, as mentioned in Chapter 1, Larson [2001] developed a "hierarchical model"(v1.0) that generalizes the theory of Milner and McLeish [Milner and McLeish (1997 and 1998); Milner et al. (1998); McLeish (1999)] for mixtures of monodisperse star-branched and linear polymers. Nowadays, there are two well- generalized advanced tube models, namely "hierarchical model" (v3.0) and "BOB" model (v2.3). Both of these models include reptation, primitive path fluctuations of chain ends, and constraint release by "constraint release Rouse motion" or "dynamic dilution." [Milner and McLeish (1998); Milner and McLeish (1997); Milner et al. (1998); McLeish (1999); McLeish (2002); Larson (2001)] The model of Das et al. also accounts for branches on branches, i.e., hyper-branching. There are some differences among these two models in relaxation mechanisms and model parameters, as well as in the way the equations are solved and what approximations are used for the fluctuation potential.

2.2.1 Relaxation mechanisms

After a small step strain is applied to the materials, the stress relaxes over a wide range of time scales. Depending on time scale and molecular weight and branching distributions, different relaxation physics are employed. We will compare the form of the relaxation mechanisms for the two advanced tube models.

(1)High-frequency relaxation

In the "BOB" model, Das et al. [2006] included Rouse motion inside the tube at times faster than the equilibration time τ_e and thus can account for relaxation at a higher frequency than the inverse equilibration time, while this physics is not included in the original "hierarchical model (v1.0) [Larson (2001)] but is included in the latest version (V3.0) [Wang et al. (2010)].

(2) Arm retraction

At a short time after a small step strain, for both "BOB" model (v2.3) and the "hierarchical model"(v3.0), the calculation of early-time fluctuations in these two models is essential the same, using the formula of Milner and McLeish [Milner and McLeish (1997)], namely

$$\tau_{early}(\xi) = \frac{9}{16}\pi^3 \tau_e S_a^4 \xi^4 \qquad (1)$$

with $S_a = M_a / M_e$, where M_a is the arm molecular, M_e is the entanglement molecular weight. In Eq. (1), τ_e is the equilibration time and ξ is "an arm coordinate that runs from zero to unity as one moves along the contour of the arm from the free end to the branch point"[Larson (2001)], or to the center of chain for a linear polymer (which can be viewed as a "two-arm star"). For these two models, the late-time arm retraction is calculated based on the numerical integration of Eq. (2) below [Milner and McLeish (1997)]:

$$\tau_{late}(\xi) = \frac{L^2}{D_{eff}} \int_0^{\xi} d\xi' \exp[U_{eff}(\xi')] \int_{-\infty}^{\xi} d\xi'' \exp[-U_{eff}(\xi'')] \qquad (2)$$

where L is the contour length of the tube and D_{eff} is the effective curvilinear diffusion constant of the retracting arm in the tube. In the Section 2.1.3, we will discuss the different approximation methods used in the numerical integration of late time relaxation.

The "BOB" model of Das et al. [Das et al. (2006)] uses a Rouse model to determine the depth of fluctuation of "compound arms" – arms that contain a short side arm that relaxes and mobilizes deeper penetration of the longer arm to which it is attached. The original "hierarchical model"[Larson (2010)] uses a "waiting time" to account for the friction of the side arm on fluctuations of the compound arm, while the "hierarchical model" (v2.0) [Park and Larson (2005)] and (v3.0) [Wang et al. (2010)] use a modified frictional prefactor in the expression for the relaxation time of the compound arm. All the three versions of "hierarchical model" (v1.0, v2.0 and v3.0) assume that the retraction potential governing fluctuations of the compound arm is based on the total length of the compound arm, and that this length is used to calculate the potential as the side arm relaxes. On the other hand Das et al. adopt a moving coordinate to define the length of the compound arm that is used in the expression for the fluctuation potential

after relaxation of the side arm. See the original papers for more details [Das et al. (2006)].

In Eq. (2), D_{eff} has similar definitions in the models of Wang et al. [2010] and of Das et al.[2006]; that is, $\frac{1}{D_{eff}} = \frac{1}{D_b} + \frac{1}{D_c}$, where D_b is the effective curvilinear diffusion constant of the branch point along the tube of the backbone and D_c is the Rouse diffusion constant for the linear chain without the effect of the branch point. When a simple arm with no side branch retracts, only Rouse drag plays a role; thus, L^2/D_{eff} is defined as $\frac{L^2}{D_{eff}} = \frac{3}{2}\pi^2 \tau_e S_a^3$. When a side arm collapses onto a compound arm, the effective drag caused by this side arm can be much larger than the Rouse drag of the rest of the arm and thus we must set $\frac{L^2}{D_{eff}} = \frac{3}{2}\pi^2 \tau_e S_a^3 + \frac{2}{p^2}\tau_a S_a^2$, where p is a numerical constant and τ_a is the relaxation time of the collapsed side arm.

(3) Reptation

For a branched polymer, as more and more arms relax or collapse, if there are only two arms left on a given molecule, the polymer finally becomes an effectively "linear" molecule, consisting of just the backbone of the original molecule [Das et al. (2006); and Larson (2001)]. We continue computing the retraction of the free ends of the effectively linear chain until a time is reached at which reptation takes over. Based on the work of Milner and McLeish [1997], Larson [2001] assumed that reptation occurs when the current time t reaches a value numerically equal to the reptation time τ_d of the effectively linear chain. As long as t remains smaller than τ_d, the chain continues to relax by arm retractions, while when t finally exceeds τ_d, the chain finally relax by reptation.

Both models ("hierarchical model" and "BOB" model) use this approach to describe final relaxation by reptation and compute drags similarly. For the "hierarchical model" (v3.0), besides the Rouse drag, the reptation time of the effectively "linear" chain (or backbone) can be approximated as $\tau_d \propto \frac{L_b^2}{D_R}$, where L_b is the backbone contour length and D_R is the reptative diffusion coefficient. In the case of the branched polymers, most

of drag is contributed by the branch point, so that $D_R \approx \frac{p^2 a^2}{2q\tau_a}$ where p is the numerical constant, and a is the tube diameter, q is the number of arms attached to the backbone, and τ_a is the relaxation time of the arm. Therefore, the reptation time of backbone in the modified "hierarchical model" is given as $\tau_d = \frac{2}{\pi^2}(1-\xi_d)^2 S_b^2 \phi_b^\alpha [\frac{3}{2}\pi^2 \tau_e S_b + \frac{\tau_a q}{p^2}]$, where S_b is the number of entanglements per backbone (effectively linear chain), ξ_d is the depth of the fluctuation along the chain coordinate ξ, and ϕ_b is the volume fraction of backbone material. The first term in square brackets is due to Rouse drag on the backbone, while the second term is for the drag contributed by the branch points. Similarly, for "BOB" and the model of Larson (v1.0), the total drag coefficient also has contributions from the backbone, and the arms that have been collapsed into the backbone.

(4) Constraint-release Rouse motion

When at a time t some polymer chain relaxes suddenly, typically by reptation, the unrelaxed volume fraction Φ is suddenly decreased to account for the loss of the contribution to the modulus represented by that chain. However, the effective orientational constraints that this chain impose on other chains do not disappear abruptly, but rather allow other chains to explore a new and larger tube by a process of "supertube relaxation" [McLeish (1989); Milner et al. (1998)]. Both models account for this process by using a function,

$$\Phi_{ST}(t) = \Phi_{ST,0}(\frac{t}{t_0})^{-1/2\alpha} \qquad (3)$$

which accounts for relaxation due to Rouse motion of the tube in which the polymer is confined. $\Phi_{ST,0} = \Phi(t_0^-)$ is the volume fraction of unrelaxed material just before the abrupt relaxation. So Φ_{ST} decreases gradually, while Φ drops suddenly. The model of Das et al. [2006] assumes that retraction occurs in a "thin" tube during constraint release Rouse relaxation rather than in a widening tube ("fat" tube) as assumed by Larson [2001], while in the model of Park and Larson [2005] ("hierarchical model" v2.0) retraction is frozen during constraint-release Rouse motion, as suggested by Milner and McLeish [1997]. The latest version of "hierarchical model" [Wang et al. (2010)] incorporates all three mechanisms, i.e. "thin" tube, "fat" tube, and arm-frozen. No conclusion has been

reached that one constraint-release Rouse motion mechanism is better than the other two. In my dissertation here, I use arm-frozen mechanism for all my predictions.

(5) Disentanglement relaxation

According to Larson's [2001] definition, "disentanglement relaxation occurs when the density of surviving entanglement $S_a\Phi(\xi)$ for an arm falls below the entanglement threshold; i.e., $S_a\Phi(\xi)$ drops to a threshold value $S_{a,min}$." Both the original theory of Milner and McLeish (1998) and the model of Das et al. [2006] did not consider the disentanglement relaxation. However, the need for this relaxation mechanisms has been discussed by Larson [2001], Lee and Archer [2002], and Park and Larson [2003]. The value of $S_{a,min}$ is somewhat arbitrary. In the original "hierarchical model" [Larson (2001)], the entanglement threshold was taken to be around unity. For the second version of "hierarchical model", $S_{a,min}$ was set to be unity for the HDB series polymers [Park and Larson (2005)] and to 3 for star-linear polybutadiene [Park and Larson (2003)]. However, we would like to use a single constant value for all materials. Thus, we stick to value "unity" for our studies using the latest version of the "hierarchical model" (v3.0).

2.2.2 Model parameters

(1) Dilution exponent

Park and Larson [2003] discussed and summarized the values of the dilution exponent. The concept of "dynamic dilution" was proposed by Marrucci [1985] to explain the constraint release motion in the relaxation of linear polymer. The dilution exponent α plays a role in Eq. (3). As summarized by Park and Larson [2003], in terms of the value of α, the experimental data presented in Tao et al. [1999] are fit somewhat better by α=1. However, according to the scaling principles, Colby and Rubinstein [1990] claimed that the "dilution exponent" ought to have a universal value of α=4/3, and Raju et al. [1981]'s experimental results also show evidence of the value α=4/3. Since the value of the dilution exponent has a significant effect on the relaxation of polymers as shown in Eq. (3), it is important to choose the correct value for quantitative predictions. In previous studies [Larson (2001); Park and Larson (2003)], α was set to 4/3 for the "hierarchical model" because the value of M_e obtained from a best-fit of viscosities of both linear and star polymers is closer to the value determined from the value of G_n^0

using the standard formula relating these quantities. However, the "BOB" model of Das et al.[2006] uses a "dilution exponent" α of unity rather than 4/3. As discussed in the paper of Das et al. [2006], α=1 predicts data well for H shaped polymers, comb polymer and branched m-PE polymers. However, when α=1, "BOB" model cannot predict well data for star polymers and linear polymers in Das et al.'s paper [2006]. For the latest version of the "hierarchical model" (v3.0), we stick to the value of α=4/3 for all predictions.

(2) Coefficient of branch point drag, p^2

As discussed above, p^2 appears in the prefactor for the drag contributed by the branch point. This numerical constant plays a role for the branched polymers with respect to compound arm retractions or reptation of the backbone. Das et al. [2006] use a value $p^2 = 1/40$ rather than the value of 1/12 used in the "hierarchical model".

2.2.3 Calculation of late time retraction

For the "BOB" model and the "hierarchical model", the late-time arm retraction is calculated from Eq. (2) [Milner and McLeish (1997)]

In the "hierarchical model" (v3.0), for ξ not close to ξ=1, the potential $U_{eff}(\xi)$ has finite slope and τ_{late} can be approximated by the formula in Milner and McLeish [1997] i.e.

$$\tau_{late}(\xi) \approx \frac{L^2}{D_{eff}} \frac{\exp[U_{eff}(\xi')]}{U_{eff}'(\xi)} \left(\frac{2\pi}{2U_{eff}''(0)}\right)^{1/2} \tag{4}$$

For ξ near ξ=1, the potential $U_{eff}(\xi)$ becomes flat, i.e. $U'_{eff}(\xi)$ becomes small, and the approximation is then no longer accurate, resulting in a divergence of τ_{late} [Milner and McLeish (1997)]. However, because of the disentanglement mechanism included in the "hierarchical model", before ξ gets very close to unity, the arm becomes disentangled and relaxes and so there is no need to repair the approximation above.

Das et al. [2006] approximate the inner integral in Eq. (2) in the same way, i.e. they use Eq. (5), but they have different strategy to deal with the outer integral.

$$\tau_{late}(\xi) \approx \frac{L^2}{D_{eff}} \left(\frac{2\pi}{2U_{eff}''(0)}\right)^{1/2} \int_0^{\xi} d\xi' \exp[U_{eff}(\xi')] \tag{5}$$

They build the potential from the differential form $\frac{\partial U(\xi, N_e(\xi))}{\partial \xi} = \frac{dU_{eff}(\xi)}{d\xi}$ [Milner and McLeish (1997)] and approximate the potential U by a Taylor expansion out to the second derivative. They then take the logarithm of τ_a and finally solve a second order equation to get the value of $\Delta\xi$ [Das et al. (2006)].

In sum, we have compared the similarities and differences between the "BOB" model and "hierarchal models" (v1.0, v2.0 and v3.0) and discussed the tube-model theory in detail. The "hierarchical model" (v3.0) will be applied into following projects to study the relationship between linear viscoelastic properties and polymer structures, thereby to test the tube model theory.

2. 3 Effect of branch point position on the linear rheology of asymmetric star polymers

These "hierarchical" models (v1.0, v2.0 and v3.0) have only been tested for a few different model branching structures, namely stars, H, and comb polymers, which have one or more branch points. These tests allow for the effect of number and length of branches to be studied, but the effect of branch position has not been systematically examined.

Recently, however, Archer and coworkers [2005] reported synthesis and rheological measurements for simple model asymmetric star polymers with a single branch point connecting a short "arm" to a long "backbone," with two different positions of the branch point along the backbone. The samples are 1, 4-polyisoprene "T shaped" A_2B73K and "Y shaped" AB_2110K shown in Figure 2-1 (a) and described in Table 2-1. Archer and coworkers showed that these data were consistent with a model they developed for asymmetric stars. In their model, they allowed a numerical coefficient "p^2" that relates the length of an attached arm to the mobility of its branch point, to be a function of the entanglement density of unrelaxed backbone segments [Lee et al. (2005)], while in the "hierarchical model" it is set to a constant value, $p^2 = 1/12$. While the model of Archer et al. gives good agreement with their data, here, we use their data to evaluate independently whether or not the "hierarchical model", which is a general model applicable to a wide range of polymer architectures, also accurately predicts the effect of

branch point position on rheology, but without varying the parameter p^2 from the canonical value of 1/12. The parameters needed in the "hierarchical model" are the plateau modulus G_N^0, the entanglement spacing M_e, and the equilibration time τ_e, which can be obtained from Lee et al. [2005], namely Me =4200[g/mol], G_N^0= 0.6 [MPa], and τ_e =7.4 ×10-6 [s] at T=28℃. These parameter values are similar to those used by Park et al. [2005] and Wang et al. [2010] at T=25℃. In the "hierarchical model", the "dilution exponent" α is set to the value 4/3, which was found to produce accurate predictions of other polyisoprene branched structures, such as symmetric stars [Park et al. (2005); and Wang et al. (2010)].

In Figures 2-2 and 2-3, we compare the predictions of the "hierarchical model" with experimental data for the storage and loss moduli of A_2B73K and AB_2110K. The basic idea of the "hierarchical model" is as follows. We consider the response of the melt to a small step strain, and calculate the time-dependent linear viscoelastic relaxation modulus, which can then be converted to frequency-dependent storage and loss moduli G' and G'' using standard methods. At a short time after a small step strain, only the arms can relax inward from their tips by early-time fluctuations and late-time retraction. We estimate early-time fluctuations by the function used by Milner and McLeish,[1997] namely $\tau_{early}(\xi) = \frac{9}{10}\pi^3 \tau_e S_a^4 \xi^4$ and the late-time arm retraction is then calculated directly from the numerical integration of Eq.(2)

$$\tau_{late}(\xi) = \frac{L^2}{D_{eff}} \int_0^{\xi} d\xi' \exp[U_{eff}(\xi')] \int_{-\infty}^{\xi} d\xi'' \exp[-U_{eff}(\xi'')], \qquad (2)$$

with $\frac{L^2}{D_{eff}} = \frac{3}{2}\pi^2 \tau_e S_a^3 + \frac{2}{p^2}\tau_a S_a^2$. In calculating the relaxation spectrum of an arm, we need the crossover equation between the early time and the late-time functions. To obtain this, we use the equation developed by Milner and Mcleish [1997], which is

$$\tau_a(\xi) = \frac{\tau_{early}(\xi)\exp[U_{eff}(\xi)]}{1 + \tau_{early}(\xi)\exp[U_{eff}(\xi)]/\tau_{late}(\xi)}. \qquad (6)$$

At any time t, the arm will have relaxed from its free end to a point ξ obtained

by equating τ_a with t; hence $t = \tau_a(\xi) = \dfrac{\tau_{early}(\xi)\exp[U_{eff}(\xi)]}{1+\tau_{early}(\xi)\exp[U_{eff}(\xi)]/\tau_{late}(\xi)}$. When an arm is fully relaxed, it is conceptually pruned away and replaced by a bead at the branch point, which schematically represents the frictional drag contributed by that arm. Eventually the unrelaxed molecule becomes a "linear" molecule. The final relaxation then occurs by reptation of an effectively "linear" chain, which, however, reptates slowly because of the beads representing the drag produced by the arms. The details of the "hierarchical model" are given by Wang et al. [2010] and Larson [2001].

Figure 2-4 shows that, over most of the frequency range, computed dynamic storage moduli, G' (ω), of A_2B73K and AB_2110K are quite similar, except that the "Y shaped" AB_2110K polymer relaxes somewhat slower in the terminal regime than does the "T shaped" A_2B73K. In the high frequency range, the "T shaped" and "Y shaped" molecules behavior similarly, because they both experience relaxation of the tips of each of their three arms. For the "T shaped" star molecule, the short arm completely relaxes at time t=1.28 s, while for "Y shaped" molecule, the two short arms completely relax at a similar time t=1.36 s. We have marked on Figure 2-4 the inverse times (as frequencies) at which the first short arm completely relaxes.

The difference between the rates of relaxation of the two molecules in the terminal regime can be explained as follows. For both molecules, the branch point is immobile until the short "B" arm has relaxed, after which the chain becomes effectively linear. At this point, for the "T shaped" molecule A_2B73K, as shown at the top of Figure 2-1 (b), fluctuations are still active at both ends of what has become effectively a linear chain. If the reptation time of linear molecule, τ_d, is bigger than the present time t, the chain is not yet ready to relax by reptation [McLeish (2002)]. The calculations using the "hierarchical model" show that no reptation occurs for the "T shaped" molecule before both of the remaining arms have completely relaxed by contour length fluctuation to the point of disentanglement by dynamic dilution. On the other hand, for the "Y shaped" molecule AB_2110K, both short arms relax at the same time, leaving an effectively linear chain, but with a low-mobility branch point at one end. Thus, further fluctuations are limited to the remaining long arm, which relaxes slowly by fluctuations due to its long length. The calculations with the "hierarchical

model" show that at t=33.3 s, the long arm of the "Y shaped" molecule abruptly relaxes by reptation. Therefore, in the relaxation process that occurs immediately after the molecules have become effectively linear, A_2B73K has two free ends that can relax through fluctuations while AB_2110K has only one free end that can relax fluctuations; hence the former relaxes faster than the latter.

2. 4 Conclusions

The differences among the two well-generalized tube models are compared in relaxation mechanisms and model parameters, as well as in the way the equations are solved and what approximations are used for the fluctuation potential.

The "hierarchical model" given by Larson [2001] and modified by Wang et al.[2010] yields good agreement with experimental data for long-chain branched polymers for two different branch point positions along a backbone of fixed length. Combined with earlier studies, we conclude that the "hierarchical model" not only captures the effects of the number and length of long-chain branches (as shown in earlier work), but also the position of the branch point.

.

Table 2-1. Molecular characterization of T and Y shaped 1,4-polyisoprene asymmetric stars

Sample	Mn (SEC with LS) [g/mol] (×10-3)			M in model [g/mol] (×10-3)	
	(1)short	(2)long	(3)total	(1) short	(2) long
A_2B73K	33	73.4	169	33	73.4
AB_2110K	32.78	110.06	170.06	32.8	110

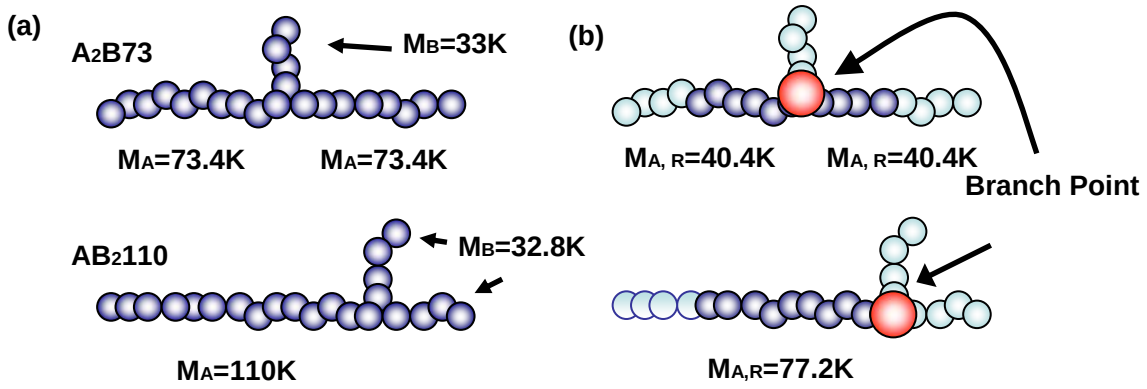

Figure 2-1. (a) Structure of "T shaped" A_2B73K and "Y shaped" AB_2110K 1,4-polyisoprene asymmetric star polymers. (b) The unrelaxed remaining backbones after relaxation of the short arms are shown in dark blue.

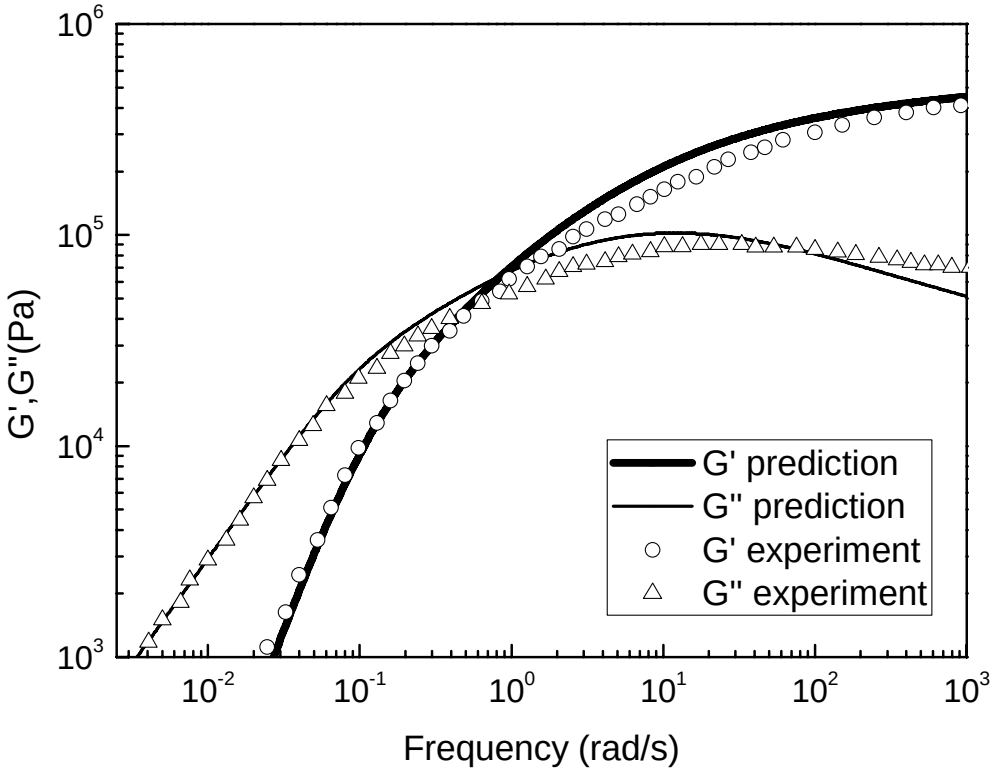

Figure 2-2. Dynamic moduli, G' (ω) and G''(ω), of "T shaped" A_2B73K 1,4-polyisoprene asymmetric star polymer. The symbols are experimental data from Lee et al. [2005] . The solid lines are the predictions of the "hierarchical model".

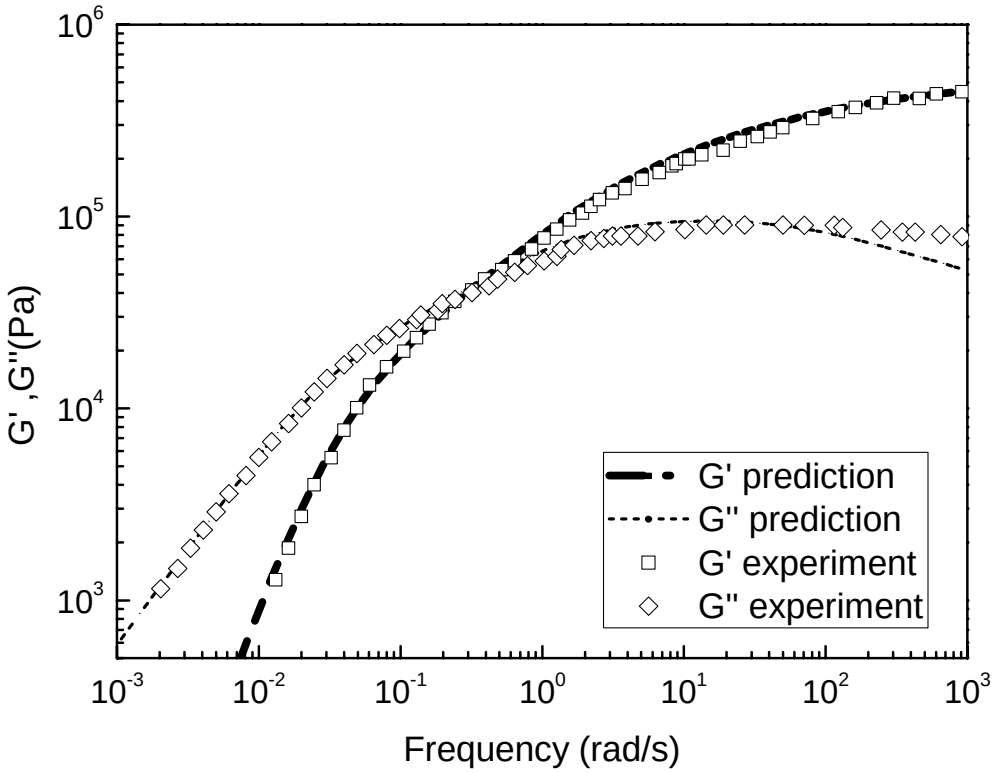

Figure 2-3. The same as Figure 2-2, except for the"Y Shaped" $AB_2$110K 1,4-polyisoprene asymmetric star polymer.

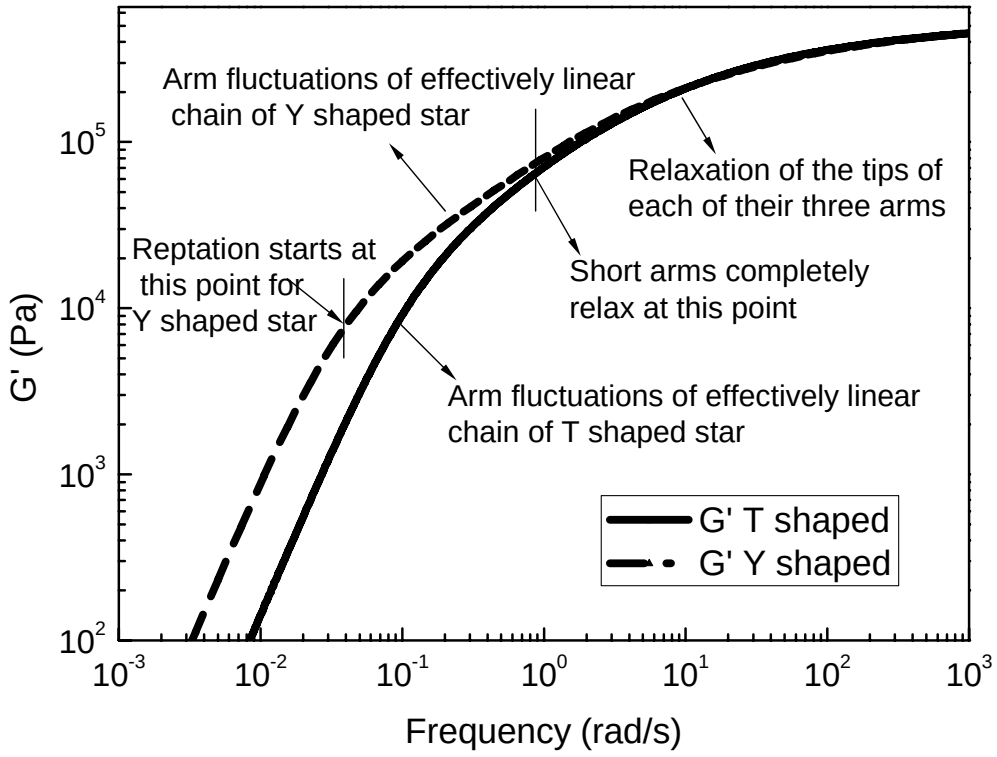

Figure 2-4. Comparison of dynamic moduli, G’ (ω), of “T Shaped” and “Y Shaped” 1,4-polyisopreneasymmetric star polymers, as predicted by the “hierarchical model”.

2.5 References

Colby, R. H, and N. Rubinstein, “Two-parameter scaling for polymers in θ solvents,” Macromolecules 23, 2753–2757(1990).

Daniels, D. R., T. C. B. McLeish, R. Kant, B. J. Crosby, R. N. Young, A. Pryke, J. Allgaier, D. J. Groves, and R. J. Hawkins, “Linear rheology of diluted linear, star and model long chain branched polymer melts,” Rheol.Acta. 40, 403-415 (2001).

Das, C., N. J. Inkson, D. J. Read, M. A. Kelmanson, and T. C. B. McLeish, “Computational linear rheology of general branch-on-branch polymers,” J. Rheol. 50, 207-235 (2006).

Ferry, J. D. Viscoelastic properties of polymers. John Wiley and Sons, New. York, (1980).

Fetters, L. J., D. J. Lohse, D. Richter, T. A. Witten, and A. Zirkel, “Connection between polymer molecular-weight, density, chain dimensions, and melt viscoelastic properties,” Macromolecules 27, 4639-4647 (1994).

Inkson, N. J., R. S. Graham, T. C. B. McLeish, D. J. Groves, and C. M. Fernyhough, “Viscoelasticity of monodisperse comb polymer melts,” Macromolecules 39, 4217-4227 (2006).

Janzen, J., and R. H. Colby, “Diagnosing long-chain branching in polyethylenes,” J. Mol. Struct. 485, 569-584 (1999).

Larson, R. G., “Combinatorial rheology of branched polymer melts,” Macromolecules 34, 4556-4571 (2001).

Lee J. H. and L. A. Archer "Stress relaxation of star/linear polymer blends," Macromolecules 35, 5587-6696 (2002).

Lee, J. H. and L. A. Archer "Tube dynamics in binary polymer blends," Macromolecules 38, 10763 (2005).

Marucci, G. J. “Relaxation by reptation and tube enlargement: A model for polydisperse polymers, ” Polym. Sci., Polym. Phys. 23, 159-177 (1985).

McLeish, T. C. B., J. Allgaier, D. K. Bick, G. Bishko , P. Biswas , R. Blackwell , B. Blottiere , N. Clarke , B. Gibbs , D. J. Groves , A . Hakiki , R. K. Heenan , J. M. Johnson , R. Kant , D. J. Read, and R. N. Young, “Dynamics of entangled H-

polymers: Theory, rheology, and neutron-scattering," Macromolecules 32, 6734-6758 (1999).

McLeish, T. C. B., J. Allgaier, D. K. Bick, G. Bishko , P. Biswas , R. Blackwell , B. Blottiere , N. Clarke , B. Gibbs , D. J. Groves , A . Hakiki , R. K. Heenan , J. M. Johnson , R. Kant , D. J. Read, and R. N. Young, "Dynamics of entangled H-polymers: Theory, rheology, and neutron-scattering," Macromolecules 32, 6734-6758 (1999).

McLeish, T. C. B., "Tube theory of entangled polymer dynamics," Adv. Phys. 51, 1379-1527 (2002).

Milner, S. T., and T. C. B. McLeish, "Parameter-free theory for stress relaxation in star polymer melts," Macromolecules 30, 2159-2166 (1997).

Milner, S. T., and T. C. B. McLeish, "Reptation and contour-length fluctuations in melts of linear polymers," Phys. Rev. Lett 81, 725-728 (1998).

Milner, S. T., T. C. B. McLeish, R. N. Young, A. Hakiki, and J. M. Johnson, "Dynamic dilution, constraint-release, and star-linear blends," Macromolecules 31, 9345-9353 (1998).

Milner, S. T., and T. C. B. McLeish, "Reptation and contour-length fluctuations in melts of linear polymers," Phys. Rev. Lett. 81, 725–728 (1998).

Park, S. J., S. Shanbhag, and R. G. Larson, "A hierarchical algorithm for predicting the linear viscoelastic properties of polymer melts with long-chain branching," Rheol.Acta 44, 319-330. (2005).

Park, S. J., and R. G. Larson, "Dilution exponent in the dynamic dilution theory for polymer melts," J. Rheol. 47, 199-211 (2003).

Park. S. J., and R. G. Larson, "Long-chain dynamics in binary blends of monodisperse linear polymers," J. Rheol. 50, 21-39 (2005).

Raju, V. R., E. V. Menezes, G. Marin, and W. W. Graessley, "Concentration and molecular weight dependence of viscoelastic properties in linear and star polymers," Macromolecules 14, 1668–1676 (1981).

Tao, H., C. Huang, and T. P. Lodge, "Correlation length and entanglement spacing in concentrated hydrogenated polybutadiene solutions," Macromolecules 32, 1212–1217 (1999).

Wang, Z. W., X. Chen, and R. G. Larson, "Computational models for predicting the linear rheology of branched polymer melts," J. Rheol. 54, 223-260 (2010).

Watanabe, H. "Viscoelasticity and dynamics of entangled polymers," Prog. Polym. Sci., 24, 1253-1403 (1999).

Chapter 3

Combined synthesis, TGIC characterization, and rheological measurement and prediction of symmetric H polybutadienes and their blends with linear and star-shaped polybutadienes

3.1 Abstract

We report the synthesis and characterization by temperature gradient interaction chromatography (TGIC) and rheometry of a symmetric H-shaped polybutadiene (PBd) that we call "HA20B40," and of a symmetric star-shaped synthetic precursor of HA20B40, and the use of these characterization data to test and validate an advanced tube model (the "hierarchical model") for long-chain branched polymers. Furthermore, by deliberately adding additional well-characterized linear and star-branched polymers into HA20B40, we mimic the effect of impurities in the sample to test the ability of the "hierarchical model" to account for the effect of similar such impurities, which are detected by TGIC. Our modeling predictions for HA20B40 and its blends with star and linear polymers show very good agreement with measured rheological data, indicating that the modeling validation is successful for the symmetric H-shaped polymers. We then test the "hierarchical model" further using literature data for symmetric H PBds, for which the TGIC and experimental rheology data were published. We find that as long as the polymer composition is accurately determined, the "hierarchical model" can calculate the rheological behavior accurately. The theory can therefore be used to help to identify the composition or impurities, which are almost always present at low levels at least in such topologically complex samples.

In this Chapter, the synthesis work was done by Jimmy May's group at University of Tennessee. The TGIC characterization was done by Taihyun Chang's group in Pohang University of Science and Technology, Korea. X.Chen acknowledges their contributions.

3.2 Introduction

Long chain branching is found in a large fraction of the polymers that are made and used commercially, particularly polyolefins, which is the highest-volume class of synthetic macromolecules manufactured worldwide. Previous studies indicate that it is often difficult or impossible to characterize low levels of long-chain branching from characterization methods other than rheology [Janzen and Colby (1999)]. Although linear viscoelastic properties are sensitive to polydispersity and long chain branching, rheological data alone do not directly reveal such information quantitatively. Such information could be obtained, in principle, however, by using molecular rheological theory to infer branching information from rheology. Fortunately, modern "tube theories" have greatly advanced our understanding of the relaxation dynamics and rheology of macromolecules with various branched architectures, such as star-shaped polymers with multiple arms of identical or different lengths [Chen and Larson (2008)]. However, understanding remains incomplete regarding the relaxation of complex branching structures in entangled polymer melts with multiple branch points, such as H- or comb-shaped polymers, especially for polymers with branches of differing lengths, such as asymmetric H polymers.

As the simplest species that contains two branching points, H-shaped polymers of polystyrene, polyisoprene or polybutadiene have been previously studied rheologically by various research groups, and the data were used to test the accuracy of appropriate tube models for these structures [Roovers and Toporowski, (1981); McLeish (1988); Hakiki et al. (1996); McLeish et al. (1999); Daniels et al. (2001a); Perny et al. (2001)]. However, the tube theory cannot be truly tested unless the polymer is completely pure, or unless the topology, molecular weight, weight fraction and polydispersity of each component in the sample are well determined. It is thus significant that recent temperature gradient interaction chromatography (TGIC) analysis of anionically synthesized H-shaped polybudiatene polymers has shown that such samples can contain substantial amounts of branched byproducts of both low and high molecular weight, whose presence is not always evident in more conventional size exclusion chromatography traces [Perny et al. (2001); Li et al. (2011)]. Taking into account the real polymer structural distributions in such samples is obviously essential to assess the true accuracy of the model predictions.

In this work, we describe the synthesis of a symmetric H polymer "HA20B40" and its characterization by TGIC. To be confident about the structure of each component in the final product, we also perform TGIC analysis of a precursor symmetric star polymer to help infer the possible structures in the final products. After validating our model on this cleanest sample, we analyze data on some previously studied symmetric H samples which were also well characterized by TGIC, but for which structures in the final products were inferred in part from assessment of the likely byproducts of the synthesis [Li et al. (2011)]. Here, we use the "hierarchical model" [Wang et al. (2010)] to help infer the most likely structures in these literature H samples. This paper is organized as follows: Section 3.3 describes the materials and experimental methods. In Section 3.4, we describe the "hierarchical model" and modeling details. In Section 3.5, we present and discuss our synthesis products, molecular characterization results, experimental rheological measurements as well as the "hierarchical model" calculations. We also describe modeling of other H-shaped PBds from the literature to further test our theory. In particular, we show that the "hierarchical model" not only yields quantitative predictions for our symmetric H and its blends with star or linear polymers, but also helps to identify the impurities in the sample. Conclusions and perspectives are drawn in Section 3.6.

3.3 Materials and experimental methods

3.3.1 Materials and blends preparation

Three 1,4-polybutadiene (PBd) polymers, namely a linear, a star (½H) and a symmetric H polymer, as well as blends of these, were investigated. The chemical composition of *cis* 1,4 and *trans* 1,4 was found to be 52% and 42% respectively. All these samples shows ~94% 1,4 and ~6% 1,2 vinyl configurations. The linear PBd was purchased from Polysciences Inc. Its weight-average molecular weight and molecular weight distribution are 22.6kg/mol and 1.05, respectively, provided by Polysciences Inc. As discussed below, this characterization was confirmed by comparison of its rheology with rheological predictions of the "hierarchical model", which has been shown to be accurate for linear polymers. The three-armed symmetric star or ½H, which is an intermediate in the synthesis of the symmetric H-PBd, has three identical arms of targeted molecular weight of 20 kg/mol. The targeted H-PBd sample is named based on the target

molecular weight of the arms and backbones. For example, "HA20B40" stands for a sample with four identical arms of a molecular weight of 20 kg/mol and a backbone of a molecular weight of 40 kg/mol.

Two kinds of blends, i.e., a blend of 50% weight fraction of HA20B40 with 50% weight fraction of the star (½H), and a blend of 50% weight fraction of HA20B40 with 50% weight fraction of the linear PBd, were designed. These two blends were prepared by dissolution of the polymers in toluene that was filtered with 0.2μm pore-size sterile filters, and then placed in a fume hood for about a week for initial evaporation of the solvent. The samples were then dried under vacuum at room temperature for another two weeks or more to ensure removal of the excess toluene. Two methods were used to determine the complete removal of the excess toluene: (1) no toluene smell after drying under vacuum; (2) the weight of the sample become constant over a period of three days. The blends after drying were stored in a refrigerator ready for rheological measurements.

3.3.2 Synthesis and purification[1]

Synthesis of symmetric H-shaped polybutadienes (H-PBd) has been described in detail in our previous contribution [Rahman et al. (2008)]. Briefy, the synthetic steps shown in Figure 3-1 involve (a) growing a living PBd chain using *s*-BuLi as initiator in benzene at room temperature, (b) titration of 4-(dichloromethylsilyl)diphenylethylene (DCMSDPE) with living PBdLi, (c) addition of *s*-BuLi to activate the double bond of diphenylethylene (DPE), (d) subsequent addition of butadiene to generate a living "1/2 H", which has two arms and half of the final cross-bar, and (e) finally coupling the two "1/2 H" molecules with dichlorodimethylsilane to produce an H-PBd, which has two arms attached to each end of the cross-bar. The raw final polymers were stabilized with butylated hydroxytoluene (BHT) and precipitated into a large excess of methanol. Fractionation was performed using toluene/methanol as the solvent/nonsolvent pair. Fractionation was repeated to obtain optimal results. The fractionated polymer was precipitated in an excess of methanol and vacuum-dried prior to characterization.

[1] The work of synthesis and purification on H-PBd was done by our collaborators Jimmy May's group at University of Tennessee. The manuscript of Section 3.3.2 and Figure 3-1 were prepared by Dr. M. Shahinur Rahman. X. Chen acknowledges their contributions.

3.3.3 SEC and TGIC characterizations[2]

A size exclusion chromatography (SEC) column connected to a Wyatt miniDAWN LS detector with 60 mW power at a wavelength of 658 nm, and a Shodex RI-101 RI detector with two PLgel mixed-C columns (300 × 7.5 mm, 5 μm) were used to characterize precursors and final H polymers. This characterization was performed at 40 °C with THF as the mobile phase at a flow rate of 0.8 mL/min; dn/dc was 0.128 mL/g.

The TGIC separations were carried out using a standard high-performance liquid chromatography(HPLC) system equipped with a C18 bonded silica column (Phenomenex, Kromasil, 300A ° pore, 150_4.6 mm, 5 μm particle size); the mobile phase was 1,4-dioxane at a flow rate of 0.5 mL/min, and dn/dc was 0.095 mL/g. The system was equipped on-line with a Wyatt miniDAWN LS detector and a Shodex RI-101 RI detector. The column temperature was programmed from 18~30°C to cover the range of molar mass of each sample.

3.3.4 Further TGIC analysis

The raw TGIC data provide us with the molecular weight of each component in the sample and based on the synthesis mechanism, we can infer the possible structures of each peak. However, in addition to information on molecular weight of each peak, the weight fractions and polydispersity indexes (PDI's) are needed as inputs for theoretical predictions of rheology. The TGIC data shown in Figure 3-5 allow us to estimate the concentration and PDI of the main products as well as byproducts in the ½H (star), and HA20B40 PBds. The method for obtaining this information is summarized in Figure 3-2. Refractive index signals, Δn, were first de-convoluted using peak integration and Gaussian fitting to calculate the weight fraction of each component and the variance of each peak, σ_{peak}. Since refractive index signals, Δn, and molecular weight, M, are linearly correlated, a correlation between M and t_R in the form of $M = a \times t_R + b$ can be set up, where a and b are constants, respectively, and t_R is the elution time of the peak. From

[2] The TGIC characterization was done by Taihyun Chang's group in Pohang University of Science and Technology, Korea. The SEC characterization was done by Jimmy May's group in University of Tennessee. The manuscript of Section 3.3.3 was prepared by Chang's and May's groups. X. Chen acknowledges their contributions.

equations (1) and (2), the PDI of each component, assuming a normal distribution, can be calculated:

$$\sigma_M^2 = \sigma_{peak}^2 \times a^2 \quad (1)$$

$$PDI = 1 + \frac{\sigma_M^2}{M} \quad (2)$$

where σ_M is the standard deviation of the molecular weight, σ_{peak} is the standard deviation of each refractive index peak in TGIC figures, and M is the molecular weight.

3.3.5 Rheological Experiments

The very viscous, "solid-like" samples, i.e. HA20B40 and the blend of HA20B40 with the ½H, were compression molded into circular disks which have the diameter of 25mm and the height of 1.2mm on a hot press. The less viscous "liquid-like" samples, i.e. ½H (star), linear and the blend of HA20B40 with linear, were loaded onto the bottom plate of the 25-mm parallel plate geometry directly. Then the bottom plate with the sample was placed into a vacuum oven at room temperature under vacuum to get rid of the air bubbles trapped in the "liquid-like" samples.

For each sample, linear viscoelastic measurements were performed on an ARES strain-controlled rheometer with a 25-mm parallel plate geometry and around 1 mm gap. Dynamic strain sweep measurements were firstly conducted to select the strains in the range of linear response. Dynamic frequency sweep tests with the selected strains were conducted at a constant temperature of 25°C with frequency sweeps from 0.0001 to 100 rad/s. In order to ensure sample stability, a nitrogen measurement atmosphere and added antioxidant were applied. In all cases, the terminal region was reached.

3.4 Theory and modeling

The model we wish to validate and use for inferring most likely component structures in the sample is the "hierarchical model" (v3.0) [Wang et al. (2010)]. This "hierarchical model" has been previously successfully validated on linear, symmetric star, "T" and "Y" shaped asymmetric star, linear-linear blends, linear-star blends as well as commercial metallocene polyethylene copolymers which are characterized by GPC [Chen and Larson (2008); Wang et al. (2010); Park and Larson (2005); Park et al. (2005); Chen et al. (2010a); Chen et al. (2010b)]. Here we will validate this "hierarchical model"

(v3.0) on a relatively "clean" H-shaped PBd (HA20B40), characterized by a more sensitive and accurate characterization tool (TGIC), and on its blends with linear and star polymers.

According to the concept of polymer hierarchical relaxation proposed by Larson [2001], for a symmetric H-shaped polymer, as shown in Figure 3-3, immediately after a small step strain, only the arms can relax inward from their tips. Later, after the four identical arms are fully relaxed, these arms are conceptually replaced by a frictional bead at the branch point at each end of the backbone. The unrelaxed molecule finally thus becomes conceptually a linear chain with two branch points at the two ends, illustrated in Figure 3-3 (b). The final relaxation then occurs by arm retractions and reptation of an effectively "linear" chain. The beads incorporate the friction added to the chain backbone by the side branches. A detailed description of this model is given elsewhere [Larson (2001); Wang et al. (2010)].

To predict the rheological behaviors of our samples, we use the default parameters of the "hierarchical model", that is α=4/3 and $p^2 = 1/12$, where α is dilution exponent and p^2 is coefficient of branch-point drag. Two of the material-dependent tube model parameters used here, namely the plateau modulus G_N^0 and the entanglement molecular weight M_e, were taken from previous reported values for 1,4-PBd [Wang et al. (2010)], that is, G_N^0 = 1.095MPa, and M_e = 1620g/mol. Another tube model parameter, the frictional equilibration time τ_e, is obtained by fitting the value to the experimental rheology data for star(½H) and linear PBds studied in this work, which gives a value of τ_e = 5E-7s. We then use these values of the three tube model parameters for modeling predictions on all the materials studied here, including HA20B40, literature H PBds synthesized in the Mays lab, as well as the star and linear PBds, without any adjustment. We note here that values of τ_e seem to be sensitive to synthesis details and the best-fit value varies from lab to lab, as we will discuss in a future publication. Our preliminary simulation results indicate that the so-called "thin-tube" option and "arm-frozen" options (see Wang et al. (2010)) of the "hierarchical model" (v3.0) yield very similar results for the same tube model parameters, because each component of the sample is nearly

monodisperse after fractionation and purification. Therefore, we use "arm-frozen" option for all our predictions.

3.5 Results and discussions

3.5.1 SEC and TGIC characterization results[3]

Figure 3-4 shows the SEC chromatogram for the symmetric HA20B40 and its precursors. SEC chromatograms recorded by a RI, UV and MALLS detector shows one dominant peak for the linear PBd arm, the star (½H) and the fractionated HA20B40. The absolute molecular weights determined from SEC-LS are summarized in Table 3-1 are in good agreement with the target molecular weights of HA20B40 and its precursors. The narrow PDI values ranging from 1.01~1.07 also suggest that these samples are nearly monodisperse. However, this does not necessarily mean that these samples are free from any side product. Specially, a small amount of byproduct with different branching degree cannot be detected by conventional SEC-LS. This is an expected behavior of SEC, which only separates the polymer chains based on their hydrodynamic volume [Lee at et. (1998); Synder and Kirkland (1979)].Thus more precise characterization using an advance technique such as TGIC is required to identify these materials and their architecture.

TGIC is an interaction chromatography technique that has much superior resolution to SEC. Additionally TGIC separation of polymer molecules is driven by an enthalpic interaction of the solute molecules with the stationary phase and this interaction is varied by changing the column temperature during the elution. Thus TGIC is less sensitive to the molecular architecture and independent of the polymer volume. TGIC can resolve biproduct species of the linking reaction, such as coupled arms, stars and H-molecules [Perny et al. (2001)]. Thus we used TGIC for a detailed characterization of our H-molecules and its precursors. In Figure 3-5 (a), a TGIC chromatogram of a linear Pbd arm is displayed. When carried out under isothermal conditions at 18°C, TGIC shows one dominant peak, just as does SEC (Figure 3-4 (a)). However, for a programmed temperature history ranging over 18-21.5°C in 35 minutes, a star (½H) sample made by multiple synthetic steps shows three clearly resolved peaks at t_R = 10 min (coupled arms),

[3] The manuscript of Section 3.5.1 and Figures 3-4 and 3-5 were prepared by Mays' and Chang's groups. X.Chen acknowledges their contributions.

17 min (three arms, desired star) and 25 min (four arms stars). The molecular characteristics of the three different peaks summarized in Table 3-1 are in good agreement with our expected values.

Similarly TGIC of HA20B40 shows four distinct peaks in Figure 3-5 (c). The molecular weight of Peaks 1-4, summarized in Table 3-2, are in good agreement with the total molecular weight of HA20B40 and its precursors. The possible structures corresponding to the TGIC peaks are discussed in next section.

3.5.2 Inference of possible by-product structures based on TGIC and synthesis mechanism

Based on the reaction mechanism and step by step analysis with SEC-LS and TGIC we can now clearly identify the possible structure in our samples. For example, Figure 3-5 (b) shows three peaks for star (½H) and four peaks for purified HA20B40 (Figure 3-5 (c)). The molecular weight of Peak 2 in Figure 3-5 (b) is 55K which is three times higher than the molecular weight of a linear arm (Table 3-1). This means Peak 2 is our desired 3-arm star (½H). Similarly the Peak 1 molecular weight of 38.5k and Peak 3 molecular weight of 74K correspond to two and four arms star respectively. The likely structures corresponding to the three TGIC peaks of Figure 3-5 (b) are shown in Figure 3-6.

HA20B40 shows four TGIC peaks in Figure 3-5 (c). The molecular weights of Peaks 1-4 are summarized in Table 3-1. Based on the reaction mechanism [Li et al. (2011)] and the known molecular weight of HA20B40's precursor, we can confidently identify all these four peaks and their structures, which are given in Figure 3-6.

3.5.3 Further analysis of TGIC data

Based on the method described in Section 3.3.4, the molecular characteristics of each component in the semi-H (star) and HA20B40 samples are summarized in Tables 3-2 and 3-3, and the possible structures corresponding to each peak are shown previously in Figure 3-6. The PDI of each component (or peak) for the star (½H) and HA20B40 are nearly unity; i.e., each component is nearly monodisperse. For the star PBd, the main product takes up about 84% of the total weight, and is nearly symmetric, with two arms having molecular weights of 19k, and the third arm, which is half of the backbone in the H polymer, has nearly the same molecular weight. As described in Section 3.3.2, we use

this unfractionated star to make the H, and we also reserved some for rheological studies. For the HA20B40, we purified the sample by conventional fractionation using toluene/methanol as the solvent/nonsolvent pair and used the purified sample for our rheology study. However, even after purification, the target product of HA20B40 has a weight fraction of only about 50%, which is, however, higher than the content (36.4%) of targeted H polymer in the sample synthesized by Perny et al. [2001].

3.5.4 Experimental and theoretical linear viscoelastic properties of HA20B40 and its blends with linear or star PBds

By applying the rheological measurement method described in Section 3.3.5, the experimental linear viscoelastic properties of the HA20B40, star (½H), and linear polymers, and their blends at 25 ˚C are shown in Figure 3-7 (H, star, and a 50/50 blend of the two) and Figure 3-8 (H, linear, and a 50/50 blend of the two) (the symbols are the experimental data). As expected, in Figure 3-7, the blend of star and H relaxes faster than the unblended HA20B40 and slower than the unblended star (½H) PBd. Similar behaviors are shown in Figure 3-8. In all the cases here, the terminal region has been reached during the testing region.

The molecular weight, weight fraction, polydispersity and possible structure of each component in the synthesized materials have been determined as described and tabulated above. Because the semi-H (or star) precursor and the final H polymer were characterized by TGIC, we can be confident of the assigned structures of each component in HA20B40. We believe that this is the first time that both the precursor and the final product were characterized by both TGIC and rheological studies. This increases our confidence in the characterization of product and the rheological modeling, the latter of which must match rheological data for both the precursor ½H (star) polymer and the final product, HA20B40.

Our accurate determination of the molecular characteristics of each component, i.e. molecular weight, weight fraction, polydispersity and likely structure, make it possible for us to do the modeling work accurately. We use the “hierarchical model” to calculate the rheological behaviors of unblended and blended melts. As shown in Figure 3-7 (H, star, and their 50/50 blends) and Figure 3-8 (H, linear, and their 50/50 blend), the rheology of these very well-characterized samples (HA20B40, ½H and the linear PBds)

are quite well predicted by the theory. Furthermore, when we deliberately add additional well-characterized star or linear polymers into HA20B40 to mimic the effect of impurities, we can predict the effect of this on the rheology of the 50/50 star-H blend as shown in Figure 3-7 and the 50/50 linear-H blend as shown in Figure 3-8.

To determine the effects of impurities on the rheology of the star (½H) and HA20B40, we predicted their rheological behaviors theoretically with and without the impurities. As shown in Figure 3-9, the ½H (star), which contains about 84 wt% targeted star molecule, is pure enough that its rheology is predicted to be almost identical to that of a 100% pure sample. For the HA20B40, however, the impurities accelerate the terminal relaxation by about a factor of two, which affects the rheology in the low-frequency region below 1 rad/s.

3.5.5 Identification of possible structures in other H-shaped polymers, using the "hierarchical model"

Recently, SEC data, TGIC data [Li et al. (2011)] and experimental linear viscoelastic data [Li (2010)] were published for four symmetric H-shaped PBds, namely HA12B40, HA12B100, HA30B40 and HA40B40, synthesized by Mays' group [Rahman et al. (2008)], using a method similar to that used to synthesize HA20B40, the H polymer described in this paper. As mentioned in this publication, SEC techniques were unable to resolve the structural compositions of the long chain branched polymers containing various byproducts due to its inherent low resolution [Li et al. (2011)]. We will therefore use the TGIC results for these samples to further test our rheological theory, using the same tube model parameters as used for HA20B40.

Table 3-4 (Table 3-4 in the previous publication [Li et al. (2011)]) summarizes the molecular characteristics of these four symmetric H-shaped PBds. Figure 3-10 shows the TGIC data for these four H-shaped PBds, which corresponds to Figure 5 in the previous publication [Li et al. (2011)]. The peaks labeled in Figure 3-10, and the structures inferred for each peak, based on a knowledge of the reaction chemistry, are listed in Table 3-4. As seen in Figure 3-10, HA12B100 and HA40B40 are the cleanest samples with the fewest byproducts. We therefore start with these two symmetric H PBds for our further model validation and possible by-product structure determination.

The possible structures corresponding to "Peak 1" in HA12B100 and in HA40B40 were each previously identified as either linear-shaped or three-armed star-shaped; see Table 3-4 and Figure 3-11. As shown in Figure 3-11, the possible linear-shaped PBd is inferred to be a combination of two arms and one half backbone based on the synthesis mechanism and molecular weight information characterized from TGIC, while the possible star-shaped PBd is inferred to have two identical arms with the molecular weight of the arm of the H PBd, and one arm with of molecular weight of the half backbone. The molecular weights of the possible linear-shaped PBd and star-shaped PBd for HA12B100 and H12B40 are listed in Table 3-5. Since these two structures have identical molecular weights, both of which are close to that of Peak 1, and both of which are reasonable bi-products of the reaction, either one might account for the presence of Peak 1 in the TGIC trace.

Here, we use our "hierarchical model" with the model parameters described in Section 3.4 to test these two possibilities. In each case, we retain the weight fractions polydispersities, and identities of all other components of HA12B100 and HA40B40 the same. We take the molecular weight corresponding to either the linear or star molecule from the molecular weight assigned from the TGIC analysis, that is, M = 103 kg/mol for HA12B100 and M=113 kg/mol for HA40B40. As shown in Figure 3-12, the modeling prediction for HA12B100 with Peak 1 corresponding to a star-shaped molecule matches the experimental rheology data well, while the choice of a linear chain for Peak 1 leads to prediction of a peak in G'' at a frequency corresponding the inverse relaxation time of the linear chain. Since this peak is not observed experimentally, the choice of a star structure for Peak 1 is more likely to be the correct assignment. Thus, the prediction of the theory is sensitive to the component structure, even when the possible structures have the same molecular weight. Therefore, in addition to TGIC characterization, theoretical modeling may be useful to determine the correct identification of impurities in the melt.

Similarly, by using the "hierarchical model" with the same model parameters, we test the two suggested possibilities for the components of HA40B40 as shown in Figure 3-13. Due to the small weight fraction for Peak 1 in HA40B40, these two structure possibilities do not generate a significant difference in the predicted linear viscoelasticity.

So far, we have validated the "hierarchical model" using the well-characterized H sample HA20B40, for which we obtained TGIC data not only on the final product but also on the intermediate to increase our confidence about the identity of each component in the final product. We has also used this model to predict the rheological behaviors of previous published relatively "clean" H-shaped PBds, namely HA12B100 and HA40B40, and to help identify the most likely structure corresponding to one of the peaks in each of these materials. These successes in modeling symmetric H polymers give us confidence to proceed to analyze the more complex melts HA12B40 and HA30B40, which have more components (peaks) in their TGIC spectra.

As summarized in Table 3-4, HA12B40 was reported to have 6 components in previous publication [Li et al. (2011)]. However, as can be seen in Figure 3-10, there is another (seventh) broad peak corresponding to efflux times ranging from 35min to 40min. By using the further analysis method on TGIC results described in Section 3.3.4, a correlation between M and t_R of HA12B40 can be established as shown in Table 3-6 and the molecular weight of Peak 7 can be estimated by using this correlation to be 96.2kg/mol. Once we add this seventh component, the weight fraction of the other components must be adjusted so that the total equals 100%. Based on the synthesis mechanism, the suggested possible structures of Peak 7 are shown in Figure 3-14 (see ref. Li et al. (2011) for details about how to determine the possible structures). The rheological predictions corresponding to these are shown in Figure 3-15. Please note here, as previously inferred [Li et al. 2011], that Peak 3 of HA12B40 might be either a linear or a star-shaped PBd. Our preliminary results indicate that either a linear or star for Peak 3 generates similar predicted rheology, and therefore we assume Peak 3 is a linear-shaped PBd in the following work for our identification of Peak 7. As we can see in Figure 3-15, any of the two choices for the high-molecular weight component greatly improves the prediction over that obtained when this component is neglected. From the synthetic route, the mostly likely structure for Peak 7 is the star-shaped PBd as shown in Figure 3-14 (1).

The fourth polymer in Figure 3-10, HA30B40, contains large quantities of impurities, as well as multiple unidentified high molecular weight peaks. The predictions of the "hierarchical model", using only the identified peaks, shows terminal relaxation at a frequency more than a decade larger than predicted (data not shown). Since

identification of the multiple high molecular weight peaks would rely largely on guesswork, we did not attempt to find a set of possible structures that might bring the predicted rheological response closer to what was observed.

3.6 Conclusions and perspective

The advent of temperature gradient interaction chromatography (TGIC) as a refined characterization method has revealed that multi-step synthesis of architecturally complex polymers, such as "H" polymers, typically leads to multiple side products that often go undetected by conventional size-exclusion chromatograms as mentioned in previous publications [Perny et al. (2001); Li et al. (2011)] and reported here. Thus, it is prudent to assume that such materials (H and comb polymers) reported on in the past, prior to the application of TGIC characterization, may also have contained such impurities, which went undetected. This might cast some doubt on previous studies, which used rheological data for such polymers to test rheological theories for long-chain-branched polymers. Indeed, the agreement of rheological predictions with experimental data for such materials has been "hit or miss," with good agreement being obtained in some cases, but with agreement being poor in other seemingly similar cases, unless parameters were arbitrarily adjusted [McLeish et al. (1999); Daniels et al. (2001a); Daniels et al. (2001b); Inkson et al. (2006)] Obviously, the testing and improvement of tube models is hindered by the uncertainty in composition of such materials, since failure of the theory to predict correctly the rheology could be attributed either to failure of the rheological model or to some undetected impurity in the material.

To address this serious problem, we here have brought to bear a combination of methodologies. These include: 1) TGIC analysis of both the product H material and its synthetic precursor star polymer. 2) Rheological characterization and modeling of both the product material and its precursor. And 3) rheological characterization and modeling of blends of the H material with star and linear polymers, to demonstrate the ability of the rheological model to account for the rheological effects of substantial quantities of impurities. In this way, we believe that we are able to develop a convincing demonstration that we have not only identified the impurities, but also can account for their effect on rheological properties.

In essence, this approach abandons the traditional approach to polymer rheological modeling, in which pristine, "monostructural" materials are targeted for synthesis and rheological measurement, in order to test rheological models in the simplified limit of ideal specimens. It has already been recognized for some time now that polymers with long-chain branching are so sensitive to polydispersity that even when GPC traces show nominal M_w/M_n values less than 1.05, or even 1.01, the samples must be treated as "polydisperse" samples for purposes of rheological modeling [McLeish et al. (1999)].

We are here taking the next logical step by assuming that these samples are not only polydisperse in molecular weight, but are also structurally polydisperse. Thus, we claim that it may not be realistic to hope to carry out clean enough chemistry, or thorough enough fractionation, to drive this structural heterogeneity down to levels low enough to make it negligible. It may therefore be better, instead, to seek to measure the compositional heterogeneity accurately and account for it in rheological models. This step, though drastic, can actually be viewed optimistically as simply propelling theoretical work towards the ultimate goal of accounting for the compositional heterogeneity of commercially synthesized polymers. We are simply recognizing that even anionically synthesized polymers of complex architecture are almost invariably mixtures of different molecular weights and different structures and therefore seek to account for the effects of the heterogeneous components on the rheology.

Following this paradigm, here we have combined knowledge of the synthesis mechanism, TGIC data, experimental rheology measurements, and advanced tube model predictions, to identify the composition of anionically synthesized symmetric H shaped PBds, and to determine the effect of impurities on their rheology.

Specifically, we here described the synthesis, purification, TGIC and rheological characterization of a new, relatively "clean" symmetric H material, HA20B40, containing only four TGIC Peaks in its chromatogram, and with 50% of the mass of the material belonging to the intended H polymer structure. We also used TGIC to analyze the composition of the synthetic precursor to this H polymer, which was composed predominantly (i.e., 84%) of the intended symmetric star, with only two side peaks, both of whose structure could be readily identified from knowledge of the reaction chemistry.

From this information, and knowledge of the reaction pathways, the composition of the final H product could be determined with high confidence. Feeding this composition into a tube model, the "hierarchical model" that accounts for the effects of multiple components on rheological predictions, we successfully predicted the rheology of both the symmetric star precursor material, and of the final melt, using pre-assigned values of the rheological parameters. We also successfully predicted the rheology of a 50/50 blend of the symmetric H melt and the precursor nearly symmetric star, as well as of a 50/50 blend of the symmetric H with a well-characterized linear polymer. All predictions agreed well with the data, confirming that the model is able to predict the rheology not only of symmetric H polymers, but also of blends of the symmetric H polymer with star and linear materials, including star and linear contaminants that appear as reaction byproducts. We also showed, using rheological modeling, that the small level (16%) impurity in the star did not significantly affect the rheology, so that this star was "pure enough" for rheological work. However, the larger impurity level (50%) in the H shifted the relaxation in the terminal region by a factor of two, according to the rheological model.

As a second step in this new direction for branched polymer characterization and rheological modeling, we re-examined four symmetric H polymers synthesized in the same lab, but for which characterization of the intermediate had not been performed, and some which contained even more impurities, or higher concentrations of them. In two cases (HA12B100 and HA40B40), only one of peaks was uncertain and could be identified as either a linear or a star molecule. By comparing rheological predictions assuming either a linear or a star molecule, we identified the star structure as the most likely impurity in HA12B100. For HA40B40, on the other hand, we found that rheological testing was not sensitive to the star or linear identity of the impurity. An additional sample, HA12B40, showed an unidentified high molecular weight peak, the neglect of which led to modestly inaccurate rheological predictions. Including any of three reasonably likely structures for this peak resulted in predictions in good agreement with the experimental rheology. For the fourth sample, HA30B40, there were multiple unidentified high molecular weight peaks, and, neglecting them, we obtained wildly

inaccurate rheological predictions. In the case of HA30B40, the uncertainties in identity of these additional peaks precluded successful rheological modeling.

The approach we have initiated here suggests that in the future, complex branched polymer synthesis, molecular weight and structural characterization, rheological measurement, and rheological modeling, might no longer be carried out separately, but rather in concert. Thus, the "characterization" will no longer considered complete until the rheological data have been compared to predictions of a rheological model. This approach is risky, since flaws in the rheological model could be covered over by miss-identifying one or two peaks in the TGIC spectrum. We recommend that this risk be minimized by taking two additional steps. The first is to characterize not only the final product, but also one or more complex synthetic intermediates, by both TGIC and rheology, to help more reliably identify impurities that show up in the final product and to provide more thorough validation of the rheological model. The second is to blend the final product with well characterized linear and star molecules that are similar in molecular weight to those of likely impurities. Only if the rheological model can accurately predict the effect of these on the rheology of the melt can the model be considered reliable enough to identify impurities in the product and account accurately for their effect on rheology.

We note that even these steps are probably not sufficient to identify the peaks present in materials as complex as HA30B40 or to account for their influence on rheology. However, in the future, it may be possible to fractionate such complex mixtures by preparatory TGIC in quantities large enough to perform rheological characterization on fractions corresponding to each peak. This may allow the high molecular weight peaks to be identified. If they could be identified, then tube models such as the "hierarchical model" could be tested even for branched melts with complex side products, such as those likely present in HA30B40. This would further advance a new methodology in which combining rheological testing and modeling with TGIC and other methods, becomes an important means of characterizing the branching structures present in polyolefins.

Table 3-1. SEC and TGIC characterization of final HA20B40 and its precursors, i.e. the linear (the arm of H), and the star (the semi-H).

	M_{w_arm} [1]	M_{w_total} [1]	PDI [1]	M_{peaks} [2] (kg/mol)			
	kg/mol	kg/mol		Peak 1	Peak 2	Peak 3	Peak 4
Linear (arm of H)	19	——	1.01	19	——	——	——
Star (½H)	19	58	1.03	38.5	54.8	73.6	
HA20B40	19	111	1.07	71	95	114	129

(1) Characterized by SEC

(2) Characterized by TGIC

Table 3-2. Further TGIC data analysis of the star (½H) PBd

Peak	Peak Type	Weight Fraction %	σ_{peak}	M g/mol	$a^{(1)}$	σ_M $\times 10^{-7}$	PDI
1	Gaussian	5.27	2.15	38500	2262.4	1.09	1.01
2	Gaussian	83.6	5.43	54800	2262.4	2.78	1.01
3	Gaussian	11.12	21.5	73600	2262.4	11.0	1.02

(1) a is the pre-factor in the correlation $M = 2262.4 \times t_R + 17664$ with $R^2 = 0.9924$

Table 3-3. Further TGIC data analysis of HA20B40 PBd

Peak	Peak Type	Weight Fraction	σ_{peak}	M	$a^{(1)}$	σ_M	PDI
		%		g/mol		$\times 10^{-7}$	
1	Gaussian	7.83	2.1	71000	9653.5	19.5	1.03
2	Gaussian	16.83	1.5	95000	9653.5	14.5	1.01
3	Gaussian	50.21	2.2	114000	9653.5	21.0	1.01
4	Gaussian	25.12	4.0	129000	9653.5	37.9	1.02

(1) a is the pre-factor in the correlation $M = 9653.5 \times t_R - 70900$ with $R^2 = 0.9973$

Table 3-4. Estimated Structures and Compositions of HA20B40, HA12B100, HA30B40 and HA40B40 (Table 4 in Ref. Li et al. (2011))

sample	peak	M kg/mol	PDI	wt%	inferred structure
HA20B40	1	22	1.01	3	linear
	2	29	1	6	linear
	3	41	1.01	15	linear or 3-arm star
	4	55	1	21	4-arm star
	5	69	1.01	25	3-arm star
	6	79	1.01	30	H
HA12B100	1	103	1.02	33	linear or 3-arm star
	2	168	1.01	15	3-arm star
	3	187	1.02	52	H
HA30B40	1	83	1.01	18	linear or 3-arm star
	2	108	1.01	21	4-arm star
	3	138	1	27	3-arm star
	4	167	1	34	H
HA40B40	1	113	1.01	6	linear or 3-arm star
	2	129	1.01	17	3-arm star
	3	205	1	77	H

Table 3-5. Comparisons of the molecular weight of two possible structures with the actual molecular weight of Peak 1 for HA12B100 and HA40B40

	M_{arm} kg/mol	$M_{backbone}$ kg/mol	M_{linear}[(1)] kg/mol	M_{star}[(2)] kg/mol	M_{peak1}[(3)]
HA12B100	15.3	125.8	93.5	93.5	103
HA40B40	41.6	38.6	102.5	102.5	113

(1) Calculated using $M_{linear} = 2M_{arm} + \frac{1}{2}M_{backbone}$

(2) Calculated using $M_{star} = 2M_{arm} + \frac{1}{2}M_{backbone}$

(3) The molecular weight of Peak 1 from TGIC trace

Table 3-6. Characterization of HA12B40 PBd

Peak	Peak Type	Weight Fraction %	σ_{peak}	M g/mol	a[1]	σ_M $\times 10^{-7}$	PDI
1	Gaussian	1.53	1.23	22000	5147	2.94	1.06
2	Gaussian	3.39	3.01	29000	5147	4.59	1.05
3	Gaussian	10.79	2.84	43000	5147	4.46	1.02
4	Gaussian	18.36	1.76	55000	5147	3.52	1.01
5	Gaussian	24.90	1.49	69000	5147	3.23	1.01
6	Gaussian	34.23	1.45	79000	5147	3.19	1.01
7	Gaussian	6.80	7.73	96200[2]	5147	7.37	1.01

(1) a is the pre-factor in the correlation $M = 5147 \times t_R - 12569$ with $R^2 = 0.9897$

(2) M of Peak 7 was calculated based on the correlation between M and t_R

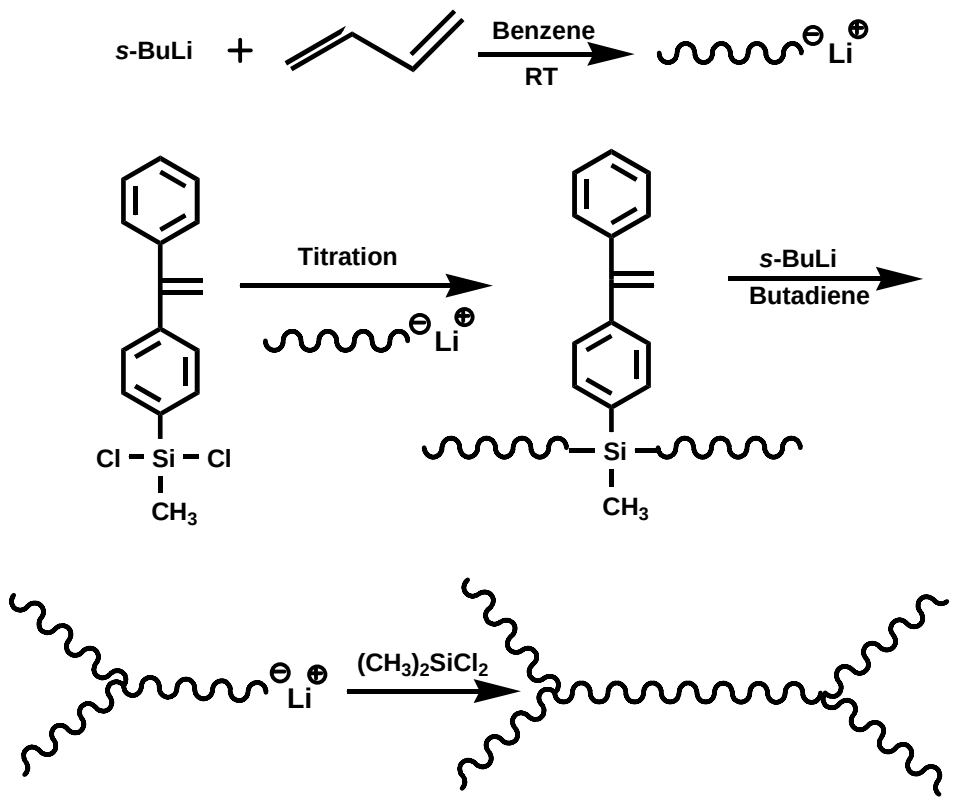

Figure 3-1. Synthetic steps of H-shaped polybutadienes

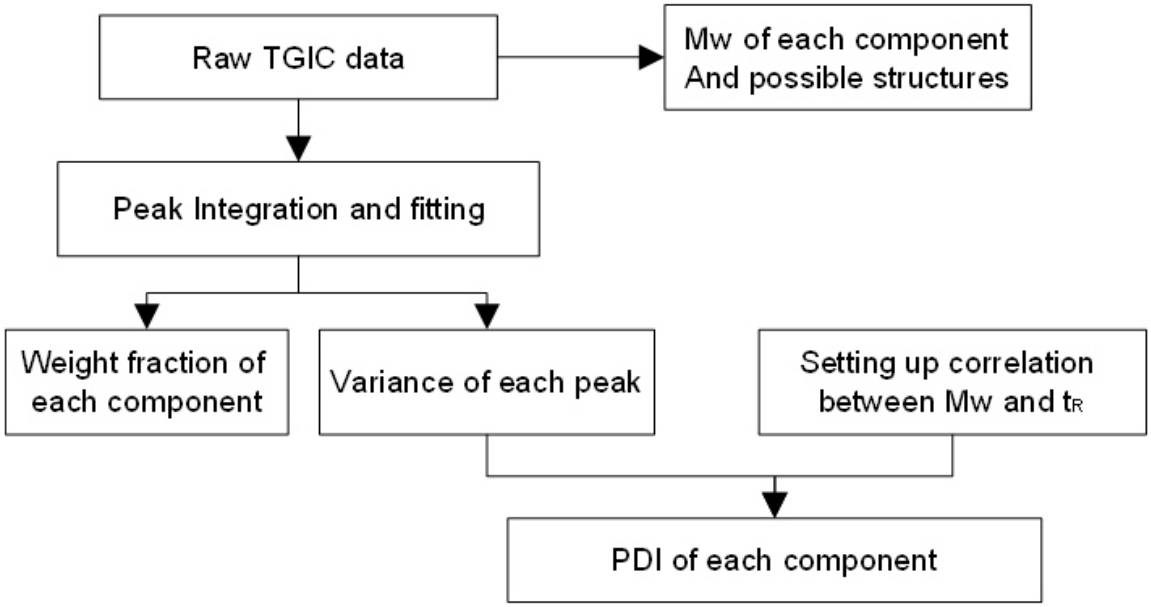

Figure 3-2. Method to characterize sample for model predictions.

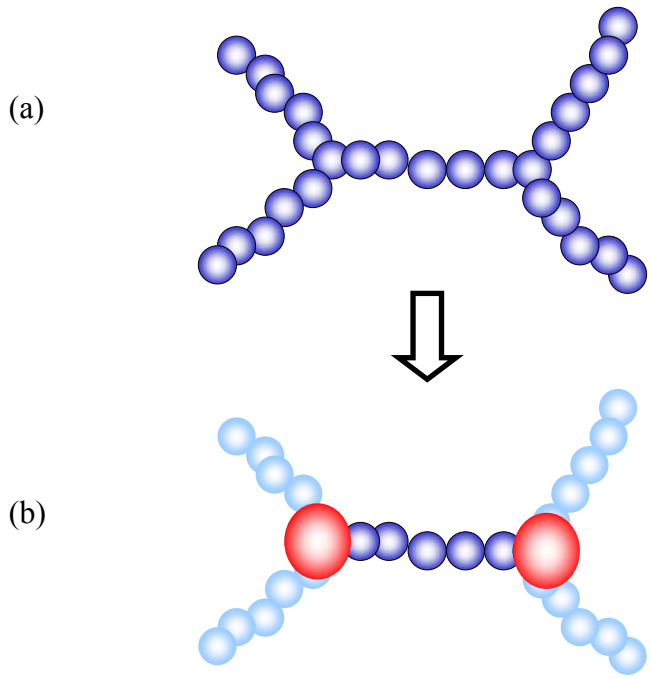

Figure 3-3. Conceptualization of algorithm for computing hierarchical relaxation of a symmetric H-shaped polymer

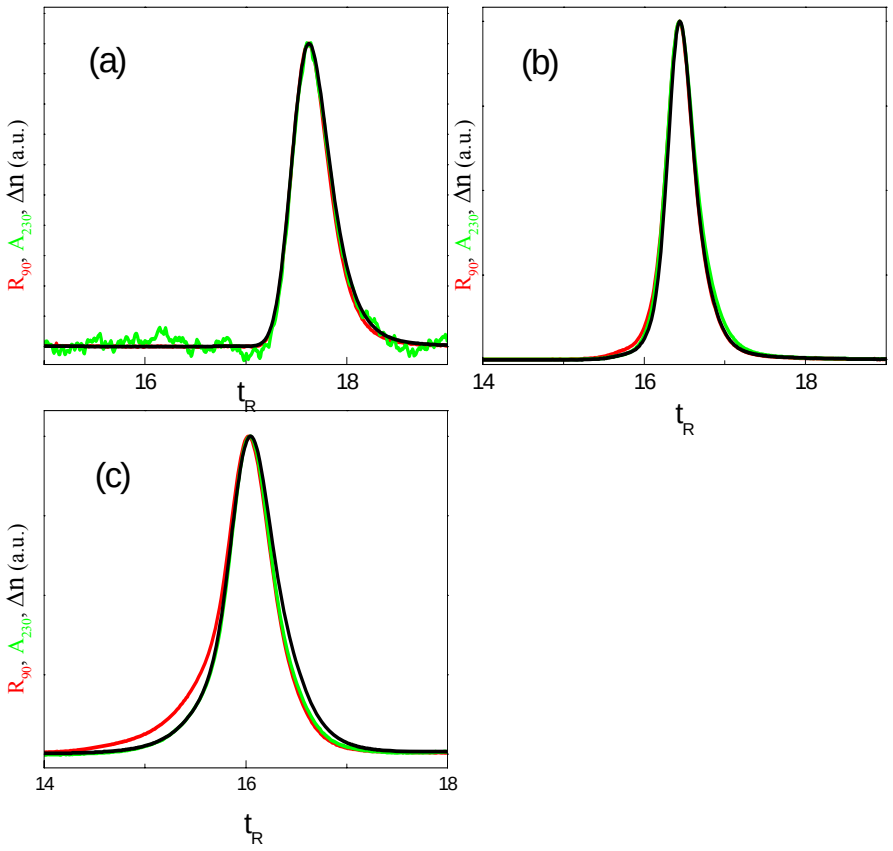

Figure 3-4. SEC (RI-Δn UV-A230 and LS at 90⁰-R90) elution profiles of precursors and H-shaped PBd: (a) linear Pbd arm, (b) star PBd (½ H) and fractionated H-PBd.

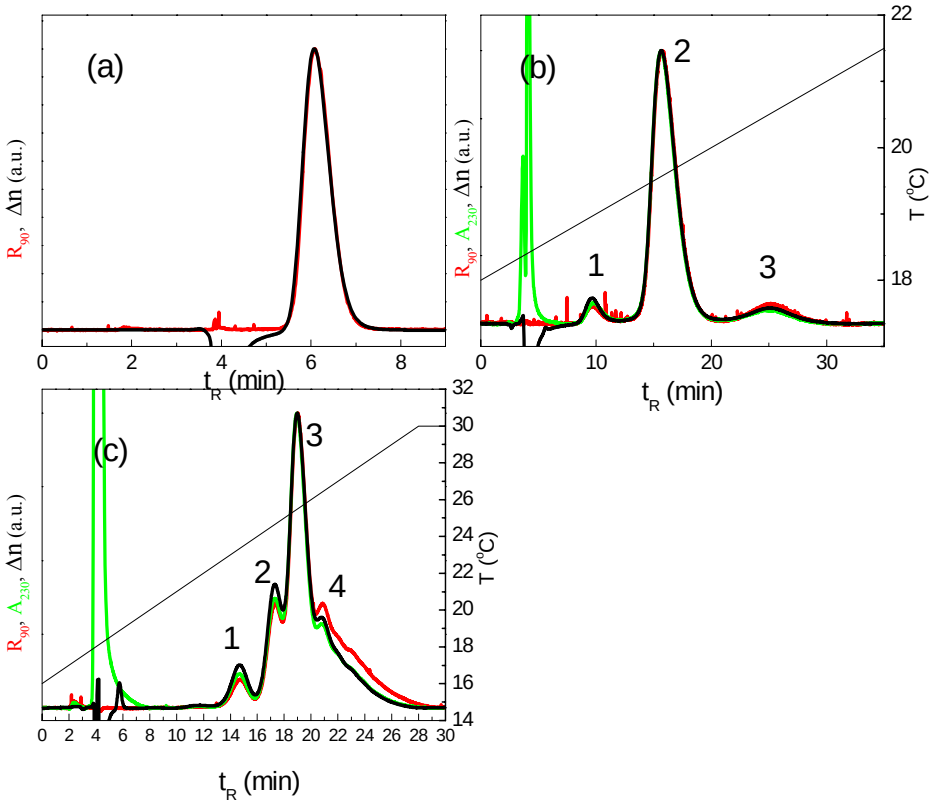

Figure 3-5. TGIC of (a) linear PBd arm (18 ˚C isothermal), (b) star PBd (½ H) (and (c) fractionated H-PBd (HA20B40).

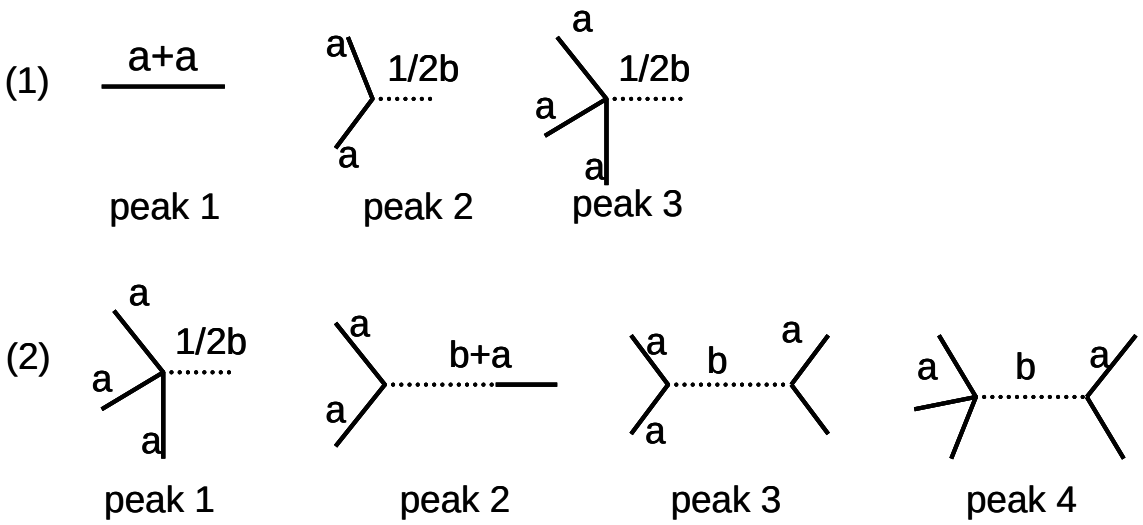

Figure 3-6. Possible structures of semi-H (Star) and HA20B40.

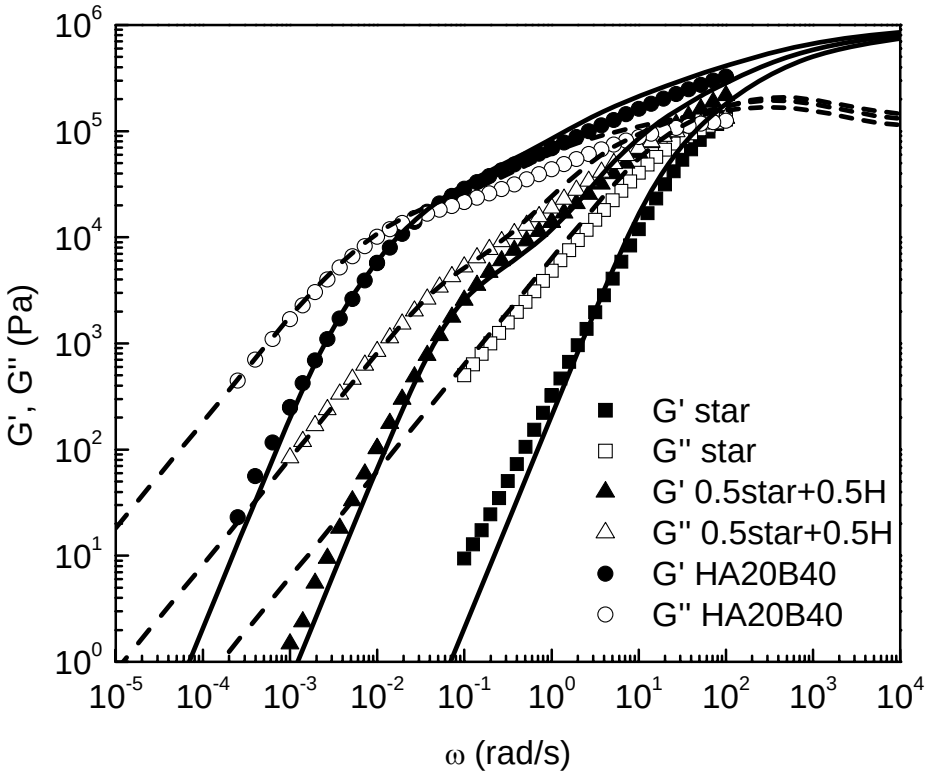

Figure 3-7. Experimental storage modulus G’ and loss modulu G’’ data, and “hierarchical model” calculations for HA20B40, star, and a 50/50 (by weight) blend of the two. Solid symbols (solid lines) and open symbols (dashed lines) are experimental data (theoretical predictions) for G’ and G’’,respectively

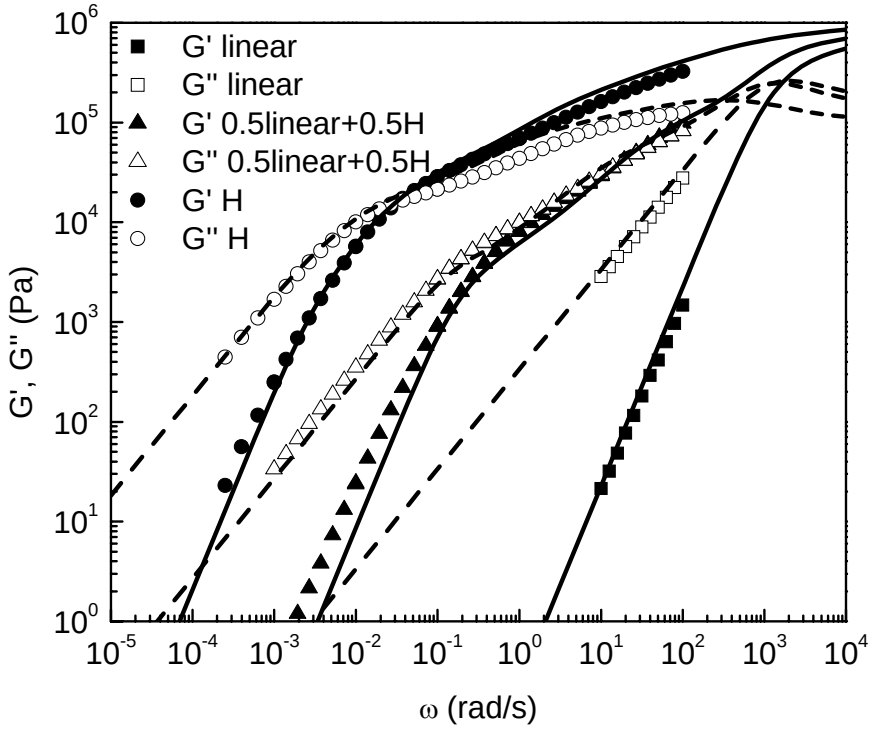

Figure 3-8. Experimental storage modulus G' and loss modulus G'' data, and "hierarchical model" calculations for HA20B40, linear PBds and their 50/50 blend. Solid symbols (solid lines) and open symbols (dashed lines) are experimental data (theoretical predictions) for G' and G''.

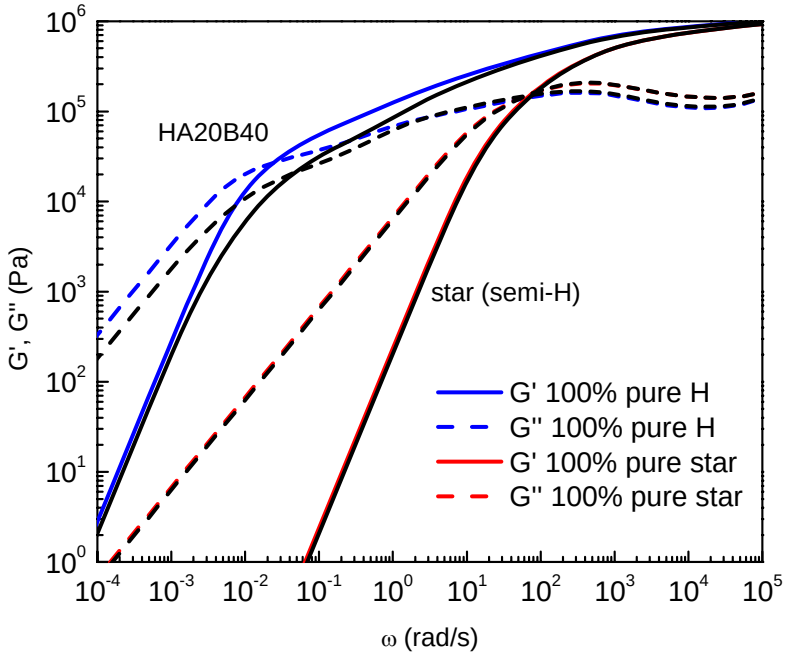

Figure 3-9. Determination of the effect of impurities on the rheology of the synthesized semi-H and HA20B40 materials by comparing the predictions of 100% pure materials with the predictions for the actual materials containing the measured concentrations of impurities. The blue solid line (dashed line) is the prediction of G' (G'') for 100% pure HA20B40; the red solid line (dashed line) is the prediction of G' (G'') for 100% pure star. The black solid lines (dashed line) are the predictions of G' (G'') for the real materials

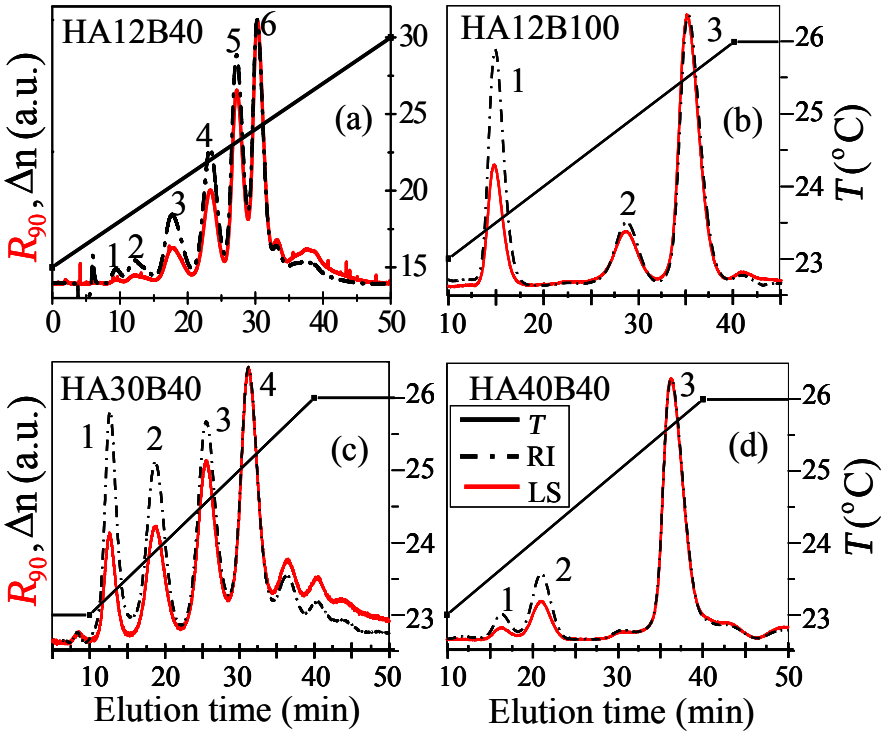

Figure 3-10[4]. TGIC chromatograms of HA12B40, HA12B100, HA30B40 and HA40B40. (Figure 5 in Ref. Li et al. (2011)).In this figure, "RI" means "refractive index", corresponding to the refractive index signal, Δn, detected by a Shodex RI-101 RI detector. "LS" means "light scattering", corresponding to the light scattering signal, R90 , detected by the Wyatt miniDAWN LS detector. The refractive index signal, Δn, is used here in our study to estimate mass fraction corresponding to each peak.

[4] Figure 3-10 is provided by Prof. Taihyun Chang of Pohang University of Science and Technology. X. Chen acknowledges his contribution.

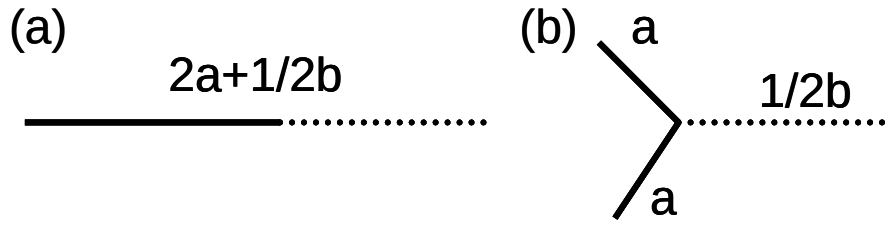

Figure 3-11. Inferred possible structures corresponding to Peak 1 in Figure 3-8 for HA12B100 and HA40B40. (a) The inferred linear shaped PBd with molecular weight equal to the sum of that of the two arms and the half backbone of the H. (b) The inferred star-shaped PBd which has two identical arms each with molecular weight equal to that of the arm of the H, and one arm with molecular weight equal to that of the half backbone of the H.

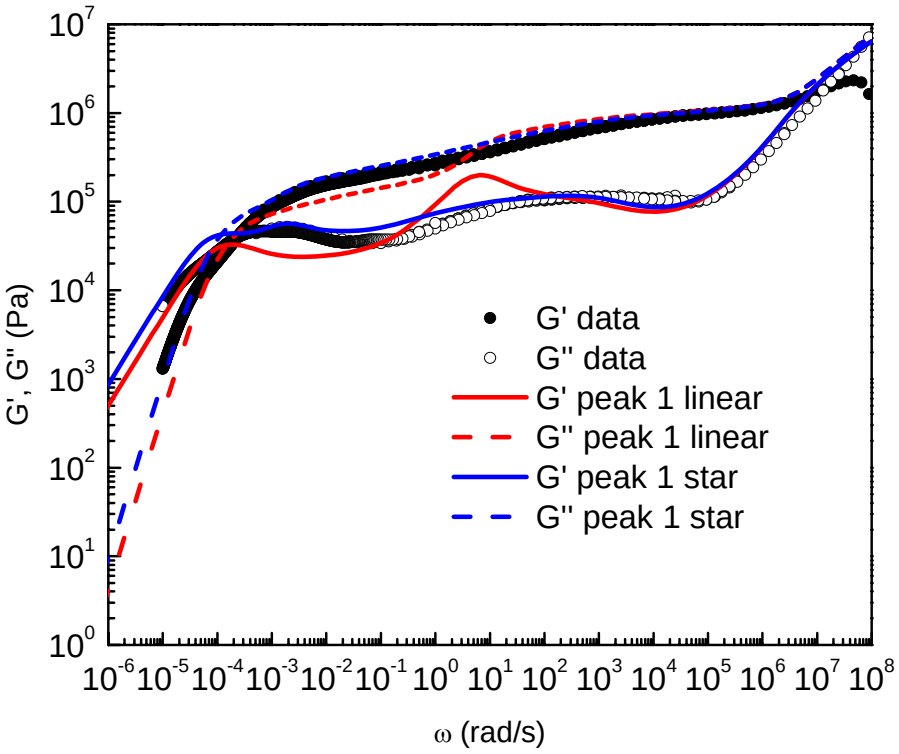

Figure 3-12. Effect of identity of Peak 1 in HA12B100 on rheological predictions from the "hierarchical model" compared with experimental rheology data. Solid symbols (open symbols) are experimental G' (G'') data. The red solid line (dashed line) is the theoretical calculation of G' (G'') assuming Peak 1 is a linear-shaped PBd, while the blue solid line (dashed line) assumes that Peak 1 is star-shaped PBd for G' (G'').

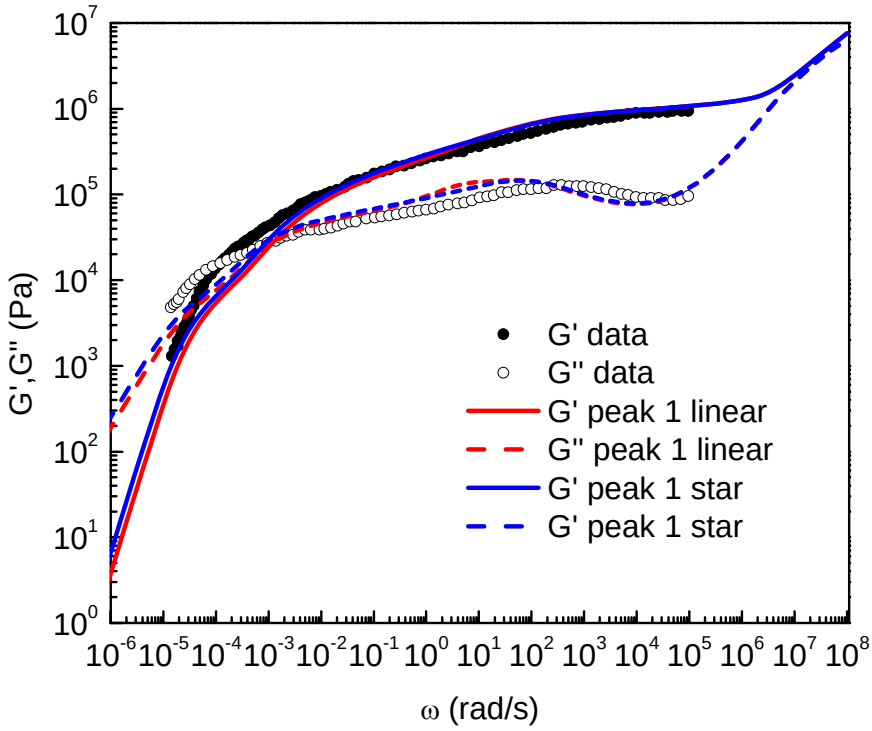

Figure 3-13. The same as Figure 3-12, except for HA40B40. As in Figure 3-13, the red solid line (dashed line) is the theoretical calculation of G' (G'') assuming Peak 1 corresponds to a linear molecule, while the blue solid line (dashed line) assumes it is a star.

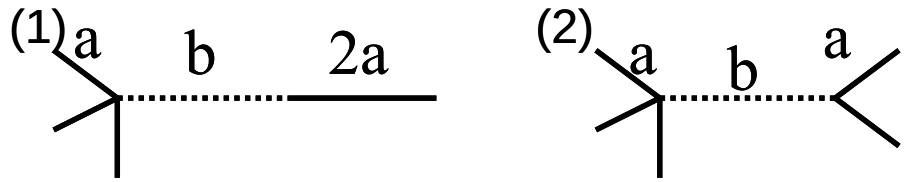

Figure 3-14. Estimated possible structures of Peak 7 in HA12B40 (1) the inferred 4-armed asymmetric star-shaped PBd which has three identical arms each with molecular weight equal to that of the arm of the H, and one arm with molecular weight equal to the sum of the backbone and two arms of the H. (2) the pom-pom shaped PBd which has three identical arms each with molecular weight equal to that of the arm of the H attached to one end of the backbone, and another two identical arms attached to the other end of the backbone

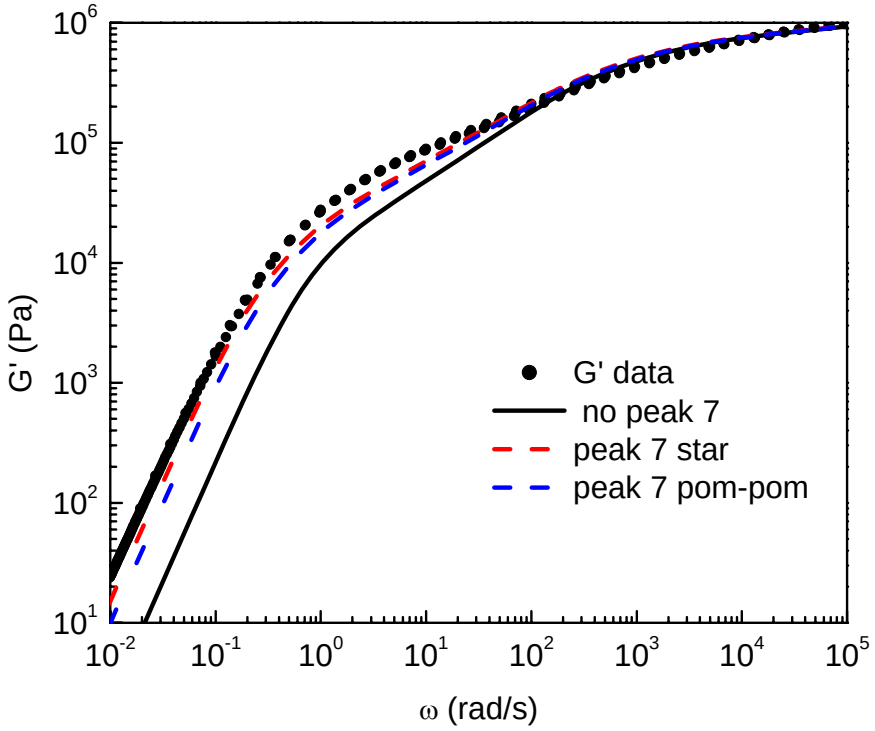

Figure 3-15. Comparisons of "hierarchical model" predictions of G' assuming different possible structures of Peak 7 in HA12B40. The solid line is the prediction without Peak 7, the red dashed line is the prediction assuming Peak 7 is star-shaped; the blue line assumes it is comb-shaped; and the green line assumes it is H-shaped.

3.7 References

Chen, X., and R. G. Larson, "Effect of branch point position on the linear rheology of asymmetric star polymers," Macromolecules 42, 6871-6872 (2008).

Chen, X., F. J. Stadler, H. Münstedt, and R. G. Larson, "Method for obtaining tube model parameters for commercial ethene/α-olefin copolymers," J. Rheol. 54, 393-406 (2010).

Chen, X., C. Costeux, and R.G. Larson, "Characterization and prediction of long-chain branching in commercial polyethylenes by a combination of rheology and modeling methods," J. Rheol. 54, 1185-1205 (2010).

Daniels, D. R., T. C. B. McLeish, R. Kant, B. J. Crosby, R. N. Young, A. Pryke, J. Allgaier, D. J. Groves, and R. J. Hawkins, "Linear rheology of diluted linear, star and model long chain branched polymer melts," Rheol.Acta. 40, 403-415 (2001).

Daniels, D. R., T. C. B. McLeish, B. J. Crosby, R. N. Young, and C. M. Fernyhough, "Molecular rheology of comb polymer melts. 1. Linear viscoelastic response," Macromolecules 34, 7025-7033 (2001).

Hakiki, A., R. N.Young, and T. C. B. Mcleish, "Synthesis and characterization of H-shaped polyisoprene," Macromolecules 29, 3639-3641 (1996).

Inkson, N. J., R. S. Graham, T. C. B. McLeish, D. J. Groves, and C. M. Fernyhough, "Viscoelasticity of monodisperse comb polymer melts," Macromolecules 39, 12, 4217-4227 (2006).

Janzen, J., and R. H. Colby, "Diagnosing long-chain branching in polyethylenes," J. Mol. Struct. 485, 569-584 (1999).

Larson, R. G., "Combinatorial rheology of branched polymer melts," Macromolecules 34, 4556-4571 (2001).

Lee, H. C.; T. Chang, S. Harville, and J. W. Mays, "Characterization of Linear and Star Polystyrene by Temerature Gradient Ineraction Chromatography with a Light Scattering Detector," Macromolecules 31, 690 (1998).

Li, S. W., Doctoral dissertation: Rheology of Branched Polybutadiene – Modeling Polydispersity. Univeristy of McGill (2010).

Li, S. W. H. E. Park, J. M. Dealy, M. Maric, H. Lee, K. Im, H. Choi, T. Chang, M. S. Rahman, and J. W. Mays, "Detecting Structural Polydispersity in Branched Polybutadienes," Macromolecules 44, 208-214 (2011).

McLeish, T. C. B., J. Allgaier, D. K. Bick, G. Bishko , P. Biswas , R. Blackwell , B. Blottiere , N. Clarke , B. Gibbs , D. J. Groves , A . Hakiki , R. K. Heenan , J. M. Johnson , R. Kant , D. J. Read, and R. N. Young, "Dynamics of entangled H-polymers: Theory, rheology, and neutron-scattering," Macromolecules 32, 6734-6758 (1999).

McLeish, T. C. B., "Molecular rheology of H-polymers macromolecules," Macromolecules 21,1062-1070 (1988).

Park. S. J., and R. G. Larson, "Long-chain dynamics in binary blends of monodisperse linear polymers," J. Rheol. 50, 21-39 (2005).

Park, S. J., S. Shanbhag, and R. G. Larson, "A hierarchical algorithm for predicting the linear viscoelastic properties of polymer melts with long-chain branching," Rheol. Acta 44, 319-330 (2005)

Perny, S., J. Allgaier, D. Y. Cho, W. Lee, and T. Y. Chang, "Synthesis and structural analysis of an H-shaped polybutadiene," Macromolecules 34, 5408-5415 (2001).

Rahman, M. S., R. Aggarwal, R. G. Larson, J. M. Dealy, and J. W. Mays, "Synthesis and Dilute Solution Properties of Well-Defined H-Shaped Polybutadienes," J. Macromolecules 41, 8225-8230 (2008).

Roovers, J., and P. M. Toporowski, "Preparation and characterization of H-Shaped polystyrenes mocromolecules," Macromolecules 14,1174-1178 (1981).

Synder, L. R., and J. J. Kirkland, Introduction to modern Liquid Chromatography, 2nd Ed.; Wiley-Interscience: New York (1979).

Wang, Z. W., X. Chen, and R. G. Larson, "Computational models for predicting the linear rheology of branched polymer melts," J. Rheol. 54, 223-260 (2010).

Chapter 4

Analytical rheology of asymmetric H-shaped model polybutadiene melts

4.1 Abstract

An asymmetric H-shaped high-quality model polybutadiene (PBd) melt with two short arms and two long arms, is carefully designed and synthesized by anionic polymerization, purified by non-solvent fraction; and both the purified and unpurified melts, labeled "H(SSLL)-P" and "H(SSLL)-UP," respectively, are characterized by thermal gradient interaction chromatography (TGIC), and by linear rheological measurement. In addition, the rheological properties of blends of H(SSLL)-P with low or modest levels of well characterized linear and star PBds are measured. From these measurements, we assess the affect of additional components, or "impurities" on the rheology of the asymmetric H polymer, and show that a rheological model, namely the "hierarchical model" for entangled branched polymers, can predict the linear rheology of pure asymmetric H polymer, and the effect of small levels of impurities on this rheology . Since all synthetic polymers, including "model" polymers contain polydispersity and low levels of sides products, and these can have significant effects on the rheology of branched polymers, our approach promises to allow the effects of these impurities on rheology to be assessed and accounted for. In this way, even the unavoidable impurities in "model" polymers can be used to help test and refine rheological theories so that they can eventually be used to help assess the molecular structure of commercial branched polymers, thus making rheometry an "analytical" technique.

In this Chapter, the synthesis work was done by Jimmy May's group at University of Tennessee. The TGIC characterization was done by Taihyun Chang's group in Pohang University of Science and Technology, Korea. X.Chen acknowledges their contributions.

4.2 Introduction

Long-chain branching has pronounced effects on rheological and processing properties of polyolefins, and the control of long-chain branching for optimal processing has long been a goal of polymer synthetic chemists. Measuring and modeling the rheology of such polymers could be of great assistance in designing and synthesize such polymers in two important ways: 1) by measuring and predicting the effect of long chain branching structures on nonlinear rheological properties, one can infer the likely processing characteristics of the polymer (for example, the "melt strength"); and 2) by measuring and predicting the linear rheological properties, one might confirm or even determine which branching structures are actually present in the melt, since these might differ from what the synthetic chemist intended to make [Dealy and Larson (2006)]. This latter use of rheology is sometimes referred to as "analytical rheology," i.e., the use of rheology as an analytical characterization tool that can augment the information gleaned from size exclusion chromatography and other analytical methods [Janzen and Colby (1999)]. To develop the understanding necessary for either of these goals, the ability must be developed to predict the rheology of branched polymers with different levels and types of branching. To this end, various researchers have studied a "zoo" of various low-polydispersity model long-chain branched polymers, with topologies ranging from star [Graessley and Roovers J (1979); Raju, et al. (1979); Pearson et al. (1983); Fetters et al. (1993); Adams et al. (1996); Frischknecht, et al. (2002)] to "H" [Daniels, et al. (2001)] to "comb" [(Roovers and Graessley (1981); Roovers (1984)], and to hyperbranched (or branch-on-branch) topologies [Lee and McHugh (2001)]. The rheology of such long-chain branched polymers is extremely sensitive to branch length and branch polydispersity, as well as to topology. In fact, failure to predict accurately the rheology of such materials might sometimes be the result of imperfections in the synthesis of these polymers, which are never completely monodisperse nor completely free of contaminating polymers, such as un-reacted branches, or complex multiply branched side products. Often conventional analytical techniques are unable to detect such impurities at the small levels that can strongly influence rheological properties as discussed in this paper.

For this reason, rheological data themselves are looked to as a means of assessing sample purity and quality. However, one confronts the problem of ill-posedness or even circular reasoning, since one is looking to such data as a means of confirming or improving rheological models. If deviations between model predictions and measured rheology could either indicate imperfections in synthesis that are difficult to pick up using the standard characterization methods, or could indicate failings of the rheological model, how is one to obtain reliable inferences from the rheological data?

Here we seek to address this conundrum through both improved sample characterization using temperature gradient interaction chromatography (TGIC), and through "combinatorial rheology." By "combinatorial rheology" we mean the measurement of the rheology of both the sample itself and of blends of the sample with simpler linear and star-branched polymers [Larson (2001)]. These measurements are then modeled theoretically and used to help confirm or determine more precisely the composition of the original sample. Combinatorial rheology seeks to overcome the ambiguity inherent in modeling a single set of rheological data for a sample of uncertain or questionable compositional purity. It does this by supplementing data for the polymer itself with multiple other sets of data obtained by blending the test polymer with polymers of known, simple, structure and by seeking to predict the rheology of all such blends using a single rheological model with fixed input parameters. By challenging both the rheological model and the presumed sample structure with multiple sets of data, one enhances the probability of correctly inferring both the compositional purity of the original sample, and the reliability of the rheological model. The compositional purity and the reliability of the rheological model can be considered coupled problems, once one recognizes that the rheology might be sensitive to impurities whose identity and concentration might not be reliably measured by standard characterization techniques. But to assess both compositional purity and model fidelity for a given model long-chain-branched polymer, more data are required than just the linear rheology of the model polymer. Hence, measuring and modeling the rheology of blends of the model polymer with well-characterized linear or simple star-branched polymers (whose synthesis is less prone to producing side products) becomes an attractive option.

We shall here illustrate this approach by studying in great detail a model "asymmetric H" polybutadiene melt specially synthesized for this purpose. We will model these data using a generalized advanced "tube" model (the "hierarchical model") that allows inclusion of multiple branching architectures and of arbitrary polydispersity in both backbone and branch molecular weights. This model is therefore able, in principle, to predict the rheology of not only ideal monodisperse H polymers, but also the effect of arm and backbone polydispersity, and the effect of impurities that might be present in the polymer due to the imperfection of the reaction and of the fractionation, or that we deliberately mix into the polymer as a means of assessing the sensitivity of the rheology to such impurities.

Our approach is thus a novel one: instead of merely purifying our sample to the extent possible and then treating it as "monodisperse" and "free of side products," we deliberately introduce linear and star-branched "impurities" to assess their effect on the rheology of the model polymer and to test our ability to predict this effect. We also measure the rheology and characterize the model H polymer both before and after fractionation, and combine this information with that obtained from the rheology of the deliberately contaminated samples, to estimate whether the purified sample is pure enough to show little influence of the remaining impurities on the rheology. The end result is a much higher level of confidence, both in the quality of our rheological data, and in the predictive power of our rheological model.

We focus here on the simplest species that contains two branching points, namely "H" polymers. H polymers composed of polystyrene, polyisoprene or polybutadiene have been previously studied by multiple groups. [Roovers and Toporowski (1981); McLeish (1988); Hakiki et al. (1996); McLeish et al. (1999); Daniels et al. (2001a); Perny et al. (2001)] However, due to the limitations of synthesis strategy and molecular characterization methods, asymmetric H polymers have not yet been investigated. We will here present the first rheological data on model asymmetric "H" polymers, which will not only be useful for testing available theories, but also is relevant for design of commercial polymers, since "H" polymers contained in commercial polymers are mostly asymmetric.

The polymer used here is anionic polymerized polybutadiene with a high concentration of 1,4 addition. Not only does 1,4-polybutadiene have a relatively low entanglement molecular weight M_e , there is an abundance of literature data on 1,4-PBd linears, stars and blends [Baumgaertel et al. (1992); Daniels et al. (2001); Rubinstein and Colby (1988); Struglinski et al. (1985); Lee and Archer (2002); Adams et al. (1996)].

Our study required completing the following tasks: 1. Synthesis of a high-quality model asymmetric H-shaped polymer that is carefully designed to test physical theories. 2. Careful characterization of the molecular weight and branching properties of the asymmetric H polymer. 3. Purification of the H polymer by fractionation. 4. Blending of the asymmetric H polymer with linear and star 1,4-PBd. 5. Measurement of the linear rheological properties of the asymmetric H polymer and its blends. 6. Comparison of the measured viscoelastic properties with predictions derived from the proposed theory. This paper is organized as follows. Section 4.3 describes the synthesis techniques and sample characterization. In Section 4.4, we describe the hierarchical tube theory and modeling details. In Section 4.5, we present and discuss our synthesized products, molecular characterization results, and rheological measurements and compare them to the "hierarchical model" calculations. In particular, we show that the "hierarchical model" yields quantitative predictions for our linear, star, and asymmetric H polymers and their blends. Conclusions are drawn in Section 4.6.

4.3 Experiments

4.3.1 Materials and Synthesis[1]

Three 1,4-polybutadiene polymers (PBd), namely a linear, a star and an H polymer, as well as blends of these, were investigated. The linear PBd was purchased from Polysciences Inc. Its weight-average molecular weight and molecular weight distribution are 22.6 kg/mol and 1.05, respectively, provided by Polysciences Inc. The three-armed symmetric star and asymmetric H-shaped PBd with targeted molecular weights were designed and synthesized as described below. As shown in Figure 4-1 (b), the three-armed symmetric star has three identical arms, with targeted molecular weight

[1] The work of synthesis and purification on S60K, H(SSLL)-P and H(SSLL)-UP was done by our collaborators Jimmy May's group at University of Tennessee. Figure 4-2 is prepared by Dr. M. Shahinur Rahman. X. Chen acknowledges their contributions.

of 20 kg/mol per arm, attached to the branch point. The asymmetric H-shaped PBd has two identical short arms attached to one end of the backbone and two identical long arms attached to another end of the backbone. To obtain high quality branched polymers, the H-shaped 1,4-polybutadienes were purified by using toluene/methanol as the solvent/nonsolvent pair. Because of our interest in developing rheological methods of identifying and characterizing the composition of complex mixtures of branched polymer species, we here study both the unpurified and purified H-shaped polymers. The samples we use here are believed to have very similar vinyl content, which is about 6%, since their synthesis mechanism and catalysts are the same. The linear, star, purified, and unpurified H-shaped polybutadienes are designated L23K, S60K, H(SSLL)-P and H(SSLL)-UP, respectively.

The strategy to synthesize asymmetric H-shaped polymer is to couple two living long arms with the end of one arm of asymmetric star-shaped molecule. We give here an outline of the synthetic route of H(SSLL) as shown in Figure 4-2 . The major product and by-products of each step are presented in Section 4.5.1.

4.3.2 Characterization[2]

The symmetric star-shaped and asymmetric H-shaped PBds were characterized by both SEC and TGIC, which have been described in Chapter 3.

4.3.3 Experimental design

To correctly infer the compositional purity of the original sample, and validate the reliability of modeling, a series of mixtures of H-shaped PBd with linear or star-shaped PBds were designed as shown in Table 4-1.

4.3.4 Preparation of blends

The detailed description of PBd blends preparation has been presented in Chapter 3, i.e. blends containing different weight fractions of linear, star, or H polymers were prepared by dissolution of the polymers in toluene that was pre-treated by filtered with 0.2μm pore-size sterile filters, allowing about a week in a fume hood for evaporation of the solvent. The samples were then dried under vacuum at room temperature for another

[2] The TGIC characterization was done by Taihyun Chang's group in Pohang University of Science and Technology, Korea. The SEC characterization was done by Jimmy May's group in University of Tennessee. X. Chen acknowledges their contributions.

two weeks to ensure removal of the excess toluene. Two methods were used to determine the complete removal of the excess toluene: (1) no toluene smell after drying under vacuum; (2) the weight of the sample become constant. The blends after drying were stored in a refrigerator ready for rheological measurements.

4.3.5 Rheological measurements

Detailed description of the rheological measurements on the samples studied here are the same as what has been presented in Chapter 3.

4.4 Theory and modeling

Here we pursue "combinatorial rheology" using the "hierarchical model" (v3.0) [Wang et al (2010)]. As mentioned in previous chapters, the "hierarchical model" has been successfully validated on linear , symmetric star , "T" and "Y" shaped asymmetric star, symmetric H-shaped polymers， linear-linear blends, linear-star blends as well as commercial metallocene polyethylene copolymers [Park and Larson, (2005).; Park, Shanbhag, and Larson, (2005); Chen and Larson (2008); Wang et al (2010); Chen et al. (2010); Chen et al. (2010)]. Here we will validate this "hierarchical model" (v3.0) on asymmetric H-shaped PBds and their blends with linear or star polymers, and infer the compositional purity of the asymmetric H PBds.

Larson proposed the "hierarchical model" to treat the relaxation of mixture of general "comb" polymers; see details in Larson [2001]. We apply this concept of polymer hierarchical relaxation into the asymmetric H-shaped polymer studied here. As shown in Figure 4-3, at a short time after a small step strain, only the arms can relax inward from their tips. When the two identical short arms are fully relaxed, they are replaced by a frictional bead at the branch point. The unrelaxed molecule becomes a "Y" shaped star molecule with two identical short arms and one long arm; see (b) in Figure 4-3. As the two short arms completely relax, the molecule finally becomes a linear chain with two branch points at the two ends; illustrate in (c). The final relaxation then occurs by arm retractions and reptation of an effectively "linear" chain. The beads incorporate the friction added to the chain backbone by the side branches.

To predict the rheological behaviors of the samples, the dilution exponent α and the coefficient of branch-point drag p^2 are set to be α=4/3 and $p^2 = 1/12$. In addition to

the material-independent parameters α and p^2, the three material-dependent tube model parameters, namely the plateau modulus G_N^0, the entanglement molecular weight M_e and the frictional equilibration time τ_e, are set to be the same as those used in Chapter 3, i.e., G_N^0 =1.095MPa, M_e =1620 and τ_e = 5E-7s. Furthermore, the "arm-frozen" option of the hierarchical model is used for all our predictions (see the definition of "arm-frozen" in Wang et al. (2010)).

4.5 Results and discussions

4.5.1 Synthesis of Asymmetric H-shaped PBd

Since the synthesis methods for linear and symmetric star PBds are very straightforward, we do not discuss their synthesis here. Perny et al. [Perny et al. (2001)] prepared a symmetric H PBd with high 1,4 addition by attaching four linear chains with the backbone to generate the H polymer. This synthetic strategy employed by Perny et al.[2001] is not able to produce regular asymmetric H-shaped polymers, because the short and long arms will randomly attach to the two ends of the backbone, thereby introducing many different products. However, a novel strategy to prepare H-PBd by anionic polymerization was developed recently [Rahman, et al. (2008)]. It is based on the idea that coupling two "half H" (i.e., star-shaped) molecules to generate an H molecule. In our work, we proposed another novel strategy to synthesize asymmetric H-shaped polymer by coupling two living long arms with the end of one arm of asymmetric star-shaped molecule as illustrated in Figure 4-2. Each synthesis step and the possible by-products are shown in Figure 4-4**.**

4.5.2 SEC and TGIC characterization of Star-shaped PBd and H-shaped PBd

As shown in Figure 4-5, the SEC characterization reveals that the S60K and H(SSLL)-P have only one single peak, while the peak of H(SSLL)-UP has some bumpers, indicating there might be some other components in the material. However, the traditional SEC characterization is not able to identify the actual components in the sample accurately. Luckily, as shown in Figure 4-6, the TGIC characterization indicates there are about three components in both S60K and H(SSLL)-P and five components in H(SSLL)-UP. The molecular characteristics information of these components are discussed in the following section.

4.5.3 Further analysis of TGIC data

The raw TGIC data provide us with the molecular weight of each component in the sample and based on the synthesis mechanism, we can infer the possible structures of each peak. However, in addition to the information on molecular weight of each peak, the weight fraction and polydispersity index (PDI) are needed for "hierarchical model" predictions. The TGIC data shown in Figure 4-6 allow us to estimate the concentration and PDI of the main products as well as byproducts in the star, H(SSLL)-UP and H(SSLL)-P PBds. The detailed TGIC analysis method is described in Chapter 3.

Based on that method, the molecular characteristics of each component in the star, H(SSLL)-UP and H(SSLL)-P samples are summarized in Tables 4-2, 4-3, 4-4, and the possible structures corresponding to each peak are shown in Figure 4-7. The PDI's of each component (or peak) for the star, H(SSLL)-P and H(SSLL)-UP are nearly unity; i.e., each component is nearly monodisperse. For the star PBd, the main product takes up about 83.6% of the total weight. For the asymmetric H PBds, Peaks 1, 2 and 3 of H(SSLL)-P are correspond closely to Peaks 3, 4, and 5 of H(SSLL)-UP, respectively. (There are some differences between H(SSLL)-P and H(SSLL)-UP in the molecular weights of the three peaks that they share, presumably due to imprecision of the calibration.) Peaks 1 and 2 of H(SSLL)-UP almost disappear after purification as shown in Figure 4-6. However, due to the overlap between the peak corresponding to the main product and those corresponding to the byproducts which have similar elution time (namely peaks 3 and 5 in H(SSLL)-UP and peaks 1 and 3 in H(SSLL)-P), it is difficult to remove those byproducts completely. As a result, even after purification, the main product of H(SSLL)-P has a weight fraction of about 78.6%, which is, however, higher than the content of targeted H polymer in the sample synthesized by Perny et al. [Perny et al.(2001)].

4.5.4 Linear viscoelastic properties of the samples

According to the experimental design described in Section 4.3.5, the linear viscoelastic behaviors of a series of L23K, S60K, H(SSLL)-P and H(SSLL)-UP and their blends have been measured. Figure 4-8 shows the storage moduli of the star and H(SSLL)-P PBds and their blends, while Figure 4-9 shows the storage moduli of the linear and H(SSLL)-P PBds and their blends. Except for H(SSLL)-P, rheological data for

all melts reach, or nearly reach, the terminal region. In addition, we acquired data for blends of the purified H(SSLL)-P with linear and star polymers, and thus have rheological information that reflects the relaxation of the longest components of the H(SSLL)-P polymer. A strength of our methodology ("combinatorial rheology") is that gaps in the terminal region can be "filled in" by measurements on blends for which the terminal region is shifted into the experimentally accessible window. Advanced rheological models allow the affect of this blending to be calculated, and successful comparison of data for multiple blends builds confidence that the model can predict accurately the rheology of the unblended sample, even when data for the unblended sample do not quite reach the terminal zone. Note that the length of the linear chain is almost the same as that of one arm of the symmetric 3-arm star-shaped PBd. As expected, as the concentration of star in the blends increases, the sample relaxes faster. At the same concentration of linear or star blended with H(SSLL)-P (50% of H(SSLL)-P), the blend with star relaxes slower than that with linear PBd, as expected, due to the more sluggish relaxation of the star molecule (Figures 4-8 and 4-9) .

Since H(SSLL)-UP and H(SSLL)-P come from the same batch and H(SSLL)-UP has two more components than H(SSLL)-P does according to the TGIC characterization, their rheological behaviors have also been compared. As shown in Figure 4-10, in the testing range from 10^{-4}rad/s to 10^{2}, no significant difference is observed between these two H-shaped PBd melts. However, when we use the linear-shaped PBd to dilute the H-shaped PBd melts, we can observe rheological difference between these two blends. This again reveals the strength of "combinatorial rheology." Upon dilution, each component of a topologically complex blend shifts its relaxation time to an extent that depends on its topology. Hence, components whose rheological signatures overlap on the frequency axis in the pure melt, can be shifted along that axis to different extents in the blend, thus separating them from each other and exposing the presence of components that might go unrecognized in the pure melt. Such "un-masking" by dilution becomes even more likely when dilution with multiple diluents, both star and linear, at different concentration, are employed. This is especially effective with branched species, where acceleration of relaxation can be exponential in both the degree of dilution and in the length of the arm that is diluted. Thus, different degrees of dilution can spread apart relaxations of various

branched species to varying degrees, and "un-mask" the presence of many otherwise unsuspected components of the original melt.

4.5.5 Comparison of modeling predictions with rheological measurements

As described in Section 4.4, the "hierarchical model" (v3.0) is employed here to calculate the rheological behaviors of these materials. The three key tube model parameters G_N^0 =1.095MPa, M_e =1620 and τ_e = 5E-7s are used for all of predictions without adjustment. The linear polymer (L23K) and each component of the star (S60K), and H polymers H(SSLL)-UP and H(SSLL)-P, are taken to be monodisperse, based on their PDIs of nearly unity. Using the measured molecular weight, and the suggested molecular structure and the weight fraction of each component (see Figure 4-7 and Tables 4-2, 4-3, 4-4), we predict their rheology data in Figures 4-11 and 4-12. As shown in Figure 4-11, the "hierarchical model" can successfully predict the rheological behaviors of linear, H(SSLL)-P, and their blends. As noted earlier, even though the terminal region of H(SSLL)-P has is not reached in the rheological measurement, the theory can reveal the information in this region, which can be confirmed by agreement of the theory with the experiments for the blends, for which the terminal region is accessed. For the H(SSLL)-P and star PBds blends, the comparison between theory and experimental data are shown in Figure 4-12. Basically the modeling results can capture the trend of the H and star blends except the 50/50 blend.

From previous analysis and discussion, H(SSLL)-P contains about 78.6% of the targeted asymmetric H polymer as the main product. To determine the effect of the contaminants on the rheology, we calculate the rheology of the theoretically pure monodisperse H polymer without any contaminants, i.e. the rheology that the sample should have if the weight fraction of the H component were 100%, instead of 78.6%. In Figure 4-13, we compare this predicted rheology with that predicted for the mixture of components inferred to be present in H(SSLL)-P, and with the experimental data. We also compared the 50/50 blends of linear and H(SSLL)-P, i.e., one blend is 50% L23K with 50% theoretical pure monodisperse H polymer, while another blend is 50% L23K with 50% H(SSLL)-P which has three components in the H sample. As shown in Figure 4-13, there are no significant differences between the theoretically pure monodisperse H(our targeted H PBd) and H(SSLL)-P. These results indicate that the impurities in

H(SSLL)-P produce no significant affect on the rheology of the H polymer. Thus, the fractionation of this H apparently rendered the polymer "pure enough" that its rheology is not sensitive to the remaining impurities. This example shows how rheological modeling can help determine the level of purification required to produce data that are insensitive to remaining impurities. Since no synthetic sample can be completely pure, modeling of this kind, along with measurement of the rheology of unpurified samples, and of deliberately blended samples, offers the prospect of determining when sufficient purification of a given sample has been attained.

4.6 Conclusions

An asymmetric H-shaped model polybudtadiene melt has been designed and synthesized by using novel strategy. Part of the original asymmetric H material was purified by fractionation. Both the purified H PBd H(SSLL)-P, and unpurified H PBd H(SSLL)-UP were characterized by TGIC and we have proposed possible component structures based on the synthesis mechanism and TGIC data. Although from the TGIC data, the purified and unpurified samples of asymmetric H PBds differ in their compositions, their rheological measurements show only a slight difference over the range of frequencies accessible in oscillatory rheometry. However, by blending the purified H(SSLL)-P and unpurified H(SSLL)-UP with a linear PBd, we find a distinct difference in the rheology of the blended polymers.

We also blended H(SSLL)-P with a linear PBd of high purity, and the rheological properties of these blends with predictions of the "hierarchical model" (v3.0) for entangled polymer blends. The calculation results indicate the reliability of this model, which can therefore aid in detecting compositional purity of the original materials. However, when we blended H(SSLL)-P with S60K, the prediction of 50/50 blend did not match the data very well, and the reason why the "hierarchical model" fail for this blend is unknown. It might be due to the degradation of the sample or due to the limitation of the model. We might need other new H(SSLL) sample to figure out the true reasons.

Furthermore, we used the "hierarchical model" to show that the rheology of the "purified" sample H(SSLL)-P, which is only 78.6% pure H, is virtually identical to that of a theoretically 100% pure H polymer, thus showing that the purified H polymer is "pure enough" that the remaining contaminants did not significantly affect the rheology.

The methods employed here: 1) synthesis of novel model branched structures 2) fractionation, 3) characterization of melt composition by TGIC, 4) rheological measurements on the purified and unpurified model polymer and on blends of the model polymer with well characterized linear and star diluents, and 5) rheological prediction using a generalized rheological model, provide a way to both identify impurities and their influence on rheology, and to test and validate models of complex branched polymers. Taken together, they represent a way of implementing the strategy of "combinatorial rheology," whereby inevitable limitations in synthetic purity and sample characterization can be overcome by producing multiple rheological data sets on the same polymer blended with well characterized simpler polymers, and predicting these data with advanced rheological models. This approach also builds the expertise needed to accomplish the ultimate aim, which is the development of models to predict the rheology of complex commercial melts, and to infer molecular characterization from such measurements.

.

Table 4-1. Experimental Design of linear, star, asymmetric H-shaped PBd and their blends

Name	L23K (wt%)	S60K (wt%)	H(SSLL)-P (wt%)	H(SSLL)-UP (wt%)
L23K	100	----	----	----
S60K	----	100	----	----
H(SSLL)-P	----	----	100	----
H(SSLL)-UP	----	----	----	100
88%H(SSLL)-P+12%S60K	----	12	88	----
75%H(SSLL)-P+25%S60K	----	25	75	----
50%H(SSLL)-P+50%S60K	----	50	50	----
50%H(SSLL)-P+50%L23K	50	----	50	----
50%H(SSLL)-UP+50%L23K	50	----	----	50

Table 4-2. Characterization of star PBd

Peak	Peak Type	Weight Fraction	σ_{peak}	M	a[1]	σ_M	PDI
		%		g/mol		$\times 10^{-7}$	
1	Gaussian	5.27	2.15	38500	2262.4	1.09	1.01
2	Gaussian	83.6	5.43	54800	2262.4	2.78	1.01
3	Gaussian	11.12	21.5	73600	2262.4	11.0	1.02

(1) a is the pre-factor in the correlation $M = 2262.4 \times t_R + 17664$ with $R^2 = 0.9924$.

Table 4-3. Characterization of H(SSLL)-UP PBd

Peak	Peak Type	Weight Fraction %	σ_{peak}	M g/mol	a[1]	σ_M $\times 10^{-7}$	PDI
1	Gaussian	1.5	0.95	64500	3891	1.43	1.00
2	Gaussian	11.7	5.44	87100	3891	8.23	1.01
3	Gaussian	8.8	17.07	111000	3891	25.8	1.02
4	Gaussian	62.6	23.14	144000	3891	35.0	1.02
5	Gaussian	15.5	35.61	207000	3891	53.9	1.01

(1) a is the pre-factor in the correlation $M = 3891 \times t_R + 36297$ with $R^2 = 0.9976$

Table 4-4. Characterization of H(SSLL)-P PBd

Peak[1]	Peak Type	Weight Fraction %	σ_{peak}	M g/mol	a[2]	σ_M $\times 10^{-7}$	PDI
1	Gaussian	5.75	12.8	136700[3]	2053.2	5.40	1.00
2	Gaussian	78.60	22.5	150000	2053.2	9.50	1.00
3	Gaussian	15.63	132.2	186000	2053.2	55.7	1.02

(1) Peaks 1, 2, 3 of H(SSLL)-P are related to peaks 3,4 5 of H(SSLL)-UP respectively

(2) a is the pre-factor in the correlation $M = 2053.2 \times t_R + 93418$ with $R^2 = 1$

(3) M of peak 1 was calculated based on the correlation between M and t_R.

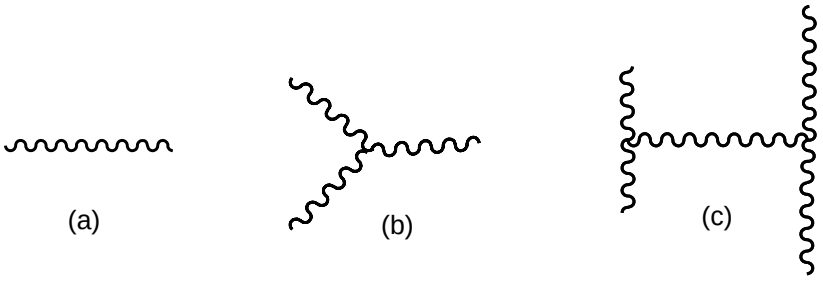

Figure 4-1. Polybudienes studied in this work: (a) linear PBd; (b) symmetric star PBd; (c) asymmetric H PBd with two identical short arms attached to one end of the backbone and two identical long arms attached to the other end.

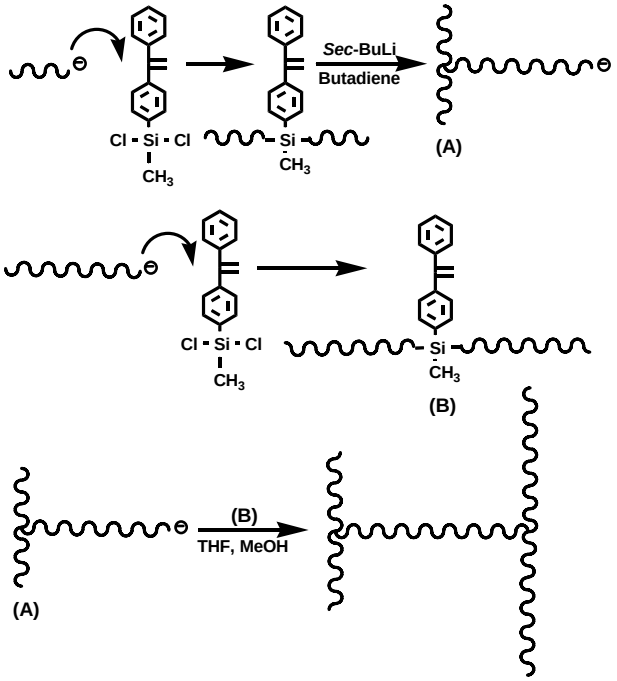

Figure 4-2. Reaction scheme for H(SSLL) synthesis

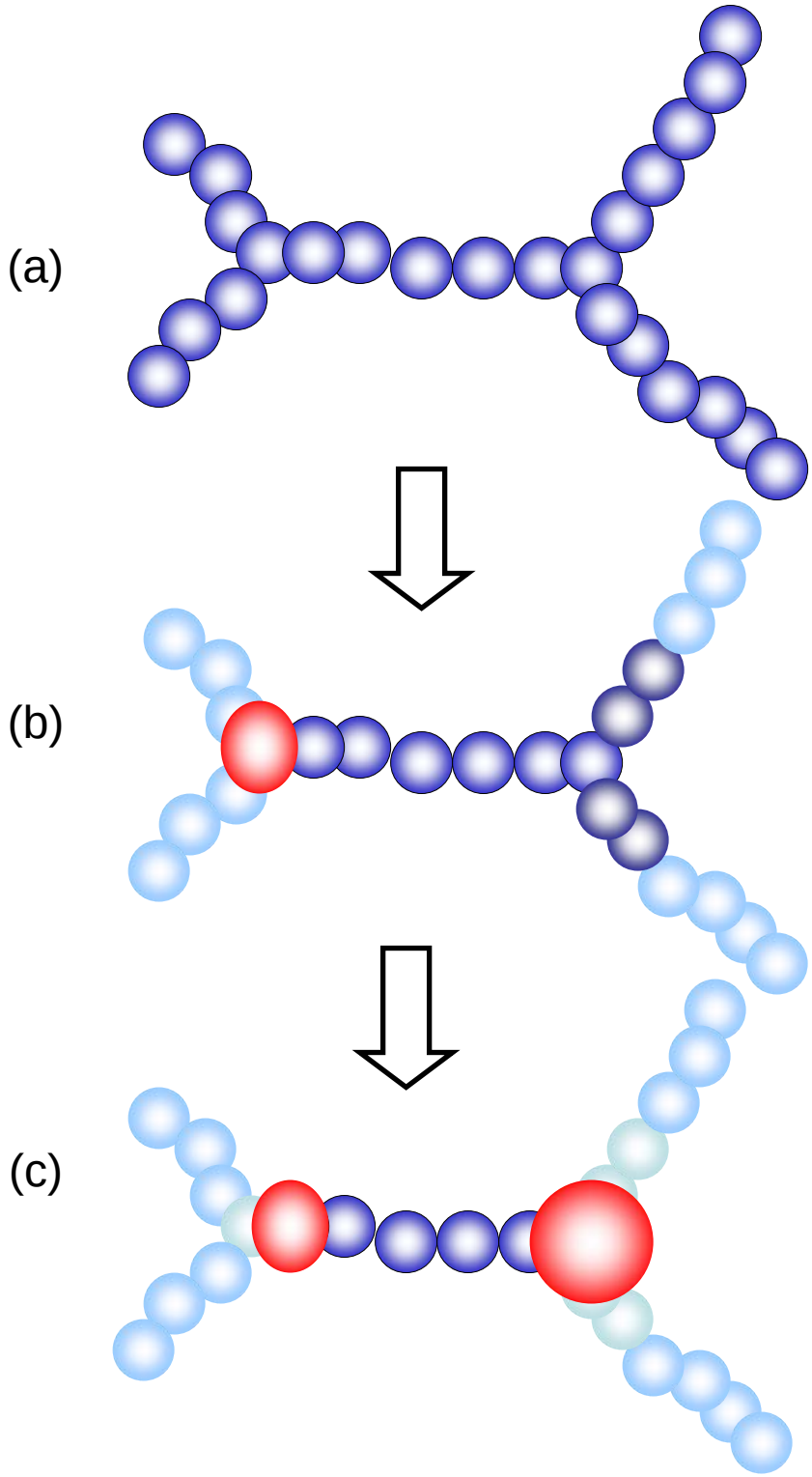

Figure 4-3. Conceptualization of algorithm for computing hierarchical relaxation of the asymmetric H-shaped polymer

Step	Reaction	Possible by-products
1	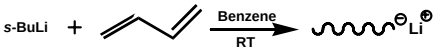	
2	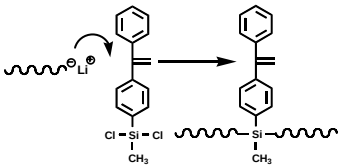	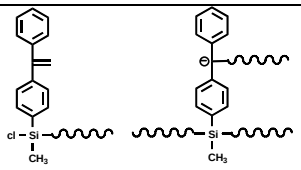 (A) (B)
3	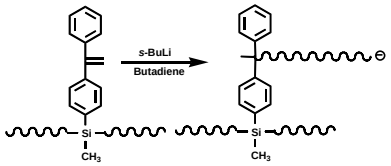	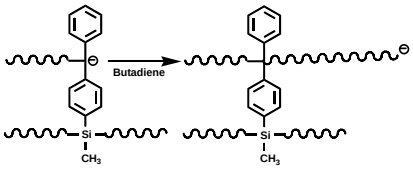 byproduct of step 2(B) (B)
4	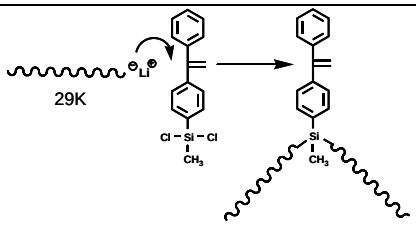	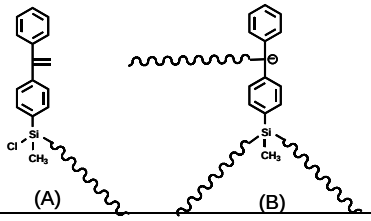 (A) (B)
5	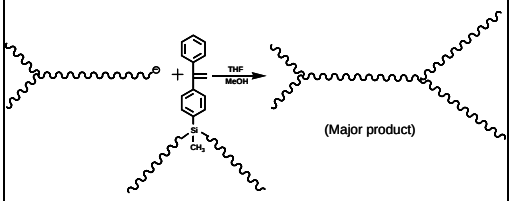	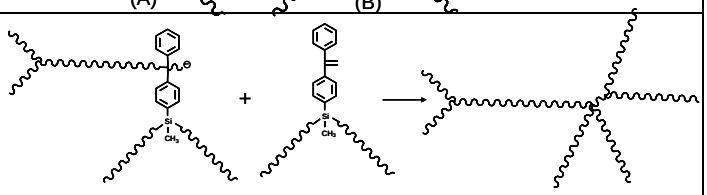 (A) 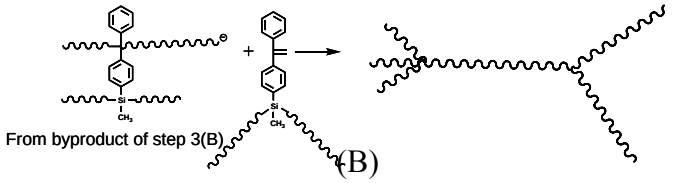 From byproduct of step 3(B) (B) 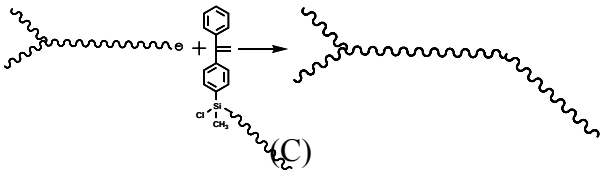 (C) From byproduct of step 4(A)

Figure 4-4. synthesis of asymmetric H-shaped PBd and possible by-products in each step[3]

[3] The by-products of each step in Figure 4 were determined by Dr. M. Shahinur Rahman. X.Chen acknowledges his contribution.

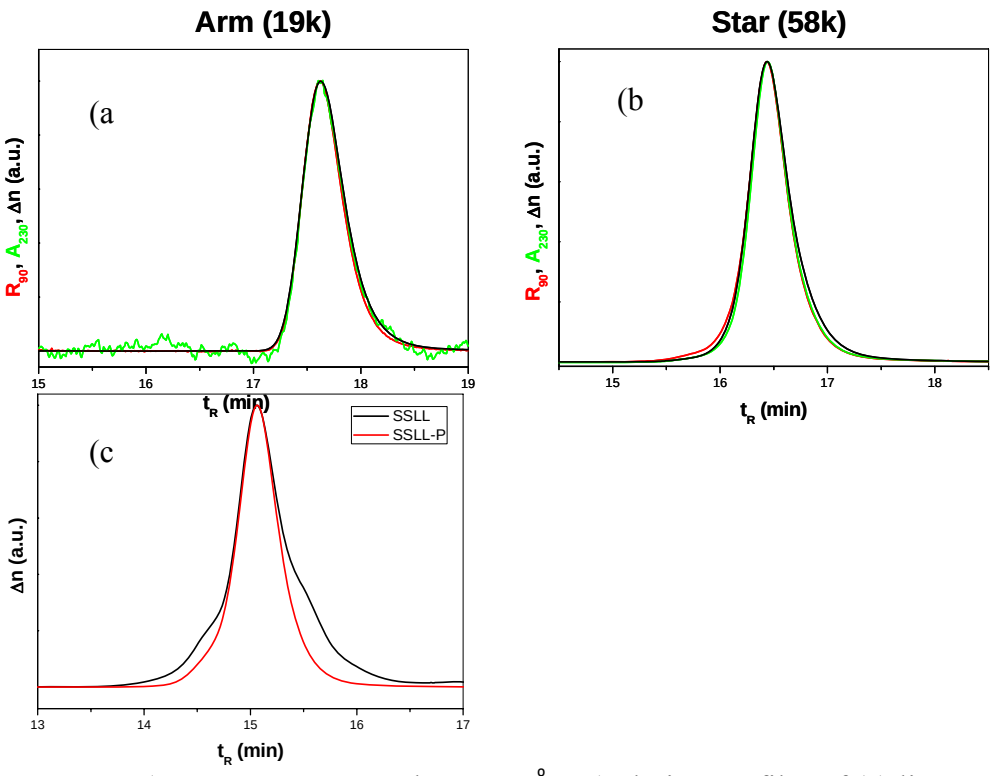

Figure 4-5. SEC (RI-Δn UV-A230 and LS at 90°-R_{90}) elution profiles of (a) linear PBd arm, the precursor of S60K, (b) S60K, and (c) purified and unpurified H(SSLL)

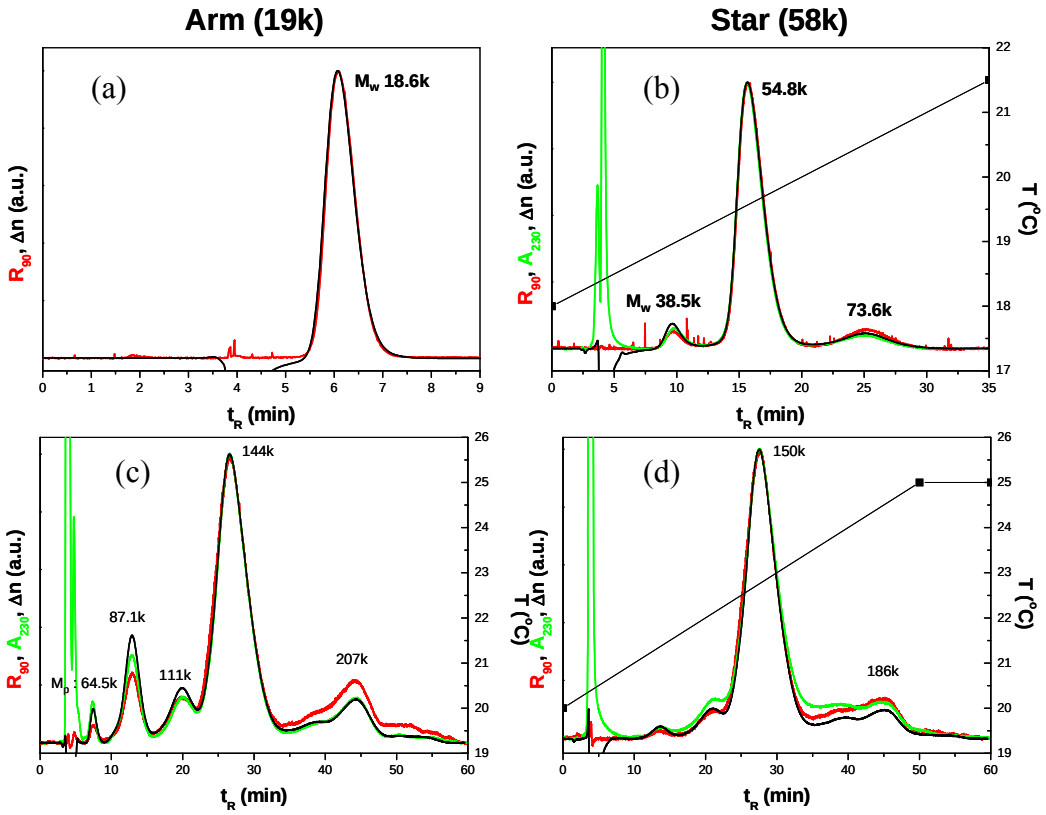

Figure 4-6. TGIC of (a) linear PBd arm, the precursor of S60K, (b) S60K, (c) unpurified H(SSLL) and (d) purified H(SSLL)

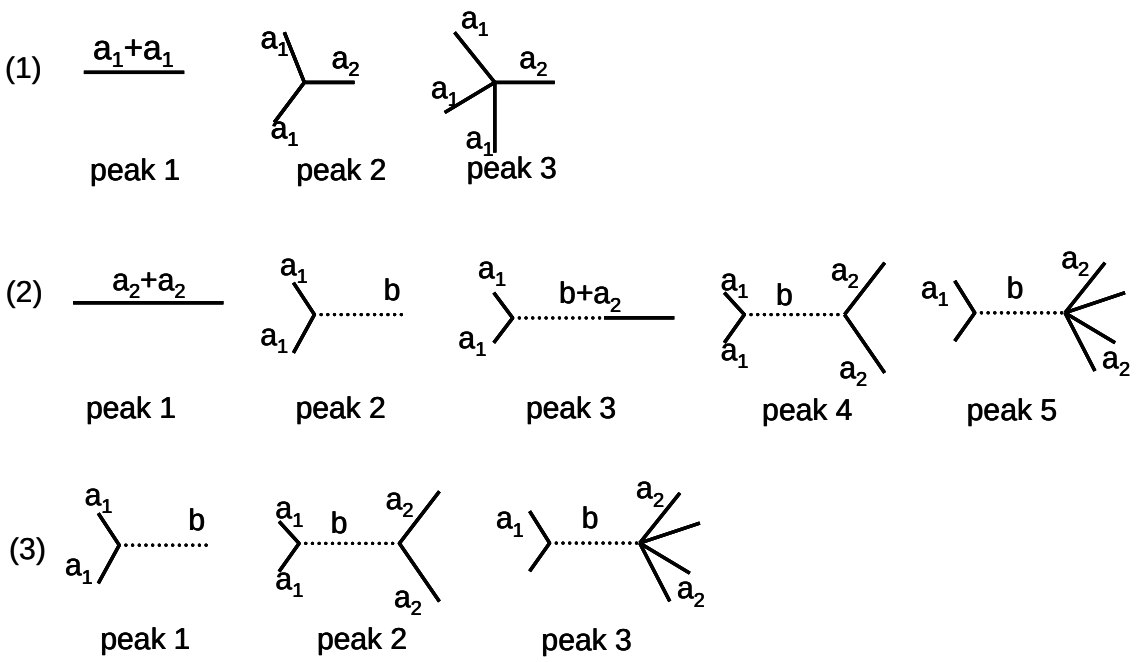

Figure 4-7. Structures of main products and possible by-products in (a) S60K, (b) H(SSLL)-UP, and (c) H(SSLL)-P and their corresponding TGIC peaks.

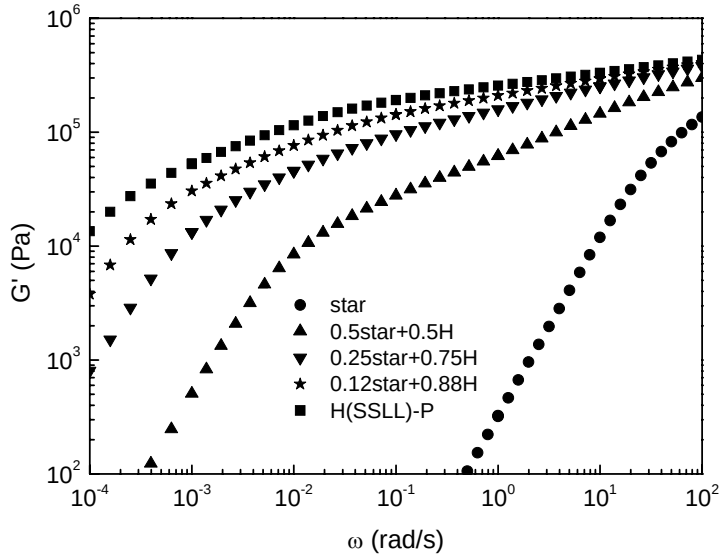

Figure 4-8. Storage modulus of individual star and H(SSLL)-P PBds and their blends

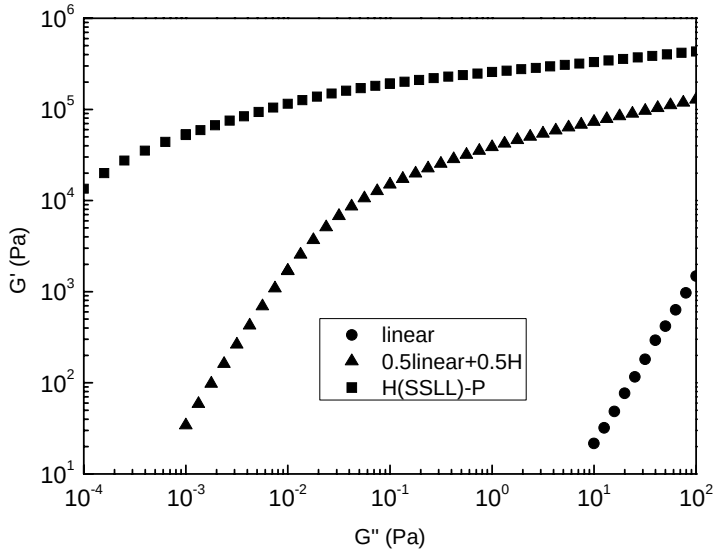

Figure 4-9. Storage modulus of individual linear and H(SSLL)-P PBds and their blends

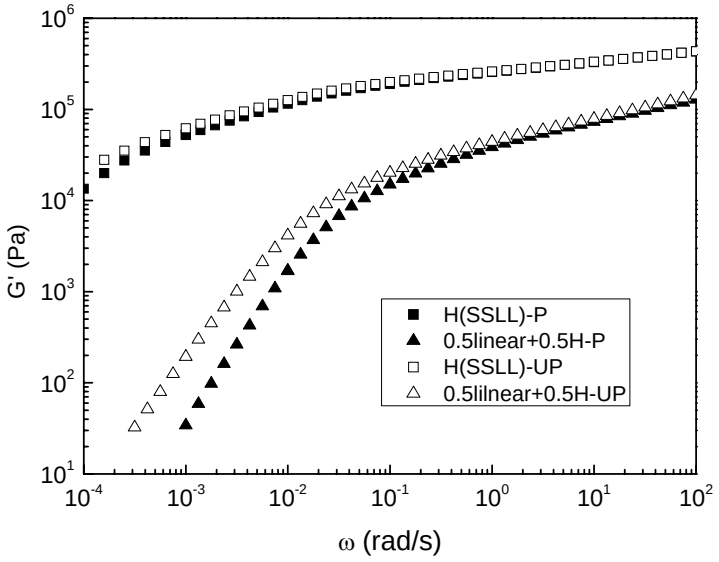

Figure 4-10. Comparison of storage modulus of H(SSLL)-UP, H(SSLL)-P and their blends with linear PBd

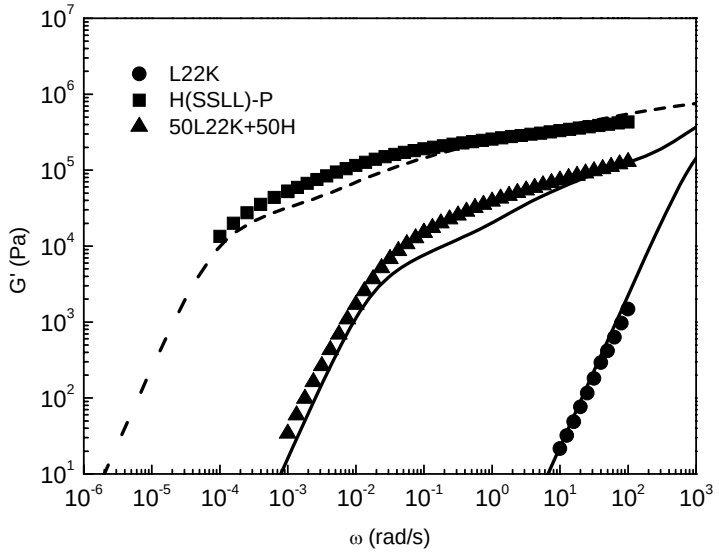

Figure 4-11. Comparison of modeling predictions with rheological data for linear polymer L23K, H polymer H(SSLL)-P PBds and a 50/50 blend of the two.

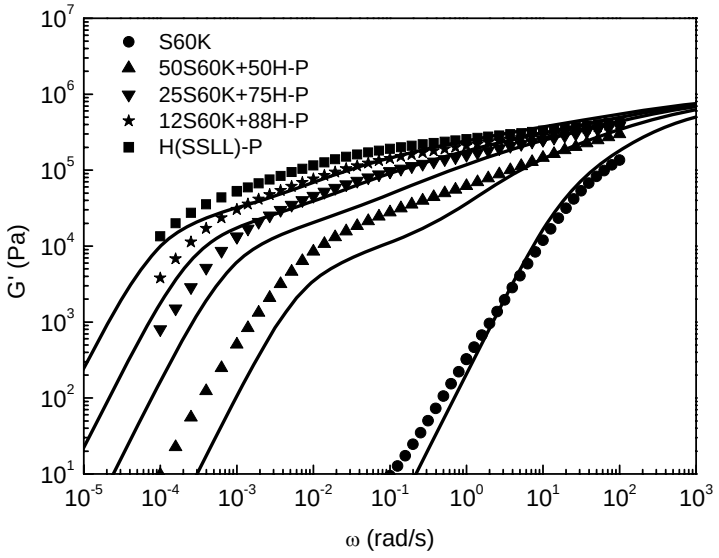

Figure 4-12. Comparison of modeling predictions with rheological data for symmetric star, H polymer H(SSLL)-P PBds and blends of the two.

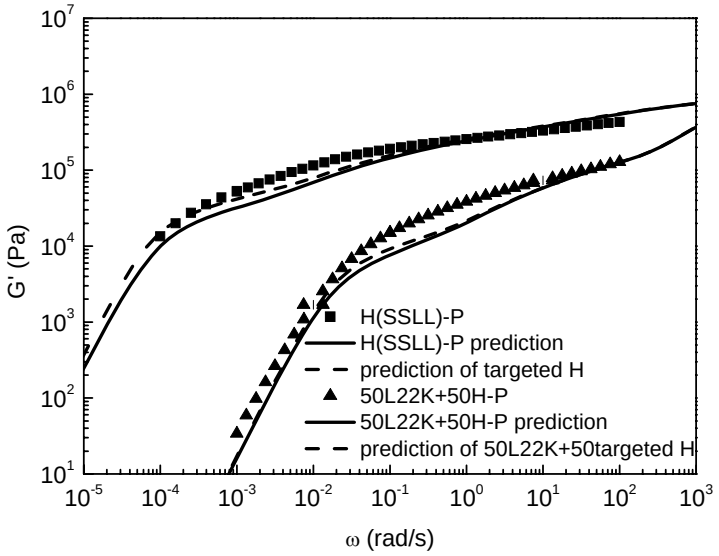

Figure 4-13. Measured storage modulus for H(SSLL)-P compared to that predicted for the pure H sample and that predicted for the mixture of components inferred from TGIC to be present in H(SSLL)-P

4.7 References

Adams, C. H., L. R. Hutchings, P. G. Klein, T. C. B. McLeish, and R. W. Richards, "Synthesis and Dynamic Rheological Behavior of Polybutadiene Star Polymers," Macromolecules 29, 5717-5722 (1996).

Baurngaertel, M., M. E. Rosa, J. Machado, M. Masse and H. H. Winter, "The relaxation time spectrum of nearly monodisperse polybutadiene melts," Rheol.Acta., 75-82 (1992).

Chen, X., and R. G. Larson, "Effect of branch point position on the linear rheology of asymmetric star polymers," Macromolecules 42, 6871-6872 (2008).

Chen, X., C. Costeux, and R. G. Larson, "Characterization and prediction of long-chain branching in commercial polyethylenes by a combination of rheology and modeling methods," J. Rheol. 54, 1185-1205 (2010).

Chen, X., F. J. Stadler, H. Münstedt, and R. G.. Larson, "Method for obtaining tube model parameters for commercial ethene/α-olefin copolymers," J. Rheol. 54, 393-406 (2010).

Daniels, D. R., T. C. B. McLeish, B. J. Crosby, R. N. Young, and C. M. Fernyhough, "Molecular rheology of comb polymer melts. 1. Linear viscoelastic response," Macromolecules 34, 7025-7033 (2001b).

Daniels, D. R., T. C. B. McLeish, R. Kant, B. J. Crosby, R. N. Young, A. Pryke, J. Allgaier, D. J. Groves, and R. J. Hawkins, "Linear rheology of diluted linear, star and model long chain branched polymer melts," Rheol.Acta. 40, 403-415 (2001a).

Dealy J. M., and Larson R. G. Structure and rheology of Molten Polymers, Hanser Gardner Publications, Inc., Ohio (2006).

Fetters, L. J., A. D. Kiss, D. S.Pearson, G. F. Quack, and F. J. Vitus, "Rheological behavior of star-shaped polymers," Macromolecules 26, 647–654 (1993).

Frischknecht, A. L., S. T. Milner, A. Pryke, R. N. Young, R. Hawkins, and T. C. B. McLeish "Rheology of three-arm asymmetric star polymer melts" Macromolecules 35, 4801-4820 (2002).

Graessley, W. W., and J. Roovers , "Melt Rheology of Four-Arm and Six-Arm Star Polystyrenes" Macromolecules 12, 959-965 (1979).

Hakiki, A., R. N.Young, and T. C. B. Mcleish, “Synthesis and characterization of H-shaped polyisoprene,” Macromolecules 29, 3639-3641 (1996).

Janzen, J., and R. H. Colby, “Diagnosing long-chain branching in polyethylenes,” J. Mol. Struct. 485, 569-584 (1999).

Larson, R. G., “Combinational rheology of branched polymer melts,” Macromolecules 34, 4556-4571 (2001).

Lee, A. T., and A. J. McHugh, “Modeling the Rheology of Concentrated AB/AB2 Hyperbranched Polymeric Systems” Macromolecules, 34, 9080–9086 (2001)

Lee, J. H., and L. A. Archer, "Stress relaxation of star/linear polymer blends," Macromolecules 35, 5587-6696 (2002).

McLeish, T. C. B., “Molecular rheology of H-polymers macromolecules, ” Macromolecules 21,1062-1070 (1988).

McLeish, T. C. B., J. Allgaier, D. K. Bick, G. Bishko , P. Biswas , R. Blackwell , B. Blottiere , N. Clarke , B. Gibbs , D. J. Groves , A . Hakiki , R. K. Heenan , J. M. Johnson , R. Kant , D. J. Read, and R. N. Young, “Dynamics of entangled H-polymers: Theory, rheology, and neutron-scattering,” Macromolecules 32, 6734-6758, (1999).

Park, S. J., S. Shanbhag, and R. G. Larson, “A hierarchical algorithm for predicting the linear viscoelastic properties of polymer melts with long-chain branching,” Rheol.Acta 44, 319-330 (2005).

Park. S. J., and R. G. Larson, “Long-chain dynamics in binary blends of monodisperse linear polymers,” J. Rheol. 50, 21-39 (2005).

Pearson, D. S., S.J. Mueller, L. J. Fetters, and N. Hadjichristidis, “Comparison of the rheological properties of linear and star-branched polyisoprenes in shear and elongational flows,”J. Polym. Sci., Polm. Phys. Ed. 21, 2287-2298 (1983).

Perny, S., J. Allgaier, D. Y. Cho, W. Lee, and T. Y. Chang, “Synthesis and structural analysis of an H-shaped polybutadiene,” Macromolecules 34, 5408-5415 (2001).

Rahman, M. S., R. Aggarwal, R. G. Larson, J. M. Dealy, and J. W. Mays, “Synthesis and Dilute Solution Properties of Well-Defined H-Shaped Polybutadienes,” J. Macromolecules 41, 8225-8230 (2008).

Raju V. R., H. Rachapudy, and W. W. Graessley, "Properties of amorphous and crystallizable hydrocarbon polymers. IV. Melt rheology of linear and star-branched hydrogenated polybutadiene," J. Poly. Sci.: Poly. Phys. Ed. 17, 1223–1235 (1979).

Roovers, J., and W. W. Graessley, " Melt rheology of some model comb polystyrenes," Macromolecules 14,766-773 (1981).

Roovers, J., "Melt rheology of H-shaped polystyrenes," Macromolecules 17,1196-1200 (1984).

Roovers, J., and P. M. Toporowski, "Preparation and characterization of H-Shaped polystyrenes mocromolecules," Macromolecules 14,1174-1178, (1981).

Rubinstein, M., and R. H. Colby, "Self‐consistent theory of polydisperse entangled polymers: Linear viscoelasticity of binary blends," J. Chem. Phys. 89, 5291-5306 (1988).

Struglinski, M. J. and W. W. Graessley, ''Effects of polydispersity on the linear viscoelastic properties of entangled polymers. I. Experimental observations for binary mixtures of linear polybutadiene,'' Macromolecules 18, 2630–2643 (1985).

Wang, Z. W., X. Chen, and R. G. Larson, "Computational models for predicting the linear rheology of branched polymer melts," J. Rheol. 54, 223-260, (2010).

Chapter 5
Method for obtaining tube model parameters for commercial ethene/α-olefin copolymers

5.1 Abstract

We propose a method of obtaining all three key "tube" model parameters, namely the plateau modulus G_N^0, the entanglement molecular weight, M_e, and the frictional equilibration time τ_e, from the molecular weight per backbone bond of ethene/α-olefin copolymers with longer co-monomers, ranging from C4 (butylene) to C26 (hexacosene). G_N^0 is obtained from a correlation by Fetters et al. [2002], and M_e is obtained from this using the standard tube-model formula, $M_e = \frac{4}{5}\frac{\rho RT}{G_N^0}$. The equilibration time τ_e is obtained from a remarkable finding by Stadler and Münstedt [2008] that, at fixed weight-average molecular weight, the zero-shear viscosity of linear ethene/α-olefin copolymers is independent of co-monomer type and content, over a wide range of α-olefin co-monomers. From this observation, and from the values of G_N^0 and M_e, we use the tube theory to construct a method for obtaining τ_e from the co-monomer type and content. We show that these a priori values of the tube model parameters, when used in two publicly available models ("hierarchical model" and "BOB" model) for predicting linear rheology, yield accurate predictions for a wide range of polydisperse copolymers. These results show that a priori predictions of linear rheology of complex commercial polyolefin copolymers are now possible.

5.2 Introduction

While the effects of long-chain branching (LCB) on polymer rheology have been much studied, and successful predictions have been made using the well known "tube" model, such predictions have for the most part been limited to "model" polymers with LCB, such as idealized star, "H" and "comb" molecules. This limitation can in principle

be overcome by use of recently developed generalized models for predicting the linear rheology of polydisperse branched polymers. One such model is the "hierarchical model" [Larson (2001)], an extension of Milner and McLeish's theory for mixtures of monodisperse star-branched and linear polymers [Milner et al. (1998)] to generalized mixtures of long-chain branched polymers. This model can, in principle, capture the effects of density of branch points, branch length, and the location of the branches along the polymer backbone, as long as there is no hyper-branching, i.e., only one level of branching is present [Larson (2001); Park and Larson (2005a); Park et al. (2005b); Chen and Larson (2008); Wang et al. (2009)]. Another publicly available generalized computer code that does include hyper-branching is called the "BOB" (for "branch-on-branch") code. It was developed recently by Das et al. [2006] and incorporates similar physical mechanisms as in the "hierarchical model", but differently implemented, and allows for hyperbranching as well.

Despite their potential applicability to commercial polymer melts with LCB, these two generalized models have only been applied to a limited number of experimental data sets for polydisperse branched melts. The models have not been more widely applied to commercial polydisperse melts, in part, because different commercial polymers use different co-monomer types and contents, and these factors affect the key tube model parameters, namely entanglement molecular weight (M_e), plateau modulus (G_N^0), and equilibration time (τ_e), that are needed to make quantitative predictions. Since these input parameters are generally not specified when experimental data are presented, generalized codes such as those discussed above cannot be truly predictive, unless a procedure is given to estimate these parameters a priori.

Fortunately, Fetters et al. [2002] recently presented empirical equations that relate the plateau modulus G_N^0 to m_b, the molecular weight per backbone bond, for co-polymers of ethylene, propylene, butene, pentene, hexene, octene, decene, and longer co-monomers up to octadecene. The plateau modulus, in turn, can be used to obtain the entanglement molecular weight M_e, using a formula that depends on the definition used for M_e, as summarized by Larson et al. [2003]. Although Garcia-Franco and coworkers [2005, 2006] discussed the effects of copolymer content on τ_e qualitatively, no

quantitative relationship between copolymer content and τ_e has been published so far. However, Stadler and Münstedt [2008] have reported extensively on the rheology of polyethylene copolymers lacking LCB and have reported an intriguing finding that the zero shear viscosity η_0 of these polymers is independent of co-monomer type and content, for fixed temperature and molecular weight, over a wide range of co-monomer types, ranging from butene to hexacosene (26 carbons long), and co-monomer mass fractions ranging up to 27%. Since within the tube model the zero-shear viscosity η_0 is proportional to τ_e, and the dependence of G_N^0 and M_e on m_b is known from the correlations of Fetters et al. [2002], this finding of Stadler and Münstedt suggests the possibility of developing a heuristic method of relating τ_e to m_b. Achieving this would yield a method of obtaining all three parameters - G_N^0, M_e, and τ_e - from the value of m_b, which can be calculated from the co-monomer composition. In what follows, we will develop such an approach and validate it by using experimental data for a variety of co-polymers, and two publicly available tube models – the "hierarchical model" (v3.0) and the "BOB" model (v2.3).

5.3 Experiments

5.3.1 Materials

As shown in Table 5-1, nine LLDPE samples were investigated: a series of copolymers published in previous work [Kaminsky et al. (2005); Piel et al. (2006a, 2006b); Stadler et al. (2006a, 2006b, 2007)]. These LLDPE samples have all been synthesized using metallocene catalysts. The number in the designation stands for the length of the co-monomer used. All of the samples studied in this work are believed to be free of long-chain branching and all have a similar molecular weight distribution (MWD), in the range 1.9 to 2.2, which is considered relatively "narrow" for polymers made using commercial catalysts. Characterizations of the samples in Table 5-1 were published in previous work [Stadler et al. (2006a, 2006b, 2007, 2008)]. As given in Eq. (1) below, the side chain weight fraction s_c is inferred from copolymer mole fraction n_c and the number of carbon atoms in the co-monomer l. The molar mass of the backbone M_w^{bb} is

determined by subtracting the molar mass of the short-chain branches $M_w s_c$ from the molar mass of molecule M_w, as shown in Eq. (2). Table 5-1 summarizes the sample properties.

$$s_c = \frac{n_c(l-2)}{n_c(l-2)+2}, \tag{1}$$

$$M_w^{bb} = M_w - M_w s_c, \tag{2}$$

5.3.2 Rheological measurements[1]

The storage and loss modulus data of L6, F18C, F26C, and F26F were previously published by Stadler et al. [2006b, 2007]. The copolymers in Table 5-1 were compression molded into circular disks of 25 mm in diameter and around 1 mm in height using a Vogt Labopress 300 in the vacuum at 180°C and 300 bar pressure for 3 min. Antioxidative stabilizers (0.5 wt.% Irganox 1010 and 0.5 wt.% Irgafos 38 (Ciba SC)) were added to the laboratory scale samples. The commercial copolymers (L4 and L6) were found to be sufficiently stable without additional stabilizer. More details are given elsewhere [Stadler et al. (2006b)].

The rheological data were acquired using a Malvern Instruments Bohlin Gemini and a TA Instruments AR-G2 with a 25 mm parallel plate geometry operated at 150°C. If the zero shear-rate viscosity η_0 was not reached by a frequency sweep (i.e. at a minimum frequency ω of 0.01 rad/s), creep and creep recovery tests were performed additionally. Depending on the molar mass M_w of the copolymer, the creep stress τ was chosen between 2 and 20 Pa. For all samples, it was proven that creep tests were performed in the linear range up to the steady state by varying the creep stress τ and the creep time t_0.

A detailed description of the definitions and the conditions necessary to determine linear and steady creep recovery data is given by Gabriel et al. [1998]. Some of the creep data presented here were confirmed by measurements with the magnetic bearing rheometer [MBR, Link and Schwarzl (1985)]. The MBR and the AR-G2 have several

[1] The rheological experimental data are from Prof. Florian J. Stadler and the manuscript of Section 5.3.2 was prepared by him. X. Chen acknowledges his contribution.

advantages over conventional air bearing rheometers when regarding creep recovery tests (see also Gabriel and Kaschta [1998]).

As the acquisition of creep recovery curves requires quite a long time (the longest tests took about two days), for samples with a high terminal relaxation time it was not possible to perform these tests on all samples, i.e. the variation of the creep time could not be performed to full extent for those samples. To ensure that the thermal stability was maintained during the duration of the creep and creep recovery test, a frequency sweep before and after the creep and creep recovery was performed and compared for signs of degradation. However the samples proved to be thermally very stable. For F18F, no significant change, i.e. no change >5%, in the rheological data, was observed within 9 days at 150°C.

The creep recovery compliance $J_r(t)$ was subsequently used to calculate the retardation spectrum according to the method of Kaschta and Schwarzl [1994]. $J'(\omega)$ and $J''(\omega)$ were then calculated from the retardation spectrum and transformed to $G'(\omega)$ and $G''(\omega)$. With this method it is possible to obtain highly accurate data in the terminal regime down to angular frequencies ω between 10^{-4} and 10^{-5} rad/s. Typically, an overlap between data acquired by frequency sweeps (ω=0.01 to 1000 rad/s) in the linear regime and the converted creep recovery tests of 1-2 decades was possible with an almost perfect match.

Additionally, F26F was also characterized using a Piezo oscillator on a Malvern Instruments Bohlin Gemini high frequency rheometer. With this method it is possible to obtain reliable rheological data in a frequency range between 10 and 32000 rad/s.

5.4 Theory

5.4.1 Models

To validate the equation that we will derive in the following work we use the latest version of "hierarchical model" (v3.0) as improved by Wang et al. [2009], and the "BOB" model (v2.3) [Das et al. (2006)] based on "tube model" theory. Both models include the mechanisms of reptation, primitive path fluctuations of chain ends, and constraint release by "constraint release Rouse motion" or "dynamic dilution," as well as branch point motion. The model of Das et al. also accounts for branches on branches, i.e.,

hyper-branching, but this feature is irrelevant for the work reported here, since we will only consider polymers that are free of LCB. There are some differences among the models in their implementation of relaxation mechanisms and choice of model parameters, as well as in the way the equations are solved and what approximations are used for the fluctuation potential. One main difference is the way to deal with "constraint-release Rouse motion". As described in Chapter 2, when at a time t some polymer chain relaxes suddenly, typically by reptation, the unrelaxed volume fraction Φ is suddenly decreased to account for the loss of the contribution to the modulus represented by that chain. However, the effective constraints that this chain imposes on other chains do not disappear abruptly, but rather allow other chains to explore a new and larger tube by a process of "supertube relaxation". Both models account for this process by using a function, $\Phi_{ST}(t) = \Phi_{ST,0}(\frac{t}{t_0})^{-1/2\alpha}$ which accounts for relaxation due to Rouse motion of the tube in which the polymer is confined. $\Phi_{ST,0} = \Phi(t_0-)$ is the volume fraction of unrelaxed material just before the abrupt relaxation. So Φ_{ST} decreases gradually, while Φ drops suddenly. The "BOB" model (v2.3) [Das et al. 2006] assumes that retraction occurs in a "thin tube" during constraint release Rouse relaxation, while in the "hierarchical model" (v2.0) [Park and Larson (2005a); Park et al. (2005b)] retraction is frozen during constraint-release Rouse motion, as suggested by Milner and McLeish [1997]. The latest version of the "hierarchical model" (v3.0) [Wang et al. (2009)] incorporates the "thin tube" as well as "arm-frozen" options for "constraint-release Rouse motion" (See previous publications for detailed description of these two models [Larson (2001); Park and Larson (2005a); Park et al. (2005b); Wang et al. (2009); Das et al. (2006)]). To validate the equation which will be derived in the following work comprehensively, we use the "BOB" model (v2.3) which makes the "thin tube" assumption and the "hierarchical model" (v3.0) with both "thin tube" and "arm-frozen" options.

While M_e and τ_e are material and temperature dependent, we expect the "dilution exponent", α, and the coefficient of branch point drag, p^2, to be independent of the material. However, different values for α and p^2 have been used, and found

optimal, for the "BOB" model and the "hierarchical model". For the "BOB" model, the value of α has been set to unity, while α has been set to 4/3 in the "hierarchical model". The value of p^2 has no effect on the results we report here, since the samples we consider here are all copolymers without LCB. In our following calculations, we retain the above values of α = 1 and 4/3 for each of these two respective models.

5.4.2 Model input parameters

Here, we explain how we infer values of the material-dependent tube model input parameters, namely G_N^0, M_e, and τ_e, from the value of m_b.

We obtain G_N^0 from Eq. (3) below in units of Pa. Eq. (3) is a correlation of plateau moduli from many ethene/α-olefin copolymers [Fetters et al. (2002)], for which only a qualitative physical explanation was given, namely that the cis-trans ratio (effectively the stiffness) depends on m_b. Since tacticity has been found to affect entanglement density, this simple correlation will not capture effects of changes in tacticity, but should be limited to atactic molecules [Rojo et al. (2004)]. The molecular weight per backbone bond, m_b, in units of g/mol, is calculated from the molecular weight M_{w_mono} of the co-monomer using Eq. (4), and the molecular weight of ethylene in units of g/mol is 28. In this paper, we use this correlation to obtain G_N^0 values for the series of samples listed in Table 5-1.

$$G_N^0 = 24820 m_b^{-3.49} \quad (m_b = 14\text{-}28 \text{ g/mol}), \tag{3a}$$

$$G_N^0 = 41.84 m_b^{-1.58} \quad (m_b = 35\text{-}56 \text{ g/mol}), \tag{3b}$$

$$m_b = [n_c M_{w\_mono} + 28(1 - n_c)] / 2, \tag{4}$$

The definition of the entanglement molecular weight M_e used here is that proposed by Fetters et al. [1994], as described in Larson et al. [2003]:

$$M_e = \frac{4}{5}\frac{\rho RT}{G_N^0} = \frac{4}{5}\frac{\rho RT}{24820 m_b^{-3.49}} = \frac{4}{5}\frac{\rho RT m_b^{3.49}}{24820}, \text{ for } m_b = 14 - 28 \text{ g/mol} \tag{5}$$

with R the universal gas constant, T the absolute temperature, ρ the density, and G_N^0 the plateau modulus. By applying Eq. (3a), we can obtain also a relationship between M_e and m_b. Since m_b of all the samples tested in this paper are in the range 14 to 28

g/mol, we did not need to derive a relationship between M_e and m_b for the second regime for m_b, ranging from 35 to 56g/mol, corresponding to Eq. (3b).

Thus, given the density ρ and m_b, one can obtain the value of M_e at a fixed temperature. Since the polymers we study here are chemically very similar and the densities will not change much from 140 °C to 150 °C, here we assume a constant density value of 788 kg/m^3, i.e. m_b ranging from 14 to 20 g/mol, based on the average of densities reported by Fetters et al. [2002] for a number of copolymers at temperature 140 °C. This choice of a constant density is justified since the densities of polyethylene copolymers reported by Fetters et al. [2002] vary from each other by less than $\pm$ 2%, and encompass a range of copolymers wider than considered here. Using a correlation of density with co-monomer content, we estimate from Fetters et al. [2002] that the densities of the polymers considered here range from around 787 to 794 kg/m^3 i.e., by only around 0.8%, and this small variation in density should thus have a comparably small effect on the entanglement molecular weight, according to Eq. (5).Therefore, we assume a constant density in our work.

Our procedure, then, is to determine τ_e using the finding that the zero-shear viscosity η_0 of ethylene/α-olefin copolymers is independent of the type or percentage of co-monomer, at least up to 26 carbon atoms and 27 wt.% of co-monomer [Stadler and Münstedt (2008)]. Previous work [Pattamaprom and Larson (2001); Likhtman and McLeish (2002)] yielded the following approximate relationship at temperature T between η_0 and τ_e (see Eq. (6)), where C, a numerical constant, depends on the model used in the previous work [Pattamaprom and Larson (2001); Likhtman and McLeish (2002)].

$$\eta_0 = C\tau_e \frac{\rho RT}{M_e}\left(\frac{M}{M_e}\right)^{3.4}, \qquad (6)$$

For many polymers the correlation between η_0 and M_w is available at a fixed temperature, presented as a phenomenological expression of the form $\eta_0(M_w) = \alpha M_w^{\beta}$, where α and β are polymer and temperature dependent [Kan et al. (1980)]. For example, Stadler et al. [2006a] found the relationship

$$\eta_0 = 9\times10^{-15} M_w^{\,3.6}, \tag{7}$$

which is also valid for the polyolefin copolymers in Table 5-1 [Stadler and Münstedt (2008)]. Thus, we take the value 3.6 for the exponent β in the following work.

We now apply Eq. (6), except we change the exponent to $\beta \approx 3.6$, and use the definition of M_e (Eq. (5)), to obtain the ratio of viscosities of two different copolymers at the same temperature:

$$\frac{\eta_{0(co_2)}}{\eta_{0(co_1)}} = \frac{\tau_{e(co_2)}}{\tau_{e(co_1)}} \frac{G^0_{N(co_2)}}{G^0_{N(co_1)}} \left(\frac{M_{(co_2)} M_{e(co_1)}}{M_{(co_1)} M_{e(co_2)}} \right)^{3.6}, \tag{8}$$

here "$M_{(co_i)}$" is the weight-average molecular weight of co-polymer i.

We can now take copolymer "co_1"as the reference polymer, and rewrite Eq. (8) to obtain the equilibration time of copolymer "co_2"in terms of the equilibration time of copolymer "co_1":

$$\tau_{e(co_2)} = \tau_{e(co_1)} \frac{\eta_{0(co_2)}}{\eta_{0(co_1)}} \frac{G^0_{N(co_1)}}{G^0_{N(co_2)}} \left(\frac{M_{(co_1)} M_{e(co_2)}}{M_{(co_2)} M_{e(co_1)}} \right)^{3.6}, \tag{9}$$

We next substitute the relationship between η_0 and M_w (Eq. (7)) into Eq. (9), and obtain the following expression for τ_e for co-polymer co_2 as a function of ratios of G^0_N and M_e for the two copolymers and the value of τ_e for co-polymer co_1:

$$\tau_{e(co_2)} = \tau_{e(co_1)} \frac{G^0_{N(co_1)}}{G^0_{N(co_2)}} \left(\frac{M_{e(co_2)}}{M_{e(co_1)}} \right)^{3.6}, \tag{10}$$

By using substituting Eqs. (3a) and (5) into Eq. (10), we get Eq. (11) below, where τ_e is a function of density and m_b.

$$\tau_{e(co_2)} = \tau_{e(co_1)} \left(\frac{\rho_{(co_2)}}{\rho_{(co_1)}} \right)^{3.6} \left(\frac{m_{b(co_2)}}{m_{b(co_1)}} \right)^{16.054}, \tag{11}$$

Since ρ is assumed to be a constant value discussed above, we can drop the density ratio from Eq. (11) and finally obtain Eq. (12), where τ_e is a function of m_b only, once one obtains τ_e for a single reference polymer co_1. In what follows, we will use

sample L4 as our reference sample and obtain its value of τ_e for both the "hierarchical model"(v3.0) with "arm-frozen" as well as "thin tube" options and for the "BOB" model by fitting each of these models to the rheological data for L4. After obtaining the value for τ_e for L4, we can obtain τ_e for any other copolymer using Eq. (12).

$$\tau_{e(co_2)} \approx \tau_{e(co_1)} \left(\frac{m_{b(co_2)}}{m_{b(co_1)}} \right)^{16.054}, \tag{12}$$

5.5 Modeling results and comparisons with experimental data

In previous efforts to predict the linear viscoelasticity of m-PE (metallocene-catalyzed polyethylene), ensembles of chains representing the distributions of molecular weights and architectures of the actual melts were generated computationally using a Monte Carlo method developed by Costeux et al. [2002]. The molecular weight distribution of a linear chain polymerized using a single-site catalyst follows the Flory (or most probable) distribution, and the corresponding polydispersity index, PDI, is theoretically exactly equal to 2 for infinite molar masses. In the range of molar masses given here, it is marginally below 2. The metallocene-catalyzed polyethylene copolymers studied in our work are all "linear" polymers; i.e., they contain only short unentangled side branches and are free of LCB. For each copolymer, we generate an ensemble of 10,000 molecules following the method described in the work of Das et al. [2006], and use the same ensemble for both simulations. Previous work has shown that 10,000 molecules constitute an adequate ensemble size to obtain results that are insensitive to further increases in ensemble size [Das et al. (2006)].

To proceed, we first determine τ_e of the reference polymer L4 by fitting the predictions of each of the two models (namely the "hierarchical model"(v3.0) and the "BOB" model (v2.3)) to linear viscoelastic data for L4. In this fit, the values of G_N^0 and M_e are calculated from the correlation of Fetters et al. [2002], as explained in Section 5.4 above, so that only the value of τ_e needs to be adjusted to obtain a fit. As shown in Figure 5-1, the model predictions match experimental data well for the values $\tau_e = 1.06 \times 10^{-8} s$ for both the "hierarchical model" with the "arm-frozen" option and for

the "BOB" model, and is $\tau_e = 2.1\times10^{-8} s$ for the "hierarchical model" with the "thin tube" option [Wang et al. (2009)]. Due to the difference of the models, the fitting values of τ_e for the reference copolymer L4 are not exactly the same, but these values are all of the same order of magnitue, namely 10^{-8} s. Next we can insert the values of τ_e and m_b for the reference copolymer L4 into Eq. (12) to obtain Eqs. (13) and (14), which allows us to use the value of m_b for any other copolymer to infer its value of τ_e.

$$\tau_{e(co_1)} = 1.06\times10^{-8}\left(\frac{m_{b(co_1)}}{14.952}\right)^{16.054} \text{ sec.} \quad \text{(for "hierarchical model" with "arm-frozen" option and "BOB" model),} \tag{13}$$

$$\tau_{e(co_1)} = 2.1\times10^{-8}\left(\frac{m_{b(co_1)}}{14.952}\right)^{16.054} \text{ sec.} \quad \text{(for "hierarchical model" with "thin tube" option),} \tag{14}$$

The resulting values of G_N^0, M_e, and τ_e for different copolymers are given in Table 5-2.

Using the values of G_N^0 and M_e in Table 5-2, we now compare the predictions of both the "BOB" model and the "hierarchical model" with the experimental data for the other polymers at 150 °C; see Figures 5-2, 5-3, and 5-4. As shown in these figures, the modulus at high frequency for each sample is consistent with the corresponding experimental measurement, indicating that the correlation of Fetters et al. [2002], Eq. (3a), gives an adequate value of the plateau modulus. In addition, except for polymer F26F for the "BOB" model, the predictions for both models match well with the experimental results for all the copolymers, except in some cases for G' at the lowest frequencies, which indicates that the value of τ_e given in Eq. (14) is an accurate one. Note in Table 5-2 that for F26C, τ_e is 19 times higher than for the reference sample L4, and yet the a priori predictions of the rheology are accurate. For F26F, the experimental data relaxes faster than predicted by the "BOB" model although the match to the "hierarchical model" is acceptable. This failure for the "BOB" model might result from the long length and high volume fraction of the side chain, because, as shown in Table 5-1, M_w^{bb} of F26F is

much smaller than M_w. It is even possible that side-chain phase separation that might occur in this case, the effect of which is obviously not accounted for in the models [Piel et al. (2006b); Stadler and Münstedt (2008)]. Whatever the explanation for this exception might be, the work here indicates that our method to determine τ_e is reasonable for copolymers up to 26 carbon atoms long and with weight fractions at least up to around 22 wt.%.

Furthermore, since at fixed molecular weight the zero shear viscosities of these copolymers are independent of co-monomer type and content, and we have used this fact to obtain modeling input parameters (G_N^0, M_e, and τ_e) as functions of m_b only (co-monomer content), the predicted G'' at fixed molecular weight in the terminal region must, by construction, be independent of modeling input parameters. However, the predictions for G' and for G'' outside of the terminal region can depend on input parameters. To see whether this dependence is significant, we consider the polymer F26F, which has the largest molecular weight and co-monomer length of the polymers we have considered here. We predict the rheology for F26F using the modeling input parameters for the reference polymer L4, and the ensemble of chains generated for F26F, using the "hierarchical model" with the "arm-frozen" option. As shown in Figure 5-5, G'' obtained for the L4 input parameters matches that obtained using the F26F parameters in the terminal region, as required by construction. However, G' obtained using the L4 parameters differs significantly from that obtained using the F26F parameters and from the experimental data. This difference, especially in the high-frequency regime, occurs, because L4 has a different plateau modulus than F26F. Therefore, the tube model input parameters should depend on co-monomer content, despite the insensitivity of the zero-shear viscosity to co-monomer content, at fixed molecular weight.

At this point, we have no explanation for the remarkable finding of Stadler and Münstedt [2008] that for fixed weight average molecular weight and temperature, the zero-shear viscosity of these co-polymers is independent of co-monomer type and content over the range considered. In terms of the tube model, this strange finding must result from the cancellation of the effects of side branches on G_N^0, which decreases with increasing side-branch content, and the effects on the equilibration time τ_e, which tends to

increase with increasing side-branch content. The decrease in G_N^0 also leads to an increase in M_e, which also tends to cause a decrease in viscosity. Finally, an increase in side branch content decreases the length of the backbone, and so this tends to decrease the viscosity at fixed molecular weight. Somehow, perhaps through sheer coincidence, these effects all cancel out for this class of copolymers, at least at the temperature considered, 150°C.

It is known, however, that the kind and content of the side-chains influence the activation energy E_a of the LLDPE and following from that their temperature dependence. The activation energies of the samples discussed in the manuscript were published by Stadler et al. [2007].They range from 27-39 *kJ*/mol. Therefore, the viscosities of various LLDPE shift differently with temperature and consequently an agreement of viscosity data found at a distinct temperature cannot exactly be valid. If one assumes that the maximum temperature at which PE still has a sufficient thermal stability for a rheological characterization is 210°C, one can calculate the effect of temperature on the validity of the η_0-M_w relation. The maximum difference ΔE_a of the activation energy of 10 *kJ*/mol leads to a shift factor change of around 30% between 150°C and 210°C. The relevance of this has to be assessed by taking into account that M_w carries an error of around ±5% which leads to an uncertainty of about ±20% for η_0 [Stadler et al. (2006a), Stadler and Münstedt (2008)].

These considerations show that the empirically found independence of the η_0-M_w-relation on the kind and content of the comonomers of LLDPE is valid only within the accuracy of the measurements but cannot be fulfilled exactly for physical reasons. We can, however, exploit this happy coincidence to obtain an a priori predictive capability for the linear rheology of commercial polydisperse ethene/α-olefin copolymers, at least over the range for which we have validated it. Given that our correlation is likely coincidental, however, it should not be used beyond the range of co-monomer lengths and content considered here, without first doing additional validation studies.

5.6 Conclusions

A procedure to determine the equilibration time τ_e of polyolefin copolymers, based on co-monomer content, has been proposed and validated. This procedure uses the

observation by Stadler and Münstedt (2008) that the zero-shear viscosity for a wide range of copolymers is independent of co-monomer type and mole fraction at fixed molecular weight and temperature. For a series of linear copolymers without LCB with co-monomers ranging from 4 to 26 carbons in length, and with copolymer content up to 22 wt.%, the relationship we derive between τ_e and m_b has been validated by both generalized models for polydisperse branched polymers, namely the branch-on-branch (or "BOB") model and the "hierarchical model"(v3.0). Since τ_e is temperature and material-dependent only, and should be independent of molecular weight and long-chain branching structure, we should be able to apply the method to copolymers with long chain branching.

Table 5-1: Sample information for mPE copolymers

Copolymer	M_w (kg/mol)	PDI	M_w^{bb} (kg/mol)	$l^{(1)}$ (l in C_lH_{2l})	$n_c^{(2)}$	$s_c^{(3)}$
L8	86	2.1	84	8	0.01	0.029
L4	114	2	106	4	0.068	0.064
L6	115	2.2	102	6	0.059	0.106
F8C	153	2	141	8	0.027	0.075
F18C	161	1.9	136	18	0.022	0.15
F26C	174	2.1	136	26	0.023	0.216
F12F	210	2	179	12	0.034	0.145
F18F	216	1.9	177	18	0.027	0.178
F26F	234	2.1	170	26	0.03	0.265

(1) Co-monomer length in number of carbon atoms.

(2) Co-monomer content in molar fraction.

(3) Side chain content in weight fraction.

Table 5-2: Model input parameters for mPE copolymers, derived from Eqs. (3a), (5), (13), (14)

Copolymer	m_b (g/mol)	N_e	G_N^0 (kPa)	M_e (g/mol)	$\tau_e^{(1)}$ ($\times 10^8$ s)	$\tau_e^{(2)}$ ($\times 10^8$ s)
L4(reference)	14.952	37.6	1973	1124	1.06	2.1
L8	14.42	34.3	2239	991	0.594	1.17
L6	15.652	42.1	1682	1319	2.21	4.38
F8C	15.134	38.7	1891	1173	1.29	2.55
F18C	16.464	47.8	1410	1573	4.99	9.86
F26C	17.864	58.5	1060	2092	18.5	36.5
F12F	16.38	47.2	1435	1546	4.60	9.08
F18F	17.024	51.9	1254	1768	8.53	16.9
F26F	19.04	68.6	849	2613	51.5	102

(1) τ_e for "BOB" model as well as "hierarchical model" (v3.0) with "arm-frozen" option.

(2) τ_e for "hierarchical model"(v3.0) with "thin-tube" option

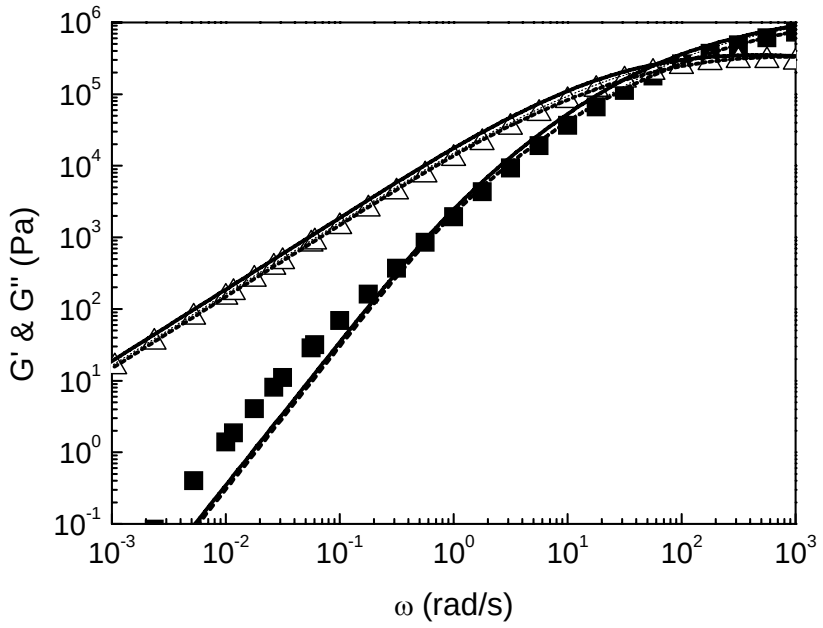

Figure 5-1. G’ and G’’ for metallocene-catalyzed polyethylene copolymer L4 (reference sample) at 150C. The symbols are experimental data; the solid lines, dashed lines and dot lines, respectively, are the fits of the “BOB” model and the “hierarchical model” with “arm-frozen” option and “thin-tube” options, yielding a best-fit value $\tau_e = 1.06 \times 10^{-8} s$ for the “BOB” model and the “hierarchical model” with “arm-frozen” option, and a best-fit value $\tau_e = 2.1 \times 10^{-8} s$ for the “hierarchical model” with “thin-tube” option.

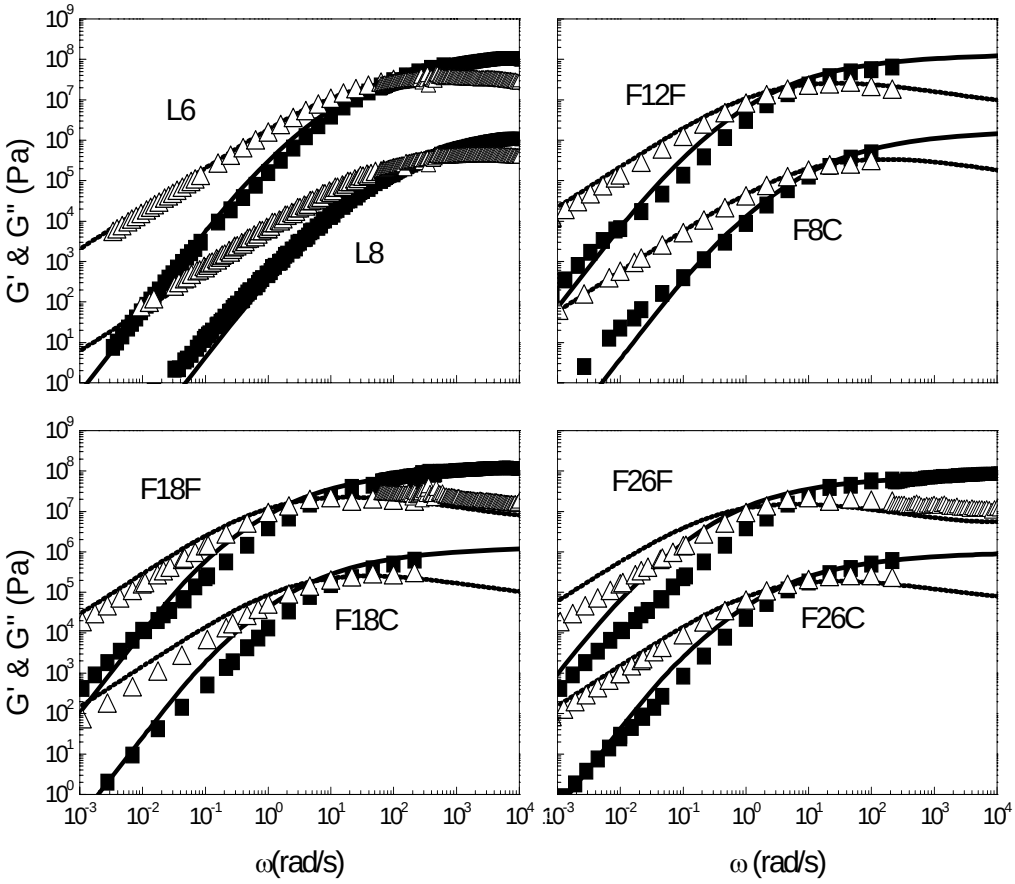

Figure 5-2. Experimental G' and G'' and "BOB" model calculations for metallocene-catalyzed polyethylene copolymers. Squares (solid lines) and triangles (dashed lines), respectively, are experimental data (theoretical predictions) for G' and G''. To separate the data sets, the data for L6, F12F, F18F, and F26F have been shifted by a factor of 100 vertically.

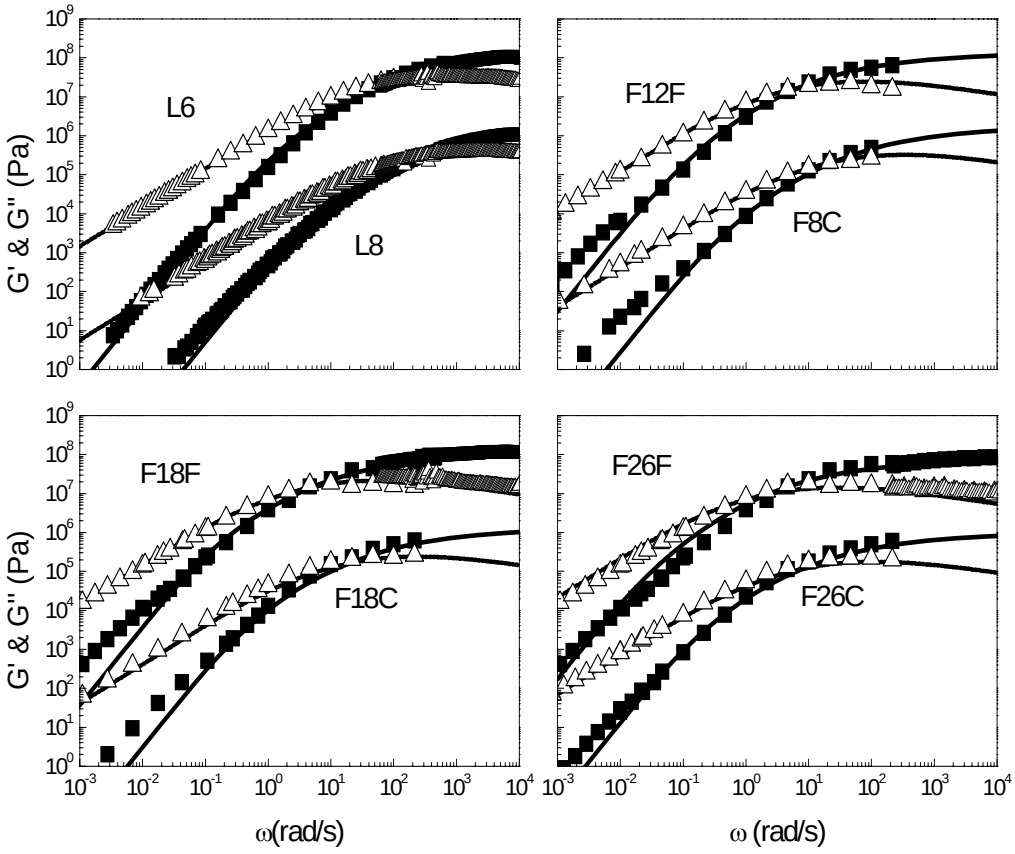

Figure 5-3. The same as Figure 5-2, except the model is the "hierarchical model" (v3.0) with the "arm-frozen" option [Wang et al. (2009)].

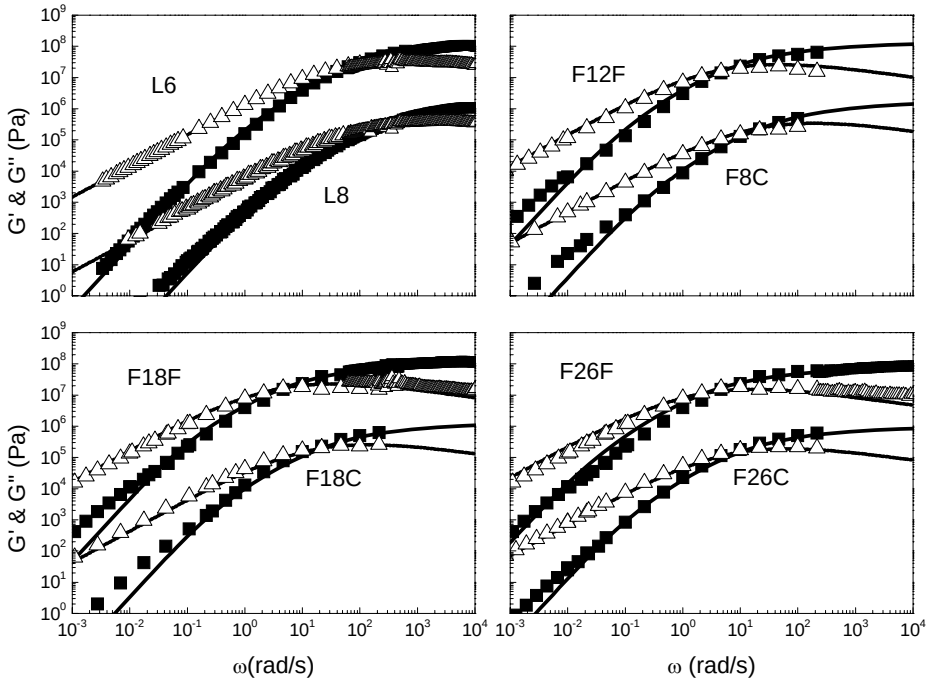

Figure 5-4. The same as Figure 5-2, except the model is the "hierarchical model" (v3.0) with the "thin-tube" option. [Wang et al. (2009)]

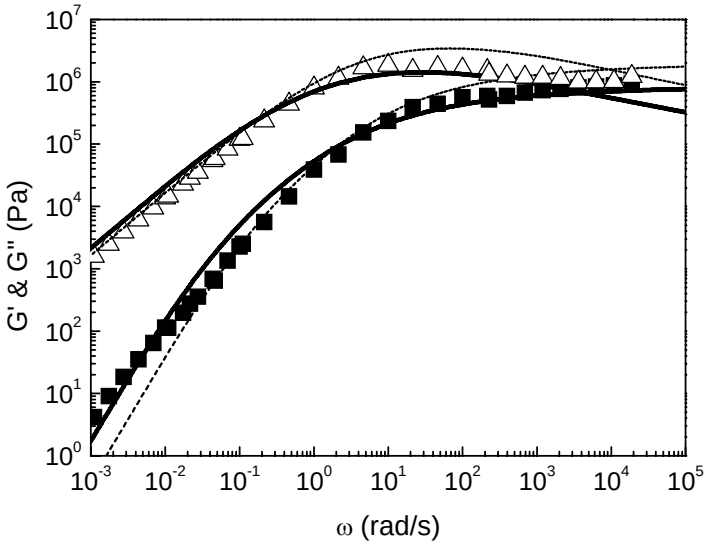

Figure 5-5. Experimental G' and G'' and "hierarchical model" (v3.0) with the "arm-frozen" option for copolymer F26F. Squares and circles, respectively, are experimental data for G' and G''. The solid lines are predictions using parameters G_N^0, M_e, and τ_e determined for F26F using the method described in the text, while dashed lines were obtained using G_N^0, M_e, and τ_e parameters for polymer L4. To separate the data sets, the data for G'' have been shifted by a factor of 10 vertically.

5.7 References

Chen, X., and R. G. Larson, “Effect of branch point position on the linear rheology of asymmetric star polymers,” Macromolecules 41, 6871-6872 (2008).

Costeux, S., P. Wood-Adams, and D. Beigzadeh, “Molecular structure of metallocene-catalyzed polyethylene: Rheologically relevant representation of branching architecture in single catalyst and blended systems,” Macromolecules 35, 2514-2528 (2002).

Das, C., N. J. Inkson, D. J. Read, M. A. Kelmanson, and T. C. B. McLeish, “Computational linear rheology of general branch-on-branch polymers,” J. Rheol. 50, 207-235 (2006).

Fetters, L. J., D. J. Lohse, D. Richter, T. A. Witten, and A. Zirkel, “Connection between polymer molecular-weight, density, chain dimensions, and melt viscoelastic properties,” Macromolecules 27, 4639-4647 (1994).

Fetters, L. J., D. J. Lohse, C. A. Garcia-Franco, P. Brant, and D. Richter, “Prediction of melt state poly(alpha-olefin) rheological properties: The unsuspected role of the average molecular weight per backbone bond,” Macromolecules 35, 10096-10101 (2002).

Gabriel, C., and J. Kaschta, "Comparison of different shear rheometers with regard to creep and creep recovery measurements," Rheologica Acta 37 358–364 (1998).

Gabriel, C., J. Kaschta, and H. Münstedt, "Influence of molecular structure on rheological properties of polyethylenes I. Creep recovery measurements in shear," Rheologica Acta 37 *(1)*, 7-20 (1998).

Garcia-Franco, C. A., B. A. Harrington, and D. J. Lohse, “On the rheology of ethylene-octene copolymers,” Rheol. Acta 44, 591-599 (2005).

Garcia-Franco, C. A., B. A. Harrington, and D. J. Lohse, “Effect of short-chain branching on the rheology of polyolefins,” Macromolecules 39, 2710-2717 (2006).

Kaminsky, W., C. Piel, and K. Scharlach, “Polymerization of ethene and longer chained olefins by metallocene catalysis, ” Macromol. Symp. 226, 25-34 (2005).

Kaschta, J., and F. R. Schwarzl, "Calculation of Discrete Retardation Spectra from Creep Data: 1. Method," Rheologica Acta 33, 517-529 (1994).

Kan, H. C., J. D. Ferry, and L. J. Fetters, “Rubber networks containing unattached macromolecules. 5. stress-relaxation in styrene-butadiene-styrene block co-polymer with unattached linear and star polybutadienes,” Macromolecules 13, 1571-1577 (1980).

Larson, R. G., “Combinatorial rheology of branched polymer melts,” Macromolecules 34, 4556-4571 (2001).

Larson, R. G., T. Sridhar, L. G. Leal, G. H. McKinley, A. E. Likhtman, and T. C. B. McLeish, “Definitions of entanglement spacing and time constants in the tube model,” J. Rheol. 47, 809-818 (2003).

Likhtman, A. E., and T. C. B. McLeish, “Quantitative theory for linear dynamics of linear entangled polymers,” Macromolecules 35, 6332-6343 (2002).

Link, G., and F. R. Schwarzl, "Measuring device for precise evaluation of torsional creep and recovery data," Rheologica Acta 24, 211-219 (1985).

Milner, S. T., and T. C. B. McLeish, “Parameter-free theory for stress relaxation in star polymer melts,” Macromolecules 30, 2159-2166 (1997).

Milner, S. T., T. C. B. McLeish, R. N. Young, A. Hakiki, and J. M. Johnson, “Dynamic dilution, constraint-release, and star-linear blends,” Macromolecules 31, 9345-9353 (1998).

Park, S. J., and R. G. Larson, “Modeling the linear viscoelastic properties of metallocene-catalyzed high density polyethylenes with long-chain branching,” J. Rheol. 49, 523-536 (2005a).

Park, S. J., S. Shanbhag, and R. G. Larson, “A hierarchical algorithm for predicting the linear viscoelastic properties of polymer melts with long-chain branching,” Rheol. Acta 44, 319-330 (2005b).

Pattamaprom, C., and R. G. Larson, “Constraint release effects in monodisperse and bidisperse polystyrenes in fast transient shearing flows,” Macromolecules 34, 5229-5237 (2001).

Piel, C., F. J. Stadler, J. Kaschta, S. Rulhoff, H. Münstedt, and W. Kaminsky, “Structure-property relationships of linear and long-chain branched metallocene high-density polyethylenes and SEC-MALLS,” Macromol. Chem. Phys. 207, 26-38 (2006a).

Piel, C., P. Starck, J. V. Seppälä, and W. Kaminsky, "Thermal and mechanical analysis of metallocene-catalyzed ethene-alpha-olefin copolymers: The influence of the length and number of the crystallizing side chains," J. Polym. Sci.,Part A: Polym. Chem. 44, 1600-1612 (2006b).

Rojo, E., M. E. Munoz, A. Santamaria, and B. Pena, "Correlation between conformational parameters and rheological properties of molten syndiotactic polypropylenes," Macromolecules 25, 1314-1318 (2004).

Stadler, F. J., C. Piel, J. Kaschta, S. Rulhoff, W. Kaminsky, and H. Münstedt, " Dependence of the zero shear-rate viscosity and the viscosity function of linear high-density polyethylenes on the mass-average molar mass and polydispersity," Rheol. Acta 45, 755-764 (2006a).

Stadler, F. J., C. Piel, K. Klimke, J. Kaschta, M. Parkinson, M. Wilhelm, W. Kaminsky, and H. Münstedt, "Influence of type and content of various comonomers on long-chain branching of ethene/alpha-olefin copolymers," Macromolecules 39, 1474-1482 (2006b).

Stadler, F. J., C. Gabriel, and H. Münstedt, "Influence of short-chain branching of polyethylenes on the temperature dependence of rheological properties in shear," Macromol. Chem. Phys. 208, 2449-24 (2007).

Stadler, F. J., and H. Münstedt, "Terminal viscous and elastic properties of linear ethene/alpha-olefin copolymers" J. Rheol., 52, 697-712 (2008).

Wang, Z. W., X. Chen, and R. G. Larson, "Computational models for predicting the linear rheology of branched polymer melts" (submitted to J. Rheol.).

Chapter 6
Characterization and prediction of long chain branching in commercial polyethylenes by a combination of rheology and modeling methods

6.1 Abstract

By blending commercial long-chain branched polyethylenes, Dow AFFINITYTM PL 1840 POLYOLEFIN PLASTOMER and Dow AFFINITYTM PL 1880 POLYOLEFIN PLASTOMER, with the linear polyethylenes ExxonMobile Exact 3132 and Exact 3128 of very similar molecular weight and molecular weight distribution, we detect the effect of ultra-low levels of chain branching (LCB) on linear rheological properties, and validate a generalized "tube" model (the "hierarchical model") for predicting this effect.

6.2 Introduction

The introduction of metallocene-based catalysis is revolutionizing the plastics world, in part by allowing more controllable synthesis of Long Chain Branched (LCB) polymers. This could lead to more optimized polymer processing and higher quality plastic products. To fully realize their potential, the architecture of these metallocene-catalyzed polymers must be accurately characterized, and the relationship between branching type/number and the rheology must be determined. Furthermore, it is well known that very low levels of long chain branching have significant effects on specific processability of polymers, such as extensibility, melt strength, drawability, etc., without undue detrimental effects on mechanical properties. Sensitive and accurate methods to detect long chain branching of sparsely branched polymers are thus very important,

TM Trademark of The Dow Chemical Company

especially those providing information on the number, length and position of the branches.

There are several techniques for determining LCB content [Gabriel et al. (2002a); Simon et al. (2001); Vega et al. (1999)], the most direct ones being spectroscopic methods, in particular nuclear magnetic resonance (NMR). A major drawback of NMR detection is that branches longer than about six carbons cannot be distinguished even by the best instruments [Shroff et al.(1999;2001); Striegel et al. (2000); Gabriel et al. (2002a); Janzen et al. (1999); Liu et al.(2004)]. However, it is the long branches that are most relevant for rheological properties, where "long" means comparable to or greater than the entanglement length, which is a decade or longer than six carbons. Size exclusion chromatography – low-angle light scattering (SEC-LALLS) can determine the presence of LCB based on the hydrodynamic size of the molecule for a given mass. Rheology, on the other hand, is very sensitive to even smaller levels of branching, [Gabriel et al. (2002b); Vega et al. (1999); Liu et al. (2004); Crosby et al. (2002); Lyu et al. (2001); Vega et al. (2002)]. However, the precise sensitivity of rheology to a very low level of long chain branching has not yet been determined. For simplicity, in the following we refer to polymers that lack LCB as "linear" polymers, although they usually do contain short side branches, arising from the co-monomer.

Moreover, the rheological response alone is often ambiguous. Indeed, the rheological characteristics of a linear polymer with broad molecular weight distribution (MWD) can be quite similar to those of a long-chain-branched polymer [Doerpinghaus et al. (2003)]. If the MWD is known, however, it is possible that a detailed comparison of the rheological data with the predictions of a quantitative model that accounts for both LCB and MWD might eliminate this ambiguity [van Ruymbeke et al. (2005)].

The relaxation of a polymer with low or modest levels of LCB is in most cases slower than that of a linear polymer with the same MWD and molecular weights. Using "tube" theory, the relaxation of linear and/or branched polymers can be modeled by combining reptation along the tube, fluctuations of chain ends inside the tubes, and constraint release whereby motions of surrounding chains release entanglements on the tube. Tube-based models predicting the linear viscoelasticity of linear polymers have in some cases achieved quantitative agreement with experiments [Leonardi et al. (2000);

Likhtman et al. (2002); van Ruymbeke et al. (2002); Pattamaprom et al. (2000); Park and Larson (2005a)]. The rheological behavior predicted by the tube model depends sensitively on whether the polymer is a monodisperse linear polymer [Milner and McLeish (1998)], a star polymer [Milner and McLeish (1997); Chen and Larson (2008)], a mixture of nearly monodisperse star and linear polymers [Milner et al. (1998)], a nearly monodisperse "H" polymer [McLeish et al. (1999); Daniels et al. (2001)], or a nearly monodisperse comb polymer [Daniels et al. (2001); Inkson et al. (2006); Chambon et al. (2008)].

For metallocene-catalyzed commercial polymer melts, which are mixtures of polydisperse linear polymers with branched polymers of various architectures, assessing the role of long chain branching is complicated by the effects of molecule-to-molecule variations in the density of branch points, the branch lengths, and the locations of the branches along the polymer backbone or along the other branches, making it difficult to predict their effects on rheological properties. To predict the rheology of metallocene-catalyzed commercial branched polymer melts, then, the tube model must be generalized. Furthermore, for the model to be useful, the parameters used for prediction of simple branched polymers should not be readjusted when more complex branched structures are modeled. As a first step towards a generalized model for polydisperse branched melts, Larson [Larson (2001**)**] developed a "hierarchical model" that generalizes a theory for mixtures of monodisperse star-branched and linear polymers developed by Milner and McLeish [1998]. Park et al. [2005b] improved this "hierarchical model" by including the "early-time fluctuations." Recently the "hierarchical model" has been further improved to allow different choices for the diameter of the tube (i.e., a "thin tube" vs. a "fat tube") in which chains retract during the so-called constraint-release Rouse relaxation [Wang et al. (2010)]. Another publicly available generalized computer code, called the "bob" (for "branch-on-branch") code, developed recently by Das et al. [2006] incorporates similar physical mechanisms as in the "hierarchical model", but differently implemented, and allows for hyperbranching as well. Yet another generalized model for long-chain-branched polymers was presented recently by van Ruymbeke et al. [2006].

Another challenge to predicting the rheology of metallocene-catalyzed commercial polymers is the determination of the tube model parameters, namely the

entanglement molecular weight (M_e), plateau modulus (G_N^0) and equilibration time (τ_e). Metallocene polymers are typically co-monomers of ethylene with longer α-olefins, such as butylene, hexene, octene, etc., and the co-monomer type and percentage affect these parameters. However, we recently proposed a method of obtaining *a priori* all three of these parameters from the molecular weight per backbone bond for copolymers of ethene with longer co-monomers, ranging from C4 (butylene) to C26 (hexacosene) [Chen et al. (2010)]. We demonstrated that the method could predict the rheology of co-polymers lacking long-chain branching. Since the tube-model parameters should in principle be independent of the presence of low levels of long-chain branching, the method should apply to complex commercial polyolefin copolymers.

The objective of this paper is to show that the combined use of rheological measurements and modeling can provide ultra-sensitive detection of the branching structure of a series of polyethylene copolymers with different levels of LCB. In particular, we explore the limits of detection of long-chain branching by blending commercial long-chain branched polyethylenes with polyethylenes lacking LCB. In what follows, Section 6.3 describes the experimental techniques and samples tested. Section 6.4 describes the modeling parameters, ensembles as well as the "hierarchical model" itself. In Section 6.5, we present and discuss our rheological measurements and compare them to the "hierarchical model" calculations. In particular, we show that the "hierarchical model" yields quantitative predictions for our series of polyethylene copolymers with different levels of LCB. Conclusions are drawn in Section 6.6.

6.3 Experiment

6.3.1 Materials

Four LLDPE polymers were investigated: Dow AFFINITY™ [1] PL 1840, AFFINITY™ PL 1880, ExxonMobil Exact 3128 and Exact 3132, all of which had been synthesized commercially using metallocene catalysts. Dow AFFINITY™ PL 1840 and PL 1880, which are both copolymers of ethylene and 1-octene, contain controlled levels of sparse LCB and are commercially available. The other two samples, ExxonMobil Exact 3128 and Exact 3132, contain 1-butene and 1-hexene as the co-monomer,

[1] **™ Trademark of The Dow Chemical Company**

respectively, and are believed to be free of LCB. All four samples have relatively narrow MWD, in the range 2.11 to 2.42. Based on SEC-LALLS, the degrees of LCB for AFFINITY™ PL 1840 and PL 1880 were reported to be, respectively, 0.057 and 0.018 long-chain branches per 1000 carbon atoms [Doerpinghaus and Baird (2002)]. The number of branches per molecule, b_m, was calculated from degree of LCB and M_w using a method described in Costeux et al. [2002], and presented in Table 6-1. The characterization of LCB by SEC-LALLS is based on the smaller hydrodynamic volume and smaller radius of gyration in solution of the long-chain-branched polymers relative to a linear polymer of the same molecular weight. The MWDs of AFFINITY™ PL 1880 and PL 1840 polymers, provided by The Dow Chemical Company, and of Exact 3128 and Exact 3132, provided by ExxonMobil Chemical Co., were determined using SEC. The co-monomer mole fraction n_c of Dow AFFINITY™ polymers and Exxon Exact polymers were provided by The Dow Chemical Co. and ExxonMobil Chemical Co., respectively. Table 6-1 summarizes the properties of these four commercial copolymer polyethylenes.

6.3.2 Experimental Design

To study the effect of long-chain branching on rheological behaviors, we designed a series of mixtures of long-chain branched AFFINITY™ PL 1880 with linear-shaped Exact 3132 (Table 6-2), which have very similar MWDs and molecular weights. The mixtures were blended using 50g Haake mixing bowl at 160^{o}C for 10 min. The labeling "PL1880_xx" in Table 6-2 denotes that xx weight percent of AFFINITY™ PL 1880 was mixed into Exact 3132. For example, PL1880_02 is a mixture of 2% AFFINITY™ PL 1880 in Exact 3132. We also measured the rheology of pure Exact 3132 and pure AFFINITY™ PL 1880 as references. The lowest non-zero level of long-chain branching obtained was 0.355 long chain branches per million carbon atoms by calculation from the blending ratio, as given by Equation (1). The weight-average molecular weight Mw and the co-monomer mole fraction n_c of the blends are calculated by Equations (2) and (3) respectively.

$$\lambda_{blend} = w_{PL1880}\lambda_{PL1880} \tag{1}$$

$$Mw_{blend} = w_{PL1880}Mw_{PL1880} + w_{Exact3132}Mw_{Exact3132} \tag{2}$$

$$n_{c_{blend}} = w_{PL1880} n_{c_{PL1880}} + w_{Exact3132} n_{c_{Exact3132}} \quad (3)$$

where λ is the number of long chain branches per 1000 carbon atoms, and w denotes the polymer weight fraction.

As shown in Tables 6-3, 6-4, and 6-5, we also designed a series of blends of AFFINITY™ PL 1880 with Exact 3128, AFFINITY™ PL 1840 with Exact 3132, and AFFINITY™ PL 1840 with Exact 3128 to explore the detectability of a low level of LCB and compare the results with those for the blends of AFFINITY™ PL 1880 and Exact 3132.

6.3.3 Rheological Measurements

Samples were compression molded into circular disks of 25mm diameter and around 1.2mm in height on a hot press.

For each blend, linear viscoelastic measurements were performed in triplicate, each time on a fresh sample for each polymer, in oscillatory shear mode with an ARES strain-controlled rheometer with a 25-mm parallel plate geometry and around 1 mm gap. Small-strain oscillatory shear tests were conducted at a constant temperature of 150°C with frequency sweeps from 0.01 to 100 rad/s. This temperature was chosen to stay well above the crystallization temperature (around 100°C), and well below temperatures at which thermal degradation becomes a danger. The strain used during the frequency sweeps at constant temperature was varied within the range 5% at the highest frequencies to 70% at low frequencies in or near the terminal zone to maintain adequate sample torque response while ensuring that the measurements were within the linear viscoelastic region as verified by strain sweeps.

After the first run, a limited set of repeat oscillatory tests for the same sample with frequency sweeps from 0.1 rad/s to 100rad/s were carried out to verify the thermal stability of the sample.

6.4 Modeling

6.4.1 Model Description

In the following work we use the latest version of “hierarchical model” (v3.0) based on the generalized tube theory. This model includes the mechanisms of reptation, primitive path fluctuations of chain ends, and constraint release by “constraint release

Rouse motion" and "dynamic dilution," as well as branch point motion. The model accounts for relaxation of branched structures by allowing branches to relax by arm fluctuations. After a branch is completely relaxed, the backbone connected to it can relax by reptation, but this reptation is slowed down by the force drag produced by the relaxed branches. The model does not account for branches on branches, i.e., hyper-branching, but this feature should not have much effect on the work reported here, since the branched polymers AFFINITY™ PL 1880 and AFFINITY™ PL 1840 have a relatively low level of LCB, and hence little hyperbranching. There are some choices in this model's implementation of relaxation mechanisms and model parameters. One main choice is the way to deal with "constraint-release Rouse motion". "When at a time t some polymer chains relax by reptation, the unrelaxed volume fraction Φ is abruptly decreased to account for the loss of the contribution to the modulus represented by those chains. However, the effective constraints that these chains impose on other chains do not disappear abruptly, but rather allow other chains gradually to explore a new and larger tube by a process of "supertube relaxation". The "hierarchical model" accounts for this process by using a function, $\Phi_{ST}(t) = \Phi_{ST,0}(\frac{t}{t_0})^{-1/2\alpha}$ which accounts for relaxation due to Rouse motion of the tube in which the polymer is confined, where α is the "dilution exponent," discussed below. $\Phi_{ST,0} = \Phi(t_0-)$ is the volume fraction of unrelaxed material just before the abrupt relaxation. Thus, Φ_{ST} decreases gradually, even when Φ drops suddenly" [Chen et al. (2010)].

The "bob" model (v2.3) [Das et al. (2006)] assumes that retraction occurs in a "thin tube" during this constraint release Rouse relaxation. In the original "hierarchical model" (v1.0) [Larson (2001)], on the other hand, retraction was assumed to occur in a "fat tube" during constraint release Rouse relaxation, while in the more recent "hierarchical model" (v2.0) [Park and Larson (2005a); Park et al. (2005b)] retraction is frozen during constraint-release Rouse motion, as suggested by Milner et al. [1998]. The latest version of the "hierarchical model" (v3.0) [Wang et al. (2010)] incorporates the "thin tube," "fat tube," as well as "arm-frozen" methods as separate options for constraint-release Rouse motion (See previous publications for a detailed description of the "hierarchical model" [Larson (2001); Park and Larson (2005a); Park et al. (2005b);

Wang et al. (2010)]). Predictions of the "hierarchical model" (v3.0) using the "thin-tube" option with the "dilution exponent" α =4/3 and the coefficient of branch point drag $p^2 = 1/12$ did not accurately predict the rheology of "HDB" high density polyethylenes reported on by Wood-Adams et al. [2000] [Wang et al. (2010)]. (We note, however, that the tube model parameters for these "HDB" polyethylenes, namely the plateau modulus G_N^0 = 1.97MPa and the entanglement molecular weight M_e =1120, do not correspond to the values reported for pure high density polyethylenes, G_N^0 =2.5MPa and M_e =1080 by Fetters et al. [2002]. Thus, we cannot apply our method of obtaining tube parameters to these HDB melts, and we suspect that these HDB's are not pure high density polyethylenes, since their plateau modulus values do not agree with the value for other HDB polymers reported by Fetters et al. [2002].) Since in our previous work [Chen et al. (2010)] we had developed equations to calculate tube model parameters for the "arm-frozen" option with α =4/3 and $p^2 = 1/12$ (details are in Section 6.4.2), we here use the "hierarchical model" (v3.0) with the "arm-frozen" option to predict the rheology of the copolymers in this paper. We have also used the "thin tube" option, and find that the predictions are not quite as accurate as they are with the "arm-frozen" method, as discussed below.

While M_e and τ_e are material and temperature dependent, we expect the "dilution exponent", α, and another parameter, the coefficient of branch-point drag, p^2, to be independent of the material. However, different values for α and p^2 have been used in the literature, and found optimal for different models. For the "hierarchical model", α has been set to 4/3 and the value of p^2 was set to 1/12. In the following calculations, we retain the above values of α = 4/3 and $p^2 = 1/12$ for our predictions using the "hierarchical model" (v 3.0). The initial time step in the integration is set to $t_0 = 10^{-4} \times \tau_e$, and grows as $t_{n+1} = m_{st} \times t_n$ with m_{st} set to 1.00002, which is small enough to obtain converged results for our samples here. Disentanglement relaxation occurs when the density of surviving entanglement $S_a\Phi(\xi)$ for an arm falls below the entanglement threshold, which we take to be unity for our studies. The details are discussed in Wang et al. [2010].

6.4.2 Tube Model Parameters

In addition to the material-independent parameters α and p^2, three material-dependent tube model parameters are needed for predictions by the "hierarchical model", namely the plateau modulus G_N^0, the entanglement molecular weight M_e and the frictional equilibration time τ_e. A relationship between the plateau modulus G_N^0 and m_b, the molecular weight per backbone bond, was reported by Fetters et al. [2002] (Equation (4)). Using the molecular weight M_{w_mono} of the co-monomer, we can calculate the molecular weight per backbone bond, m_b, in units of g/mol (Equation (5)), and use this to obtain G_N^0. The molecular weight of ethylene is 28 g/mol. The plateau modulus G_N^0, in turn, can be used to obtain the entanglement molecular weight M_e, using a formula that depends on the definition used for M_e, as summarized by Larson et al. [2003]. From this, we can derive the relationship between M_e and m_b (Equation (6)).

$$G_N^0 = 24820 m_b^{-3.49} \quad (m_b = 14\text{-}28 \text{ g/mol}), \tag{4}$$

$$m_b = [n_c M_{w\_mono} + 28(1 - n_c)]/2, \tag{5}$$

$$M_e = \frac{4}{5}\frac{\rho RT}{G_N^0} = \frac{4}{5}\frac{\rho RT}{24820 m_b^{-3.49}} = \frac{4}{5}\frac{\rho RT m_b^{3.49}}{24820} \tag{6}$$

with R the universal gas constant, T the absolute temperature, and ρ the density. The density is taken to be 788 kg/m^3, which is an average for a variety of copolymers, whose densities vary by only around 1% [Chen et al. (2010)]. The temperature is 423.15K in this work.

Stadler and coworkers found that the zero-shear viscosity for a wide range of copolymers is independent of co-monomer type and mole fraction at fixed molecular weight and temperature [Stadler et al. (2008)]. Our procedure for determining the equilibration time of the polyolefin copolymers uses this observation. The relationships we derived between τ_e and m_b (Equations (7) and (8)) for the "hierarchical model" with the "arm-frozen" option and with the "thin-tube" option were validated by comparisons of predicted storage and loss moduli with experimental data for a series of linear polyethylene copolymers, with co-monomers ranging from butene to hexacosene (26

carbons long), and co-monomer mass fractions ranging up to 27% [Chen et al. (2010)]. Since for the four sets of co-polymer blends that we study here, the largest co-monomer mass fraction is 16.85% and the largest co-monomer is octene (8 carbons long), the correlation between τ_e and m_b should be applicable here. These correlation are:

$$\tau_{e(co_1)} = 1.06\times10^{-8}\left(\frac{m_{b(co_1)}}{14.952}\right)^{16.054} \text{ sec. (for the "hierarchical model" with "arm-frozen" option)} \quad (7)$$

$$\tau_{e(co_1)} = 2.1\times10^{-8}\left(\frac{m_{b(co_1)}}{14.952}\right)^{16.054} \text{ sec . (for the "hierarchical model" with "thin tube" option)} \quad (8)$$

Equations (7) and (8) were validated for linear copolymers [Chen et al. (2010)]. However, since τ_e is temperature and material dependent only, and should be independent of molecular weight and long-chain branching structure, we should be able to apply the same parameters to copolymers with long chain branching. The calculated tube model parameters for the "hierarchical model" with "arm-frozen" option for different blend components are shown in Tables 6-6, 6-7, and 6-8. The calculated tube model parameters for the "hierarchical model" with "thin tube" option for the blends of AFFINITY^{TM} PL1880 with Exact 3132 are shown in Table 6-9. Since the blends contain components with different co-monomer type and amount, and the "hierarchical model" does not allow assigning different tube model parameters to the different components of the melt, we determine an average value of m_b by weight averaging the values of m_b from the two components in the blend, and then we use this average value of m_b to determine the tube model parameters for the blend. Later, we will show that we get very similar results if we use the m_b value for either of the two components in the blend, and so our results are not sensitive to the averaging procedure used.

6.4.3 Modeling the Molecular Weight and Branching Distributions

In previous efforts to predict the linear viscoelasticity of m-PE (metallocene-catalyzed polyethylene), ensembles of chains representing the distributions of molecular weights and architectures of the actual melts were generated computationally using a Monte Carlo method developed by Costeux et al. [2002]. The molecular weight

distribution of a linear chain polymerized using a single-site catalyst follows the Flory (or most probable) distribution, and the corresponding polydispersity index, PDI, theoretically should approach 2 as the average molar mass becomes large. In the range of average molar masses given here, the PDI is indeed very close to 2. For the four LLDPE co-polymers, the ensembles were generated following the previous method [Das et al. (2006)], and are summarized in Table 6-10, showing their statistical compositions. All molecules in Exact 3128 and Exact 3132 ensembles are taken to be linear chains without long chain branches. (Exact 3128 and 3132 contain short-chain branches, but these are not modeled explicitly, but only through their effect on the model parameters, as discussed above.) The ensembles for AFFINITY™ PL 1840 and PL1880 contain linear, star, H, and comb shaped molecules. From Table 6-10, we can see AFFINITY™ PL 1840 has more molecules with long chain branches than AFFINITY™ PL1880 does, because the former has a higher degree of LCB. Using the generated ensembles, we calculated the number of branches per molecule as the total number of branches in the ensemble divided by total number of molecules, which gives 0.156 and 0.071, respectively, for AFFINITY™ PL 1840 and PL1880, similar to the values calculated from experimental characterization data (0.1535 for AFFINITY™ PL1840 and 0.0697 for AFFINITY™ PL1880).

For each blend, we first generate an ensemble of branched polymers and another ensemble of linear polymers, and then combine them in proportion to their concentrations in the blend, to generate a combined ensemble of 10,000 molecules, following the method described in the work of Das et al. [2006]. The number of the chains of each component is taken to be proportional to the concentration of that component, but weighted differently for each component to give the correct overall weight fraction of each component in the blend. For example, the ensemble containing 40 wt% AFFINITY™ PL1880 and 60 wt% Exact3132 contains 4000 chains of AFFINITY™ PL1880 and 6000 chains of Exact3132. Because the weight average molecular weights of AFFINITY™ PL1880 and Exact3132 differ somewhat, the weight fraction assigned to each molecule in the AFFINITY™ PL1880 ensemble in the blend differs from that assigned to the molecules in the Exact3132 ensemble, so that the total weight fraction of AFFINITY™ PL1880 chains equals 40%, as required.

Next, we transform the data format of the ensemble generated by the "bob" model to a format required to use it as input to the "hierarchical" model (v3.0). Finally, since the "hierarchical model" (v 3.0) does not deal with branch-on-branch (i.e., hyperbranched) structures, the branch-on-branch structures in the ensemble generated by the "bob" model are changed to comb shaped chains with the same arms and backbones arranged orderly. Figure 6-1 shows the structure of one hyperbranched molecule selected from the AFFINITY™ PL1840 ensemble and how it is converted to a comb shaped chain. Since AFFINITY™ PL1840 has the largest degree of LCB, some of the ensembles of PL1840 blends contain more hyperbranched structures than others do, while some blends do not contain any hyperbranched structures. To minimize the number of hyperbranched structures that need to be converted to combs, we generated several repeat ensembles for AFFINITY™ PL1840 (five ensembles), PL1840_80 (three ensembles), and PL1840_60 (two ensembles), and selected from these the ensemble containing the fewest branch-on-branch structures (one or two branch-on-branch chains). For AFFINITY™ PL1840, the total hyperbranched weight fraction for the ensemble selected was less than 0.1%, corresponding to only two hyperbranched molecules that needed to be converted to combs. Of the five ensembles generated for AFFINITY™ PL1840, the largest number of hyperbranched structures found was 8 hyperbranched chains, amounting to a weight fraction of 0.6%. We now validate our procedure for eliminating hyperbranched molecules by considering its effect on the rheology of AFFINITY™ PL1840, which has the highest LCB level of any of the melts considered here. In Figure 6-2, we compare the results predicted by the "hierarchical model" for the ensemble with two hyperbranched molecules to the one with 8 hyperbranched molecules, in both cases with the hyperbranched molecules converted to comb-shaped chains. There is very little difference in the rheology of these two ensembles, which indicates that selecting an ensemble with a minimal number of hyperbranched chains does not significantly bias the rheology, since the fraction of hyperbranched molecules is very small. As a further check, since the "bob" model is able to account for hyperbranched molecules, we ran the "bob" model on the original ensemble with 8 hyperbranched molecules as well as on the ensemble modified by changing the 8 hyperbranched molecules to combs. As shown in Figure 6-2, little difference results from changing the hyperbranched molecules to combs.

(For the same ensemble, the predictions of the "bob" model differ considerably from those of the "hierarchical" model because different model parameters are needed to optimize the predictions of the two models. Since our purpose here is only to show the effect of replacing hyperbranched molecules with combs, we do not re-optimize the parameters for the "bob" model.) Our work here and previous work [Das et al. (2006)] have shown that 10,000 molecules constitutes an adequate ensemble size to obtain results that are insensitive to further increases in ensemble size.

6.5 Results and discussions

6.5.1 Measurement Results

AFFINITY™ PL 1880 and Exact 3132 have almost identical weight and number average molecular weights and therefore should have nearly the same rheological properties, if both samples were free of long-chain branching. Figure 6-3, however, shows that G' for the pure AFFINITY™ PL 1880 is distinctly different from that of Exact 3132, despite the nearly identical molecular weight distributions of the two polymers. Some of the differences in rheology between these samples might be traced to the difference in the co-monomers used (octene for AFFINITY™ PL 1880 and hexene for Exact 3132). However, based on our earlier rheological studies on linear co-polymers of varying composition [Chen et al. (2010)], there is little doubt that for the modest levels of co-mononer present and similar co-monomer content in these polymers, the major reason for the difference in rheology between the two samples is the presence of long-chain branching in AFFINITY™ PL 1880. From the triplicate runs of each sample, we determined the relative standard error of each data point to be less than 3%, even at low frequency, which is within the size of symbols used in our data plots, and much smaller than the differences between the blends. Note from Figure 6-3 that the presence of as little as 2% AFFINITY™ PL 1880 in Exact 3132 leads to a distinguishable difference in the G' curves. This result shows clearly the effect of very small levels of long chain branches on the rheology. Figure 6-4, which presents the rheology of blends of AFFINITY™ PL 1880 with Exact 3128, also allows discrimination between pure Exact 3128 and PL1880_02, the latter containing only 2% AFFINITY™ PL 1880. Although Exact 3132 and Exact 3128 have very similar molecular weights, Exact 3132 contains

hexene as the co-monomer and Exact 3128 contains butene, and the former relaxes a little bit slower than the latter, apparently due to the small difference in friction from the small side branches, as described earlier [Chen et al. (2010)]. The blends of AFFINITY™ PL 1880 with Exact 3132 and of AFFINITY™ PL 1880 with Exact 3128 for different concentrations of AFFINITY™ PL 1880 also follow this trend; i.e. Exact 3132 blends relax slower than do Exact 3128 blends at the same composition of branched polymer (selected data sets shown in Figure 6-5).

Figures 6-6 and 6-7 show G' data for blends of AFFINITY™ PL 1840 with Exact 3132 and of AFFINITY™ PL 1840 with Exact 3128. Although the weight average molecular weight of AFFINITY™ PL 1840 is significantly smaller than that of Exact 3132 or Exact 3128, both sets of blends reveal that as the percentage of AFFINITY™ PL 1840 in the blend increases, G' increases, even though the average molecule weight of the blend decreases. This shows the dominant effect of long-chain branching on G'.

Comparing the mixtures in Tables 6-3 and 6-5, at the same percentage of branched polymer, mixtures of AFFINITY™ PL 1840 with Exact 3128 have more long-chain branches than do mixtures with AFFINITY™ PL 1880 at the same percentage of the branched polymer, while mixtures with AFFINITY™ PL 1880 have higher molecular weight at the same composition. As shown in Figure 6-8, the mixtures of AFFINITY™ PL 1840 with Exact 3128 relax slower than do those of AFFINITY™ PL 1880 and Exact 3128 at the same composition. Thus, for these blends, the level of long-chain branching, which is higher in the AFFINITY™ PL 1840 mixtures, has a more significant effect on relaxation than does the difference in molecular weight, which is higher in the AFFINITY™ PL 1880 blends.

6.5.1 Modeling Results

As discussed above, the correlations between τ_e and m_b for the "hierarchical model" (v 3.0) with the "arm-frozen" option and the "thin-tube" option are presented in equation (7) and (8). Using the values of G_N^0, M_e and τ_e in Tables 6-6 and 6-9, we now compare the predictions using each option with the experimental data for blends of AFFINITY^{TM} PL1880 with Exact3132. As shown in Figure 6-9, the "thin-tube" option

does not yield as accurate results as the "arm-frozen" option does. Thus, we use the "hierarchical model" with "arm-frozen" option in our following work.

Using the values of G_N^0, M_e and τ_e in Tables 6-6, 6-7, and 6-8, we now compare the predictions of the "hierarchical model" (v3.0) with the "arm-frozen" option (with no adjustable parameters) with the experimental data for the polymer blends at 150 °C in Figures 6-10 and 6-12. As shown in these figures, the frequency-dependent storage and loss moduli for all blends are consistent with the corresponding experimental measurements, with some exceptions near the terminal regime. Note in Figure 6-11 that for blends of AFFINITY™ PL 1880 and Exact 3128, the predictions for G' sometimes lie above the data at low frequencies, while the reverse is the case for some of the blends of AFFINITY™ PL 1840 and Exact 3132, in Figure 6-12. One possible reason of the deviation is due to the choice of tube input parameters. To test this, we used the tube parameters for Exact 3128 to predict the LVE data for pure AFFINITY™ PL 1880 (whose tube parameters differ the most from those for Exact 3128), and compare these predictions to those obtained using with the tube parameters for AFFINITY™ PL1880. As shown in Figure 6-13, the predictions using the two sets of tube parameters are almost the same. We also carried out this analysis for the blends of AFFINITY™ PL1880 with Exact3132, and for blends of AFFINITY™ PL1840 with Exact3132, and found little difference resulting from the different choices of tube parameters. The reason for this is that for co-monomers that are not too different from each other, as is the case for the blends considered here, the rheological predictions are rather insensitive to the co-monomer type and amount, for a fixed molecular weight distribution, since the effects of changes in the different parameters largely cancel each other out. Only for very large differences in co-monomer type, for example C4 (butylene) vs. C26 (hexacosene), does a significant difference in rheological predictions appear (cf. Fig. 5 of Chen et al. 2010). Thus, the discrepancy between the predicted and experimental data is likely due to our modeling of the effects of LCB, and not due to choice of parameter values. The deviation for the 5% blend of AFFINITY™ PL 1880 in Exact 3128 in Figure 6-11 may reflect a failure of the model to capture accurately the effects of very small levels of LCB. We note that blends with a very small level of long-chain branching are essentially star-linear

blends, and tube models have a particularly difficult time simulating such blends (see, for example, Fig. 6 of Wang et al. 2010).

In the low-frequency terminal zone, where only the longest relaxation times contribute to the viscoelastic behavior, G' and G'' must follow the well-known frequency dependence:

$$G' \propto \omega^2,\ G'' \propto \omega \tag{9}$$

From Figures 6-10 and 6-12, it can be seen that, for all the blends except the pure linear copolymers Exact 3132 and Exact 3128, the experiments do not reach the terminal regime. However, the predictions, if they are accurate, could be used to predict the behavior in the terminal regime. Thus the "hierarchical model" and similar models might be useful not only to detect the presence of LCB in commercial copolymers, but also to predict the rheology of branched commercial copolymers at frequencies not readily attainable experimentally.

6.6 Conclusions

A sensitive method based on the linear viscoelastic response has been successfully applied to detect and quantify the presence of long chain branching (LCB) in sparsely branched commercial polyethylenes. The predictions of the "hierarchical model", which is a tube-based algorithm for predicting the rheology of complex mixtures of branched and linear polymers, show good agreement with experimental results for most samples, although deviations occurred for some of the samples at low frequencies. The work presented here shows that rheological measurements can provide highly sensitive information on the branching structure of polyethylene copolymers with different levels of LCB.

Table 6-1. Description of the four LLDPE co-polymers

	Polymer classification	M_w (kg/mol)	M_w/M_n	n_c (1)	w_c (2)	LCB (n/1000C)	b_m (3)
AFFINITY ™ PL 1840	ethylene/1-octene	87	2.40	0.0390	0.1390	0.057	0.1535
AFFINITY ™ PL 1880	ethylene/1-octene	116	2.10	0.0482	0.1685	0.018	0.0697
Exact 3128	ethylene-butene	115	2.21	0.0580	0.1090	0	0
Exact 3132	ethylene-hexene	112	2.12	0.0530	0.1440	0	0

(1) Co-monomer content in mole fraction

(2) Co-monomer content in weight fraction

(3) Number of branches per molecule

Table 6-2. Composition and LCB levels of mixtures of AFFINITY™ PL 1880 with Exact 3132

Sample name	AFFINITY™ PL1880 (branched)	Exact 3132 (linear)	LCB (n/1000C)	n_c	M_w (kg/mol)
AFFINITY™ PL 1880	100%	0%	0.0177	0.0482	116
PL1880_80	80%	20%	0.0142	0.0492	115
PL1880_60	60%	40%	0.0106	0.0502	114
PL1880_40	40%	60%	0.00709	0.0511	114
PL1880_20	20%	80%	0.00355	0.0521	113
PL1880_05	5%	95%	0.000887	0.0529	112
PL1880_02	2%	98%	0.000355	0.0530	112
Exact 3132	0%	100%	0	0.0531	112

Table 6-3. Composition and LCB levels of mixtures of AFFINITY™ PL 1880 with Exact 3128

Sample name	AFFINITY™ PL1880 (branched)	Exact 3128 (linear)	LCB (n/1000C)	n_c	M_w (kg/mol)
AFFINITY™ PL 1880	100%	0%	0.0177	0.0482	116
PL1880_80	80%	20%	0.0142	0.0502	116
PL1880_60	60%	40%	0.0106	0.0521	116
PL1880_40	40%	60%	0.00709	0.0541	116
PL1880_20	20%	80%	0.00355	0.0560	115
PL1880_05	5%	95%	0.000887	0.0575	115
PL1880_02	2%	98%	0.000355	0.0578	115
Exact 3128	100%	0%	0	0.0580	115

Table 6-4. Composition and LCB levels of mixtures of AFFINITY™ PL 1840 with Exact 3132

Sample name	AFFINITY™ PL1840 (branched)	Exact 3132 (linear)	LCB (n/1000C)	n_c	M_w (kg/mol)
AFFINITY™ PL 1840	100%	0%	0.057	0.0390	87
PL1840_80	80%	20%	0.0456	0.0418	92
PL1840_60	60%	40%	0.0342	0.0446	97
PL1840_40	40%	60%	0.0228	0.0475	102
PL1840_20	20%	80%	0.0114	0.0503	107
PL1840_05	05%	95%	0.00285	0.0524	111
PL1840_02	02%	98%	0.00114	0.0528	112
Exact 3132	0%	100%	0	0.0531	112

Table 6-5. Composition and LCB levels of mixtures of AFFINITY™ PL 1840 with Exact 3128

Sample name	AFFINITY™ PL1840 (branched)	Exact 3128 (linear)	LCB (n/1000C)	n_c	M_w (kg/mol)
AFFINITY™ PL 1840	100%	0%	0.05695	0.0390	87
PL1880_40	40%	60%	0.02278	0.0504	104
PL1840_20	20%	80%	0.01139	0.0542	110
Exact 3128	0%	100%	0	0.0580	115

Table 6-6. Tube model parameters for blends of AFFINITY™ PL 1880 and Exact 3132 (for the "hierarchical model" with "arm-frozen" option)

co-polymers	M_w	n_c	m_b	G_N^0	M_e	τ_e
	kg/mol		g/mol	Pa	g/mol	s
AFFINITY™ PL 1880	116	0.0482	16.02	1549	1433	3.24E-08
PL1880_80	115	0.0492	15.93	1582	1403	2.94E-08
PL1880_60	114	0.0502	15.83	1618	1371	2.65E-08
PL1880_40	114	0.0511	15.72	1657	1339	2.37E-08
PL1880_20	113	0.0521	15.61	1699	1305	2.11E-08
PL1880_05	112	0.0529	15.52	1733	1279	1.93E-08
PL1880_02	112	0.0530	15.50	1740	1274	1.89E-08
Exact 3132	112	0.0531	15.49	1745	1271	1.87E-08

Table 6-7. Tube model parameters for blends of AFFINITY™ PL 1880 and Exact 3128 (for the "hierarchical model" with "arm-frozen" option)

co-polymers	M_w	n_c	m_b	G_N^0	M_e	τ_e
	kg/mol		g/mol	Pa	g/mol	s
AFFINITY™ PL 1880	116	0.0482	16.02	1549	1433	3.22E-08
PL1880_80	115	0.0502	15.83	1618	1371	2.64E-08
PL1880_60	114	0.0521	15.61	1699	1305	2.11E-08
PL1880_40	114	0.0541	15.36	1795	1236	1.64E-08
PL1880_20	113	0.0560	15.10	1907	1163	1.24E-08
PL1880_05	112	0.0575	14.89	2004	1107	9.87E-09
PL1880_02	112	0.0578	14.84	2025	1095	9.41E-09
Exact 3128	115	0.0580	14.81	2039	1088	9.11E-09

Table 6-8. Tube model parameters for blends of AFFINITY™ PL 1840 and Exact 3132 (for the "hierarchical model" with "arm-frozen" option)

co-polymers	M_w	n_c	m_b	G_N^0	M_e	τ_e
	kg/mol		g/mol	Pa	g/mol	s
AFFINITY™ PL 1840	87	0.039	15.64	1687	1315	2.18E-08
PL1840_80	92	0.0418	15.64	1686	1315	2.18E-08
PL1840_60	97	0.0446	15.62	1692	1311	2.15E-08
PL1840_40	102	0.0475	15.59	1703	1302	2.08E-08
PL1840_20	107	0.0503	15.55	1721	1289	1.99E-08
PL1840_05	111	0.0524	15.50	1739	1276	1.9E-08
PL1840_02	112	0.0528	15.49	1742	1273	1.88E-08
Exact 3132	112	0.0531	15.49	1745	1271	1.86E-08

Table 6-9. Tube model parameters for blends of AFFINITY™ PL 1880 and Exact 3132 (for the "hierarchical model" with "thin-tube" option)

co-polymers	M_w	n_c	m_b	G_N^0	M_e	τ_e
	kg/mol		g/mol	Pa	g/mol	s
AFFINITY™ PL 1880	116	0.0482	16.02	1549	1433	6.39E-08
PL1880_80	115	0.0492	15.93	1582	1403	5.79E-08
PL1880_60	114	0.0502	15.83	1618	1371	5.23E-08
PL1880_40	114	0.0511	15.72	1657	1339	4.68E-08
PL1880_20	113	0.0521	15.61	1699	1305	4.17E-08
PL1880_05	112	0.0529	15.52	1733	1279	3.81E-08
PL1880_02	112	0.0530	15.50	1740	1274	3.74E-08
Exact 3132	112	0.0531	15.49	1745	1271	3.69E-08

Table 6-10. Number of molecules of each architectural type in ensembles generated for each pure melt

Molecule shape	linear	Star	H	Comb				$b_{m\_c}^{(1)}$
Number of branches	0	1	2	3	4	5	6	
AFFINITY ™ PL 1840	8831	883	213	54	11	3	5	0.156
AFFINITY ™ PL 1880	9375	550	66	8	1	0	0	0.071
Exact 3128	10000	0	0	0	0	0	0	0
Exact 3132	10000	0	0	0	0	0	0	0

(1) Calculated number of branches per molecule for the generated ensemble

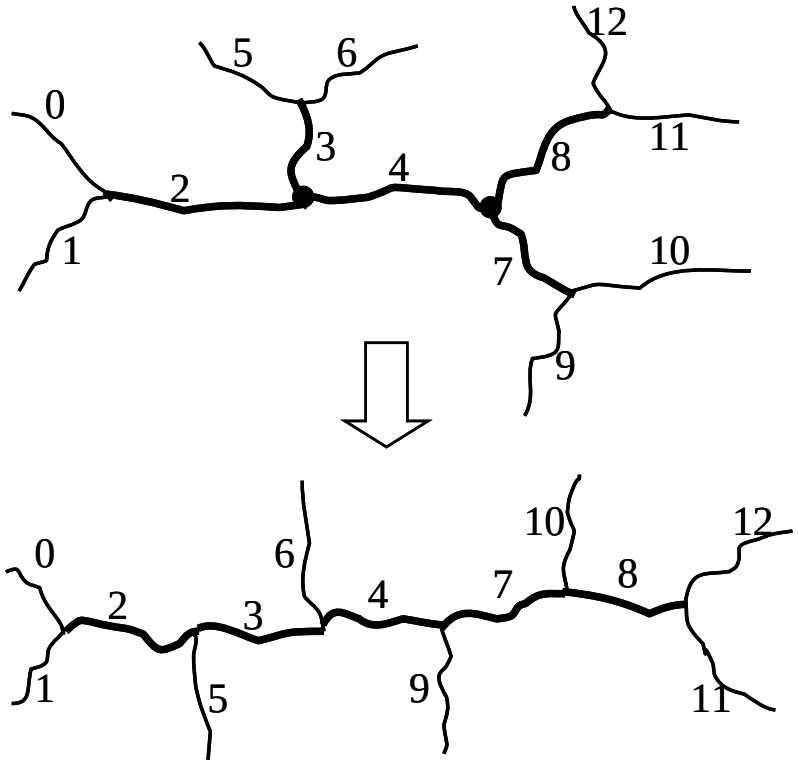

Figure 6-1. Illustration of algorithm for changing branch-on-branch structure (top) to comb shaped molecule (bottom). Segments in bold are backbone segments. Hyperbranching points (in bold) are removed by moving hyperbranching backbone segments into a single collinear comb backbone and attaching their arms directly onto this backbone, as shown.

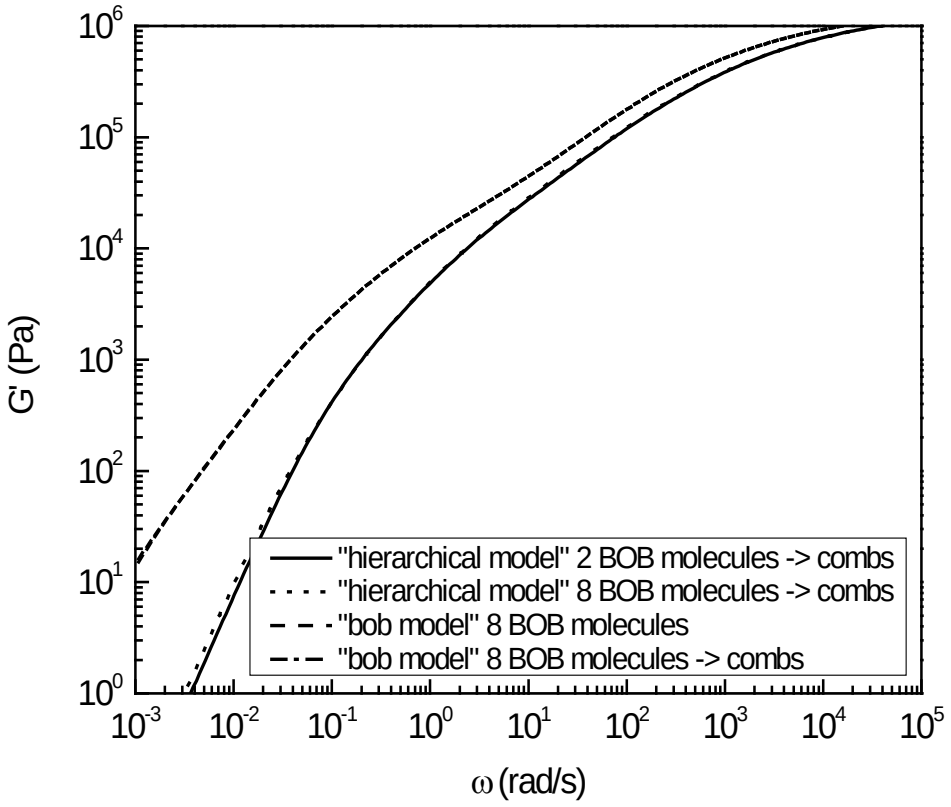

Figure 6-2. Comparisons of calculated storage moduli for ensembles with branch-on-branch (BOB) structures and with branch-on-branch structures replaced by combs. Solid and dotted lines are predictions by the "hierarchical" model for ensembles that originally contained 2 hyperbranched chains and 8, respectively. Dashed and dot-dash lines (which lie on top of each other) are predictions by the "bob" model for an ensemble with 8 hyperbranched chains and with these 8 hyperbranched chains converted to combs.

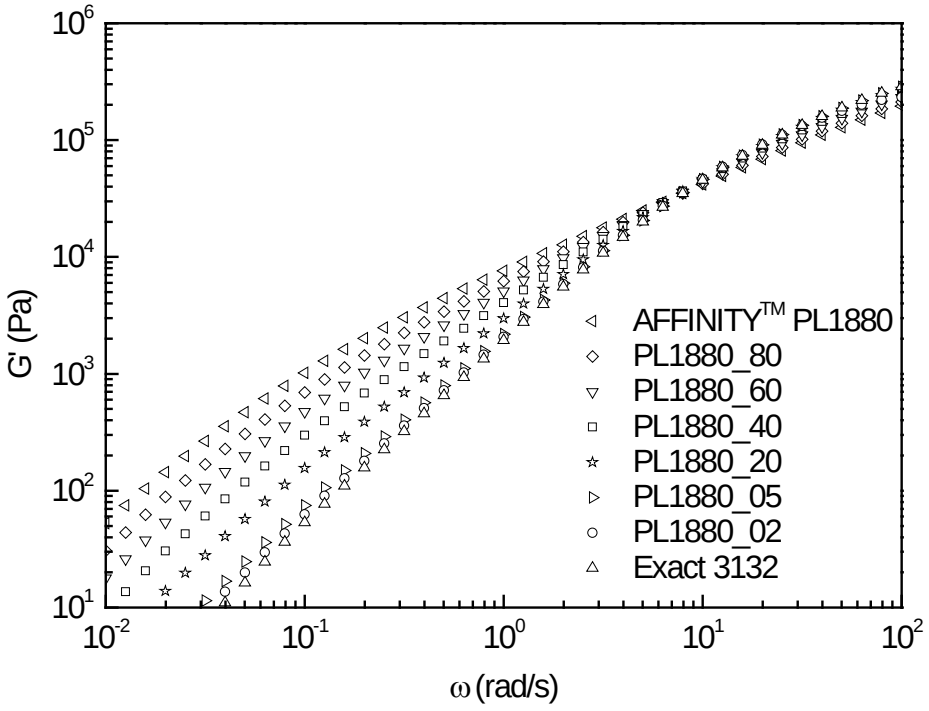

Figure 6-3. Storage modulus as a function of frequency for blends of AFFINITY™ PL 1880 and Exact 3132 at 150 °C.

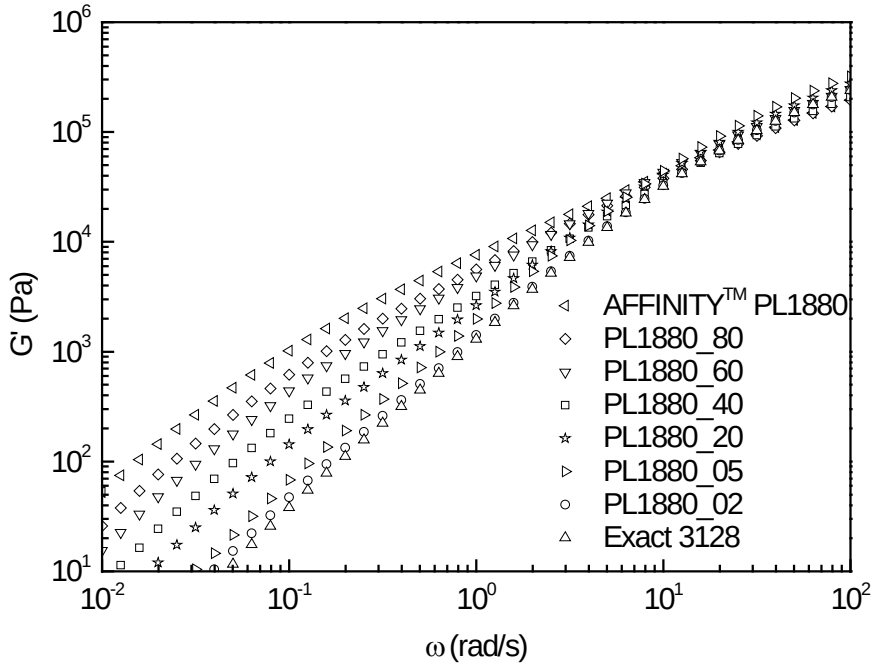

Figure 6-4. Storage modulus as a function of frequency for blends of AFFINITY™ PL 1880 and Exact 3128 at 150 °C.

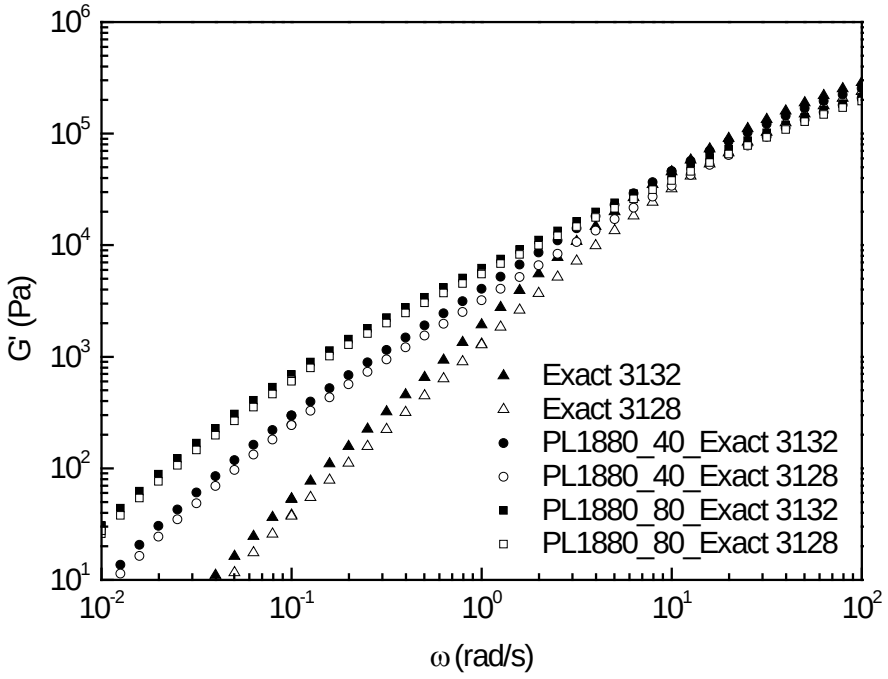

Figure 6-5. Storage modulus as a function of frequency for blends of AFFINITY™ PL 1880 with Exact 3132 and blends of AFFINITY™ PL 1880 with Exact 3128 at the concentrations 0%, 40% and 80% of AFFINITY™ PL 1880 at 150 °C.

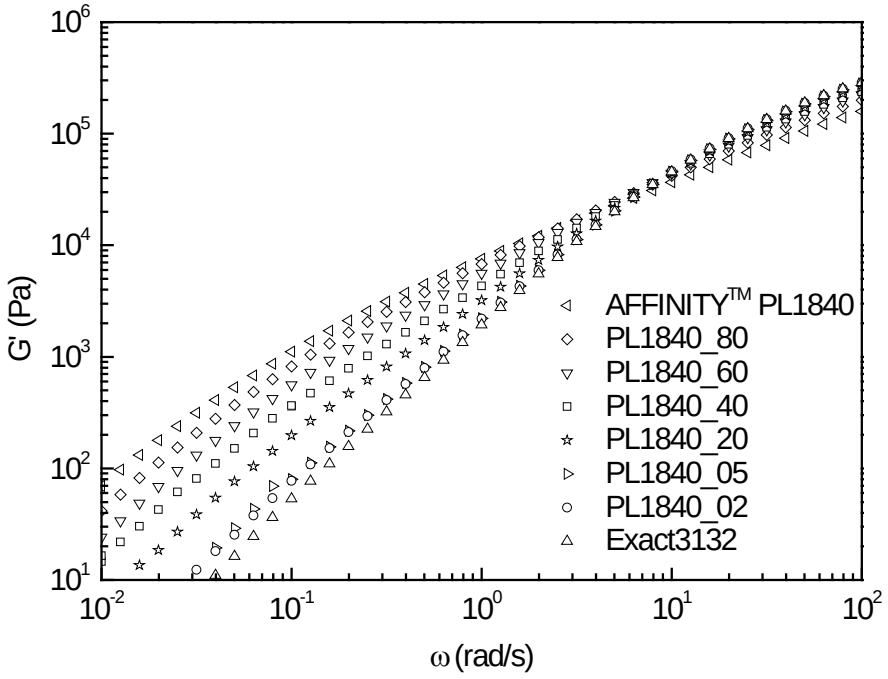

Figure 6-6. Storage modulus as a function of frequency for blends of AFFINITY™ PL 1840 and Exact 3132 at 150 °C.

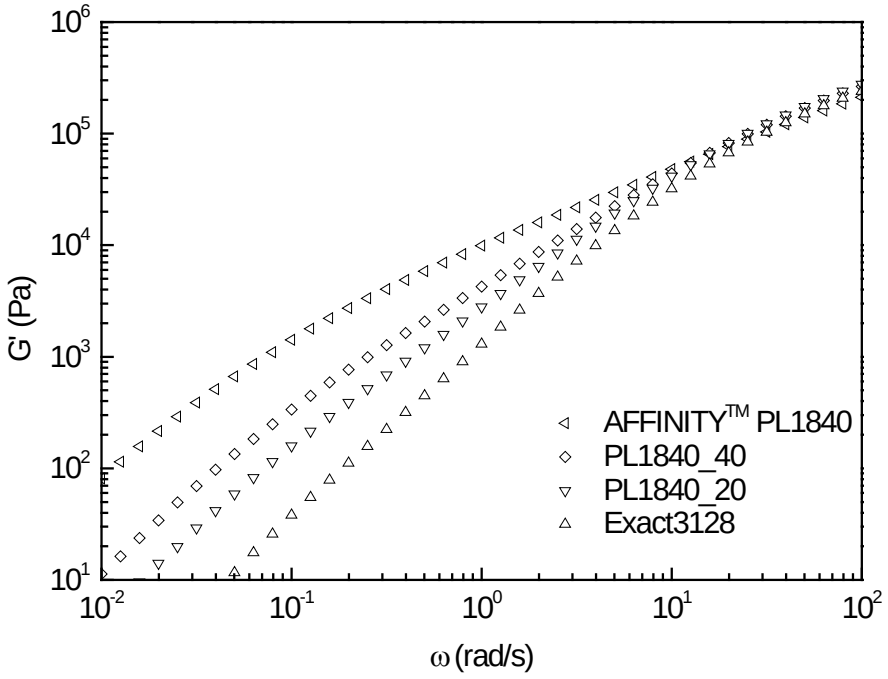

Figure 6-7. Storage modulus as a function of frequency for blends of AFFINITY™ PL 1840 and Exact 3128 at 150 °C.

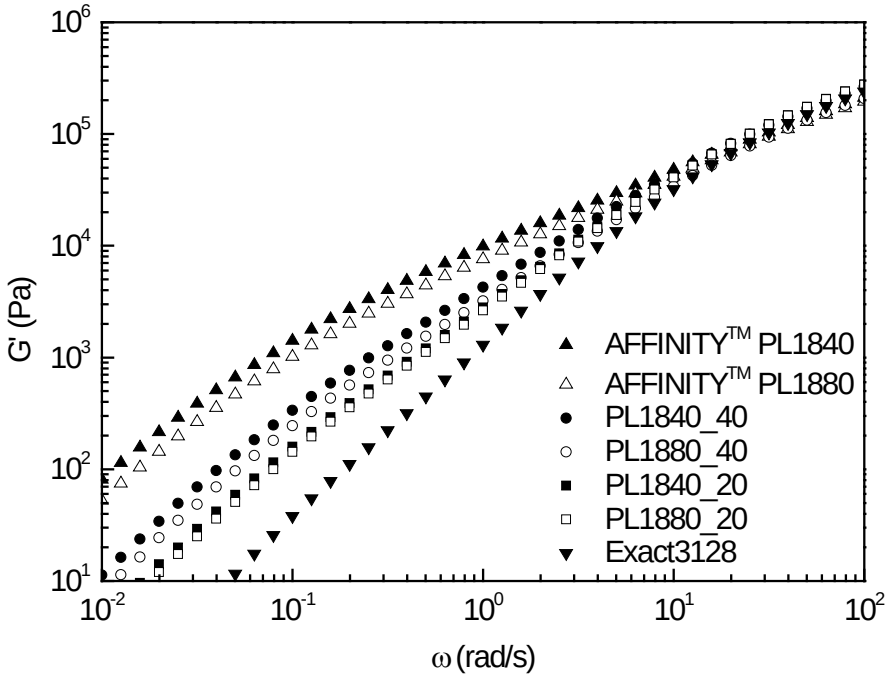

Figure 6-8. Comparison of storage modulus as a function of frequency for blends of AFFINITY™ PL 1840 (symbols) and Exact 3128 with blends of AFFINITY™ PL 1880 and Exact 3128 (dashed lines) at 150 °C.

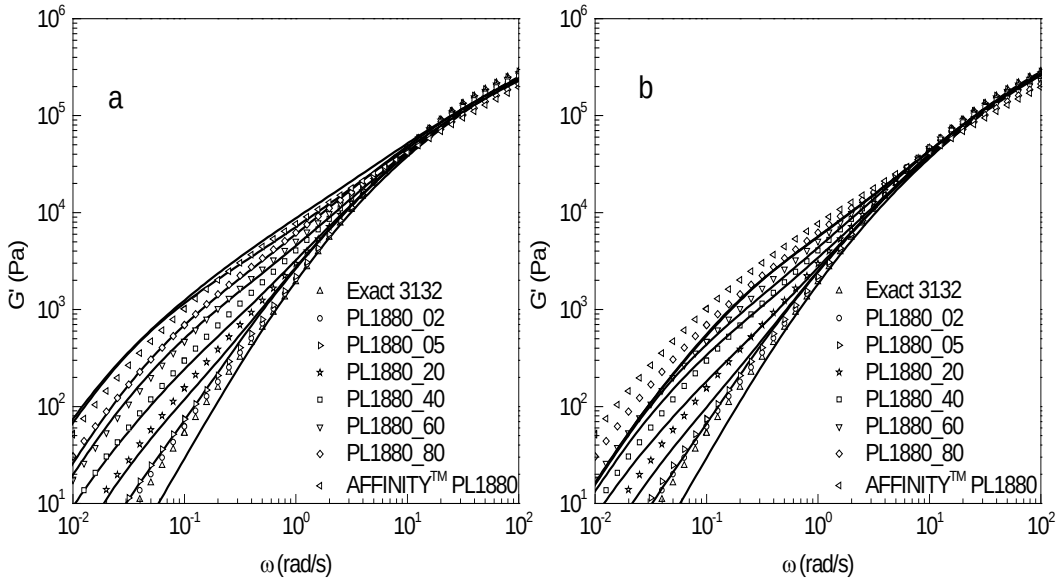

Figure 6-9. Comparisons of storage modulus for the blends of AFFINITY™ PL1880 with Exact 3132 with predictions by the "hierarchical model" with different options. In both (a) and (b), symbols are experimental G' data. (a) lines are predictions of the "hierarchical model" with the "arm-frozen" option; (b) lines are predictions of the "hierarchical model" with the "thin-tube" option.

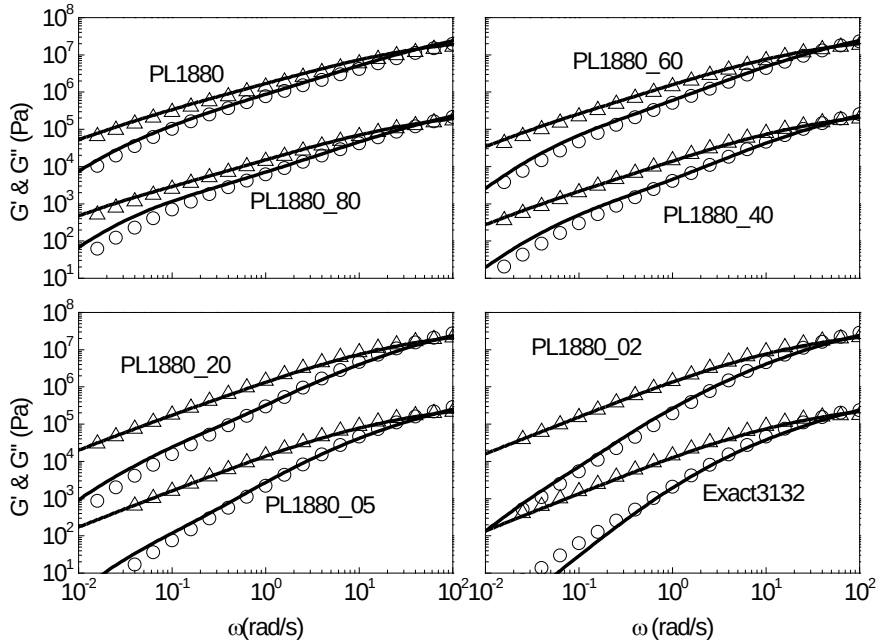

Figure 6-10. Experimental G’ and G’’ data, and “hierarchical model” calculations for blends of AFFINITY™ PL 1880 and Exact 3132. Circles (solid lines) and triangles (dashed lines) are experimental data (theoretical predictions) for G’ and G’’. To separate the data sets, the data for AFFINITY™ PL 1880, PL1880_60, PL1880_20 and PL1880_02 have been shifted vertically by a factor of 100.

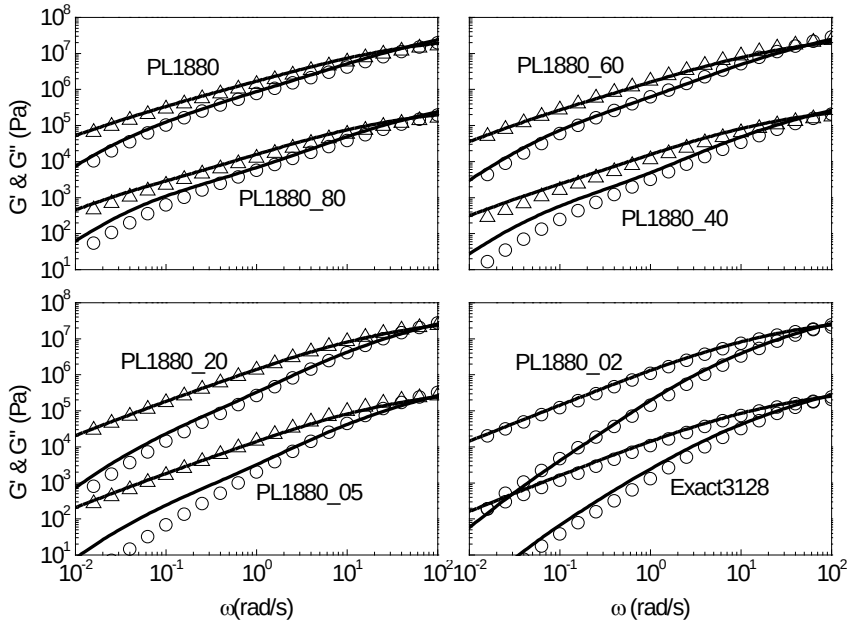

Figure 6-11. The same as Figure 6-10, for blends of AFFINITY™ PL 1880 and Exact 3128.

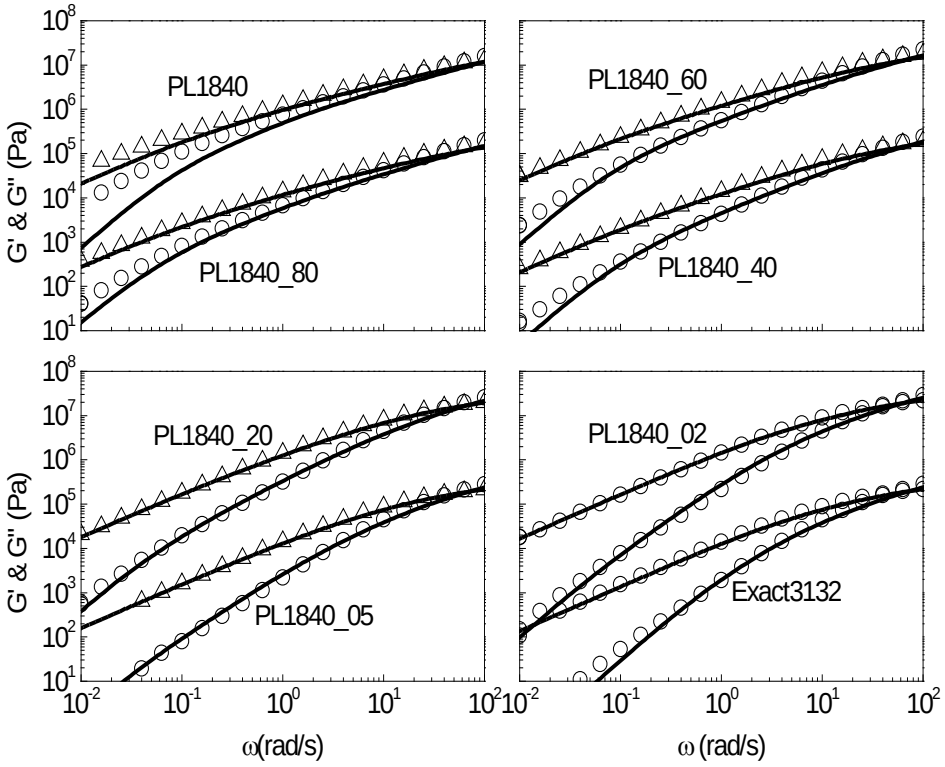

Figure 6-12. The same as Figure 6-10, for blends of AFFINITY™ PL 1840 and Exact 3132.

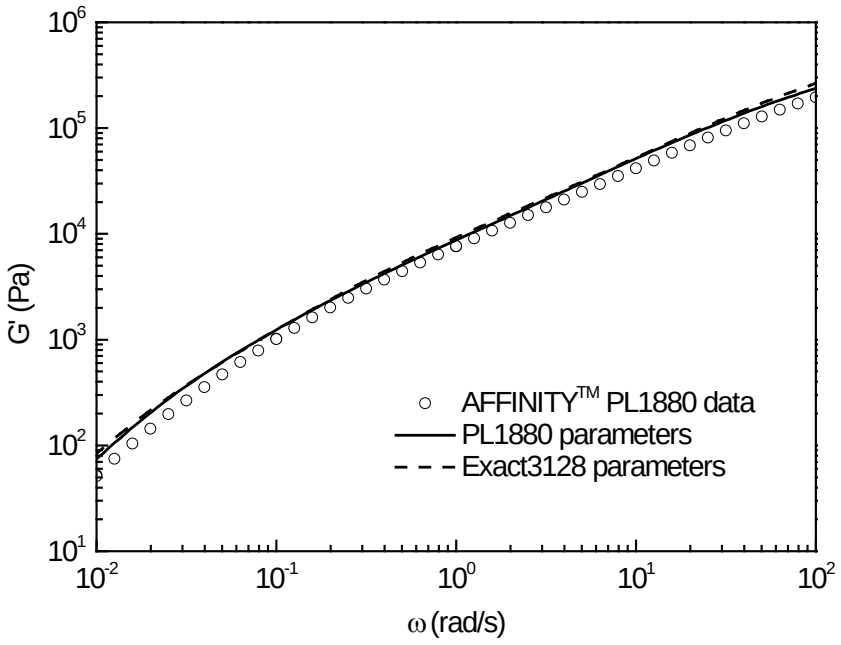

Figure 6-13. Experimental G' data, and "hierarchical model" calculations for AFFINITY™ PL 1880. Circles are experimental data for G'. Solid lines and dashed lines are calculations for the AFFINITY™ PL1880 ensemble, using tube model parameters for AFFINITY™ PL1880 and for Exact 3132, respectively.

6.7 References

Chen, X., and R. G. Larson, "Effect of branch point position on the linear rheology of asymmetric star polymers," Macromolecules 42, 6871-6872 (2008).

Chen, X., F. J. Stadler, H. Münstedt, and R. G.. Larson, "Method for obtaining tube model parameters for commercial ethene/α-olefin copolymers," J. Rheol. 54, 393-406, (2010).

Chambon, P., C. M. Fernyhough, K. Im, T. Y. Chang, C. Das, J. Embery , T. C.B. McLeish, and D. J. Read, "Synthesis, temperature gradient interaction chromatography, and rheology of entangled styrene comb polymers," Macromolecules 41, 5869-5875 (2008).

Costeux, S., P. Wood-Adams, and D. Beigzadeh, "Molecular structure of metallocene-catalyzed polyethylene: Rheologically relevant representation of branching architecture in single catalyst and blended systems," Macromolecules 35, 2514-2528 (2002).

Crosby, B. J., M. Mangnus, W. de Groot, R. Daniels, and T.C.B. McLeish, "Characterization of long chain branching: Dilution rheology of industrial polyethelenes," J. Rheol. 46, 401-426 (2002).

Daniels, D. R., T. C. B. McLeish, R. Kant, B. J. Crosby, R. N. Young, A. Pryke, J. Allgaier, D. J. Groves, and R. J. Hawkins, "Linear rheology of diluted linear, star and model long chain branched polymer melts," Rheol.Acta. 40, 403-415 (2001).

Das, C., N. J. Inkson, D. J. Read, M. A. Kelmanson, and T. C. B. McLeish, "Computational linear rheology of general branch-on-branch polymers," J. Rheol. 50, 207-235 (2006).

Doerpinghaus, P. J., and D. G. Baird, "Assessing the branching architecture of sparsely branched metallocene-catalyzed polyethylenes using the pompom constitutive model," Macromolecules 35, 10087-10095 (2002).

Doerpinghaus, P. J., and D. G. Baird, "Separating the effects of sparce long-chain-branching on rheology from those due to molecular weight in polyethylenes," J. Rheol. 47, 717-736 (2003).

Fetters, L. J., D. J. Lohse, C. A. Garcia-Franco, P. Brant, and D. Richter, "Prediction of melt state poly(alpha-olefin) rheological properties: The unsuspected role of the

average molecular weight per backbone bond," Macromolecules 35, 10096-10101 (2002).

Gabriel, C., E. Kokko, B. Lofgren, J. Seppala, and H. Münstedt, "Analytical and rheological characterization of long-chain-branched metallocene-catalyzed ethylene homopylymers," Polymer 43, 6383-6390 (2002a).

Gabriel, C., and H. Münstedt, "Influence of long-chain branches in polyethylenes on linear viscoelastic flow properties in shear," Rheol. Acta 41, 232-244 (2002b).

Inkson, N. J., R. S. Graham, T. C. B. McLeish, D. J. Groves, and C. M. Fernyhough, "Viscoelasticity of monodisperse comb polymer melts," Macromolecules 39, 4217-4227 (2006).

Janzen, J., and R.H. Colby, "Diagnosing long-chain branching in polyethylenes," J. Mol. Struct. 485, 569-584 (1999).

Larson, R.G., "Combinatorial rheology of branched polymer melts," Macromolecules 34, 4556-4571 (2001).

Larson, R. G., T. Sridhar, L. G. Leal, G. H. McKinley, A. E. Likhtman, and T. C. B. McLeish, "Definitions of entanglement spacing and time constants in the tube model," J. Rheol. 47, 809-818 (2003).

Leonardi, F., J-C. Majeste, A. Allal, and G. Marin, "Rheological models based on the double reputation mixing rule: The effects of a polydisperse environment," J. Rheol. 44, 675-692 (2000).

Likhtman, A. E., and T. C. B. McLeish, "Quantitative theory for linear dynamics of linear entangled polymers," Macromolecules 35, 6332-6343 (2002).

Liu, C. Y., C. X. Li, P. Chen, J. He, and Q. Fan, "Influence of long-chain branching on linear viscoelastic flow properties and dielectric relaxation of polycarbonates," Polymer 45, 2803-2812 (2004).

Lyu, M. Y., J. S. Lee, and Y. Pae, "Study of mechnical and rheological behaviors of linear and branched plycarbonates blends," J. Appl. Polym. Sci. 80, 1814-1824 (2001).

McLeish, T. C. B., J. Allgaier, D. K. Bick, G. Bishko , P. Biswas , R. Blackwell , B. Blottiere , N. Clarke , B. Gibbs , D. J. Groves , A . Hakiki , R. K. Heenan , J. M. Johnson , R. Kant , D. J. Read, and R. N. Young, "Dynamics of entangled H-

polymers: Theory, rheology, and neutron-scattering," Macromolecules 32, 6734-6758 (1999).

Milner, S. T., and T. C. B. McLeish, "Parameter-free theory for stress relaxation in star polymer melts," Macromolecules 30, 2159-2166 (1997).

Milner, S. T., and T. C. B. McLeish, "Reptation and contour-length fluctuations in melts of linear polymers," Phys. Rev. Lett 81, 725-728 (1998).

Milner, S. T., T. C. B. McLeish, R. N. Young, A. Hakiki, and J. M. Johnson, "Dynamic dilution, constraint-release, and star-linear blends," Macromolecules 31, 9345-9353 (1998).

Park. S. J., and R. G. Larson, "Long-chain dynamics in binary blends of monodisperse linear polymers," J. Rheol. 50, 21-39 (2005a).

Park, S. J., S. Shanbhag, and R. G. Larson, "A hierarchical algorithm for predicting the linear viscoelastic properties of polymer melts with long-chain branching," Rheol.Acta 44, 319-330. (2005b).

Pattamaprom, C., R. G. Larson, and T. J. Van Dyke, "Quantitative prediction of linear viscoelastic rheological properties of entangled polymers," Rheol. Acta 39, 517-531 (2000).

Shroff, R. N., and H. Mavridis, "Long chain branching index for essentially linear polyethylenes," Macromolecules 32, 8454-8464 (1999).

Shroff, R. N., and H. Mavridis, "Assessment of NMR and rheology for the characterization of LCB in essentially linear polyethylenes," Macromolecules 34, 7362-7367 (2001).

Simon,P. F. W., A. H. E. Muller, and T. Pakula, "Characterization of highly branched poly(methyl methacrylate) by solution viscosity and viscoelastic spectroscopy," Macromolecules 34, 1677-1684 (2001).

Stadler, F. J., and H. Münstedt, "Terminal viscous and elastic properties of linear ethene/alpha-olefin copolymers" J. Rheol., 52, 697-712 (2008).

Striegel, A. M., and M. R. Krejsa, "Complementarity of universal calibration SEC and C-13 NMR in determining the branching state of polyethylene," J. Polym. Sci., Part B: Polym. Phys. 38, 3120-3135 (2000).

Van Ruymbeke, E., R. Keunings, V. Stephenne, A. Hagenaars, and C. Bailly, "Evaluation of reputation models for predicting the linear viscoelastic properties of entangled linear polymers," Macromolecules 35, 2689-2699 (2002).

Van Ruymbeke, E., V. Stephene, D. Daoust, P. Godard, R. Keunings, and C. Bailly, "A sensitive method to detect very low levels of long chain branching from the molar mass distribution and linear viscoelastic response," J. Rheol. 49, 1503-1520 (2005).

Van Ruymbeke, E, C. Bailly, R. Keunings , and D. Vlassopoulos, "A general methodology to predict the linear rheology of branched polymers," Macromolecules 39, 6248-6259 (2006).

Vega, J. F., M. Auilar, J. Peon, D. Pastor, and J. Martinez-Salazar, "Effect of long chain branching on linear viscoelastic melt properties of polyolefins," e-Polymer paper 46 (2002).

Vega, J. F., M. Fernandez, A. Santamaria, A. Munoz-Escalona, and P. Lafuente, "Rheological criteria to characterize metallocene catalysed polyethylenes," Macromol. Chem. Phys. 200 2257-2268(1999).

Wood-Adams, P. M., J. M. Dealy, A. W. de Groot, and O. D. Redwine, "Effect of molecular structure on the linear viscoelastic behavior of polyethylene," Macromolecules 33, 7489–7499 (2000)

Wang, Z. W., X. Chen, and R. G. Larson, "Computational models for predicting the linear rheology of branched polymer melts," J. Rheol. 54, 223-260 (2010).

Chapter 7
Conclusion and future work

As a link between polymer molecular characteristics and polymer process behaviors, polymer melt rheology can be used as to tool to help to determine polymer structures as well as to predict process behaviors. This is especially true of long-chain branched polymers, because rheology is a very sensitive indicator of polymer long chain branching. This dissertation is thus focused on the study of the relationship between polymer linear viscoelastic properties and their structures using both experimental rheology measurements as well as theoretical modeling methods.

As discussed in previous chapters, the logic to present my research work is shown in Figure 7-1. We start with a description of the theory, and then test the theory on model polymers, and finally apply the theory to commercial polymers which are a mixture of model polymers. The detailed summary of each chapter is listed below:

1) Chapter 2: The theory of polymer relaxation mechanism is discussed by comparing two generalized advanced tube models, namely the “BOB” model and “hieratical model”. One example of “T” and “Y” shaped star polymers is given in this chapter to study the branch point position effect on their linear viscoelastic properties. These two advanced tube models are applied into other chapters of my dissertation.
2) Chapters 3 and 4: It is known that commercial polymers are a mixture of various molecular architectures, such as linear, star, H, comb or even the branch-on-branch molecules. In each of these advanced tube models, the polymer is represented by an ensemble of thousands of chains, representing many kinds of molecules in the melt. Then, a computer code tracks the relaxation of each molecule in the mixture, using the mechanisms of reptation, retraction and constraint release and adds up the effects of relaxation of all the molecules to produce the overall relaxation. Therefore, before accessing the theoretical predictions on the commercial polymers, we need to

validate the tube models on the model polymer melts, which are nearly monodisperse or have a few monodisperse components that can be identified. The linear and star-shaped polymers are relatively simple polymers, because it is relatively easy to synthesize the materials of high quality with few by-products. The tube models have been validated successfully on many linear and star-shaped polymers in the literature. Due to the difficulty to synthesize the H-shaped polymers of high quality, very few groups have worked on the symmetric H-shaped polymers and no group has worked on the asymmetric H-shaped polymers. The Chapter 3 and Chapter 4 are about our work on the H-shaped polymers. And we are the first group to work on the asymmetric H-shaped polymer. The novelties of Chapter 3 and Chapter 4 include: (1) we proposed a new method to synthesize the asymmetric H (H(SSLL)), that is, an asymmetric star is prepared firstly and then two long arms are attached to the end of one arm of the asymmetric star. (2) The traditional SEC characterization only identifies one peak for the purified H-shaped polymer. For a long time, previous research publications have treated the H-shaped polymer as one kind of structure. However, our work here, combining the knowledge of synthesis, TGIC, and theoretical modeling, indicates that we need to treat this kind of sample as polydisperse in structure as well. (3) The "combinatorial rheology" concept has been applied into the H shaped polymer project to detect the impurities in the samples.

3) Chapters 5 and 6: These two chapters are about the commercial polyethylene project. To predict the rheological behaviors of commercial polyethylene copolymers, there are two main barriers. Commercial branched polymers always contain mixtures of different molecular architectures, such as linear polymer, star, H, comb and branch-on-branch polymers. So we need a generalized model to predict their rheology. The second barrier is related to co-monomer's types and content. Because different commercial polymers use different co-monomer types and contents, and these factors affect the key tube model parameters, namely entanglement molecular weight, plateau modulus, and equilibration time, that are needed to make quantitative predictions. For the first barrier, the generalized tube models have been proposed. The advanced tube model, namely, the "hierarchical model" has been validated on a branch of simple model polymers (linear, star et al.) in previous publications. And it

has been validated on the model H-shaped polymer using accurate molecular characteristics information in my previous chapters. Therefore, the first problem has been solved. The second barrier is related to the model parameters include the entanglement molecular weight, the plateau modulus, and the equilibration time. Since these input parameters are generally not specified when experimental data are presented, generalized codes such as those discussed above cannot be truly predictive, unless a procedure is given to estimate these parameters a priori. In Chapter 5, we proposed a method to obtain those tube model parameters for copolymers and validate this method successfully using both of the generalized tube models (BOB model as well as hierarchal model) on the literature rheological data of linear-shaped polyethylene copolymers measured by other groups. We then applied this method into the project of commercially-available polyolefin copolymers, namely Dow Affinity PL1880, PL1840 and Exxon Mobil Exact 3132 and Exact 3128, as discussed in Chapter 6. And the "hierarchical model" can predict the experimental data of those blends successfully. The novelties of these two chapters include: (1) we are the first to create the method to calculate tube model parameters based on the copolymer type and content information. (2) By mixing the linear-shaped commercial polyethylene with the long-chain branched polyethylene, we can detect the level of long-chain branching as low as 0.355 branches per million carbon bonds by using the rheological measurements. Such a low level of long chain branching cannot be detected by any other methods and have not been reported before.

The limitations and future work have also been discussed as listed below:

1) The "hierarchical model" cannot calculate the rheology of the hyper-branched polymers. For the commercial polymers without long chain branches or with a low level of long chain branching, the "hierarchical model" works well, since we can consider the branch-on-branch structure as a comb-shaped polymer approximately, as that presented in Chapter 6. However, for the commercial polymers with a very high level of long chain branching, which means the number of the hyper-branched chains cannot be neglected, the prediction power of "hierarchical model" is limited.
2) In Chapter 4, we studied one asymmetric H-shaped polymer (H(SSLL)), which has

two identical short arms attached to one end of the backbone and two identical long arms attached to another end of the backbone. In the future, other kinds of asymmetric H-shaped polymer, such as H(SSSL), H(SLLL) and H(SLSL), can also be studied to test the theory as well as the “hierarchical model”. Furthermore, for the 50/50 blend of star and H(SSLL)-P as mentioned in Chapter 4, the “hierarchical model” cannot predict the data very much, while it works well for the 50/50 blend of linear and H(SSLL)-P. A new H(SSLL) is then needed to help us figure out the reasons.

3) This thesis focuses only on the linear visocoelasticity of polymer melts to study the relationship between polymer structures and their rheological properties. For practice, the knowledge of non-linear rheology is useful for polymer processing, such as extrusion process. Efforts in this area need more attention.

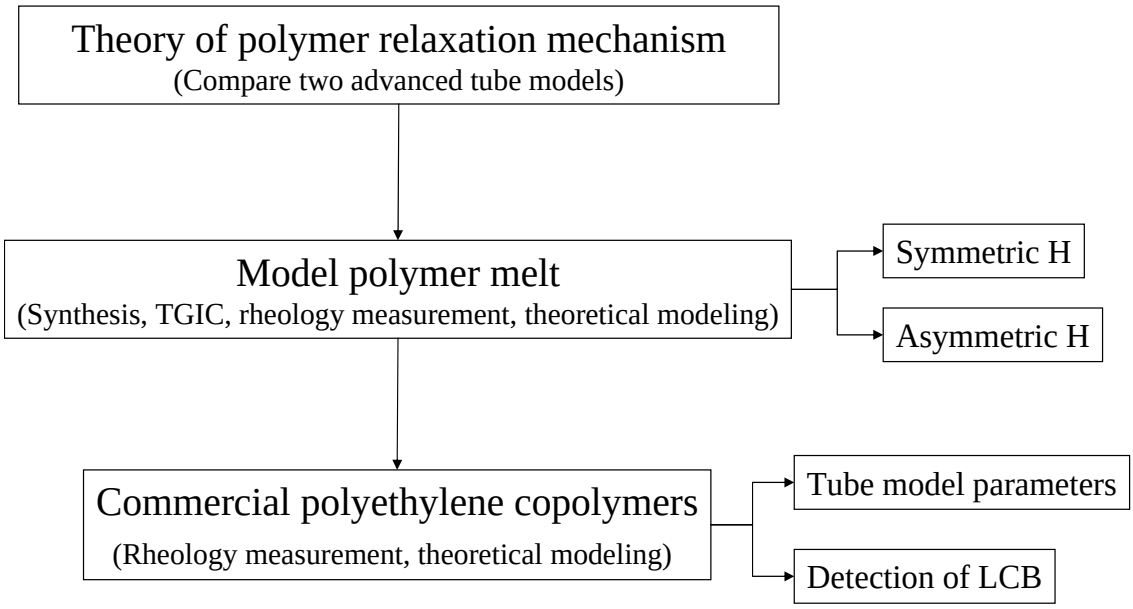

Figure 7-1. Logic of this thesis to present my research work.